PLASTICITY OF PRIMARY GUSTATORY AFFERENTS

Olivia Lynn May
Sarasota, FL

B.A., Florida State University, 1999

A Dissertation presented to the Graduate Faculty
of the University of Virginia in Candidacy for the Degree of
Doctor of Philosophy

Department of Psychology

University of Virginia
August, 2005

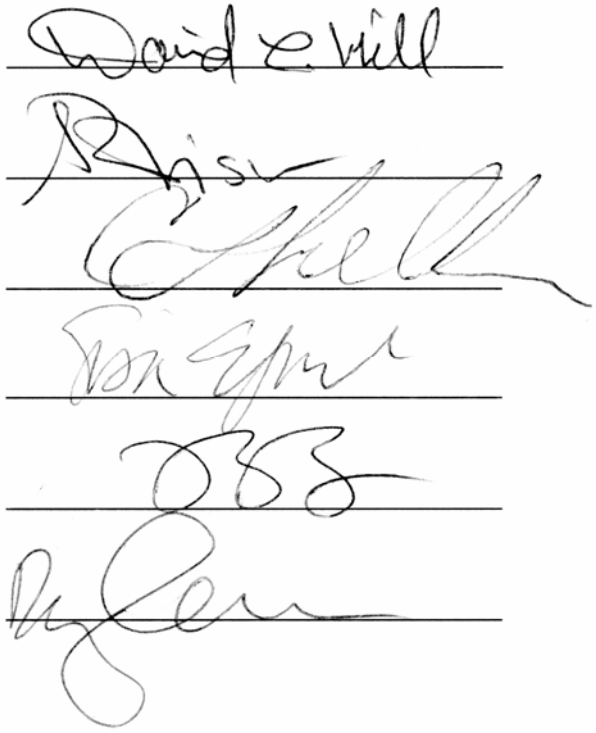

ABSTRACT

The first synaptic relay of the gustatory system is located in the brainstem in the nucleus of the solitary tract (NTS). This relay integrates input from three distinct gustatory nerves: the greater superficial petrosal nerve, the chorda tympani nerve, and the glossopharyngeal nerve. However, key information is lacking regarding the anatomical relationships among the terminations of these three nerves. Furthermore, the normal organization of these terminations in the gustatory brainstem is profoundly influenced by dietary sodium restriction during early development. The experiments in this dissertation sought to obtain an accurate characterization of the normal interactions of the three gustatory afferents in the NTS in order to further explore the neural plasticity resulting from early dietary sodium restriction. Chapter II describes a novel, triple-fluorescent confocal microscopy technique implemented to simultaneously visualize the three gustatory terminal fields in the NTS of control and sodium-restricted rats. Under normal developmental conditions, individual gustatory afferents terminated in an ordered yet overlapping array. However, dietary sodium restriction resulted in dramatic and specific alterations of these termination patterns, which increased the extent of convergence of the gustatory terminal fields. Chapter III describes the distinct ultrastructural morphology and synaptic relationships of the axon terminals of the three gustatory afferents in control rats. Chapter IV reveals evidence for plasticity in the synaptic arrangements of all three gustatory afferents as a result of dietary sodium restriction. The results of these three experiments provide new insight on how the circuitry of the gustatory brainstem is wired during distinct phases of development and how they are modified by early dietary

manipulations. These findings provide fundamental information about how taste stimulus information may be functionally processed centrally and how it may be manifested behaviorally.

DEDICATION

To the mentors that have shaped and informed my aspirations, and to the family and friends who have supported my every endeavor, I am most grateful.

ACKNOWLEDGEMENTS

In a sense, this dissertation project was a collaborative effort in that its completion would not be possible without the concerted encouragement and support of numerous people that surround my life. While there is inevitable risk of omission in compiling a list of such benefactors, I would like to acknowledge a few significant contributions.

–My parents, Harry and Barbara May, from whom I learned to balance patience and perseverance in striving to do my best. Thank you both for your unconditional love and support and for providing comic relief with numerous suggestions for experiments I can perform on rats.

–My sister and her husband, Heidi and Michael Shaw, for showing never-ending interest in my scientific research (this was a constant source of encouragement) and for giving exceptional advice on every query I presented.

–My best friend, Jennifer Stertzer, for building my confidence when it was lacking and for continually providing much needed diversions throughout my academic career, despite my better judgment. I could not imagine a truer friend.

–The members of my committee, Lisa Goehler, Cedric Williams, Barry Condron, Peter Brunjes, Alev Erisir, and Dave Hill, for their utmost cooperation in

scheduling (mostly early-morning) committee meetings and for their valuable input on the design and interpretation of the experiments of this dissertation.

–The ever-revolving members of the Erisir Lab, too numerous to list; in particular, I would like to acknowledge Alev Erisir, Marc Nahmani, and Bonnie Sheppard for their unending electron microscopy training, technical support, advice, and, above all, their friendship.

–The past and present members of Hill lab (who spanned my time at the University): Nick Guagliardo, Sue Hendricks, Dan Binder, Erika Friehling, Sukie Rayas, Jamie Mangold, Becky Reddaway, Jenny Thomas, Si-ting Wang, and Bill Goodwin, for creating a good-humored, amicable, and supportive laboratory environment.

–My advisor and friend, Dave Hill, for providing guidance and practical training through every phase of my graduate career. You instill confidence and inspire greatness yet exemplify true humility amid success. I have learned more about myself during the years I spent at the University of Virginia, than the combined life experiences I had thus far encountered. Thank you for affording me this opportunity. I hope that my achievement here has made you proud and will continue to do so in the future.

TABLE OF CONTENTS

CHAPTER I

General Introduction

The design of the taste system provides an advantageous model by which both structure and function can be studied with relative ease. Three different nerves carry information from three separate receptor cell populations to one distinct population of neurons located in the central nervous system. Neural plasticity, induced by a paradigm of altered dietary sodium during development, is evident at this first central relay located in the brainstem. However, many details regarding the normal development of the gustatory circuitry have remained undetermined. Importantly, the interactions of the three gustatory afferents relative to each other in the first central relay are largely unknown. An accurate characterization of the normal interactions of these gustatory afferents is fundamental to understanding plasticity as a consequence of environmental manipulation.

Detailed in the following paragraphs is the current knowledge of the development and plasticity of the neural components of the first central relay of the gustatory system. Through considerable effort, the principal studies cited in this introduction have provided a basic foundation for the organization of gustatory circuitry; however, in certain aspects, these researchers were largely limited by technological design. The experiments described in Chapters II-IV of this dissertation were launched from these initial studies to provide a better understanding of how the gustatory nerves interact with each other and their synaptic targets in the brainstem and how those interactions are altered upon environmental manipulation. To this end, we developed a novel technique with which the terminal fields of the three gustatory nerves could be simultaneously visualized in three-dimension in a single rat. This technique enabled me to document the relative

relationships of the terminal fields of the three gustatory afferents and to characterize alterations in those relationships in a background of plasticity (Chapter II). Additionally, I further expanded these studies to determine the general distinguishing ultrastructural morphology and the synaptic relationships of the axon terminals of the three different gustatory afferents in an effort to begin to determine the level of convergence of gustatory afferents onto postsynaptic targets (Chapter III). Finally, I described how plasticity, induced by our sodium restriction paradigm, is manifested in the synaptic arrangements of the gustatory afferents (Chapter IV).

Gustatory Circuitry

The nucleus of the solitary tract (NTS) is the site of the first-order afferent relay of the gustatory nerves in the central nervous system (Contreras et al., 1982). The chorda tympani (CT) nerve, which innervates the anterior portion of the tongue, and greater superficial petrosal (GSP) nerve, which innervates the soft palate and nasoincisor duct, comprise the VII nerve and terminate in the rostral-most portion of the NTS (Hamilton and Norgren, 1984; Lasiter, 1992). The glossopharyngeal (IX) nerve, which innervates the posterior portion of the tongue, terminates in the NTS just caudal to CT and GSP fields (Hamilton and Norgren, 1984; Lasiter, 1992). The superior laryngeal (X) nerve, which innervates the pharynx, larynx, and epiglottis, terminates in the caudal NTS overlapping with IX terminations (Hamilton and Norgren, 1984). Gustatory relay (or projection) neurons in the NTS, on which gustatory afferents terminate, transmit taste information primarily to the ipsilateral, caudal parabrachial nucleus (PBN) (Norgren, 1978). From the PBN two branches of the ascending taste pathway arise. One branch

extends into the ventral posteromedial thalamic nucleus and eventually terminates in the cortex (Benjamin and Pfaffmann, 1955; Ables and Benjamin, 1960). The other pathway ascends through the lateral hypothalamus and terminates in the central amygdala and the bed nucleus of the stria terminalis (Norgren, 1976).

Development of the Anatomical Arrangement of the NTS

Tract tracing studies of gustatory projections to the NTS have provided a preface to the gross organization of mature gustatory terminations and their developmental time course. Individual gustatory afferents and their postsynaptic targets develop in separate stages. Whereas studies of NTS development have not conclusively teased apart the developmental timelines of individual afferents (i.e., the GSP and CT nerves) due to technical limitations, collective evidence points to a successive development of afferent terminations pioneered by the GSP nerve, followed by the CT nerve, and then eventually the IXth nerve. Geniculate ganglia cells, the cell bodies of the VIIth nerve, are born on embryonic day 11 (E11), while petrosal ganglion cells, the cell bodies of the IXth nerve, are born at E14 (Altman and Bayer, 1982). The VII nerve terminal fields, which include that of both the CT and GSP nerves, already occupy the rostral NTS at P1 and develop to approximately P25 (Lasiter, 1992). In examining the CT nerve projections apart from the GSP nerve, afferent fibers of the CT nerve project to the rostral NTS in rats as early as postnatal day 1 (P1) (Zhang and Ashwell, 2001), and the volume of CT terminal field increases from about P1 to P20 as collaterals persistently branch and form terminations extending in the rostrocaudal plane (Lasiter et al., 1989). Unfortunately, the developmental time course of the GSP field alone has not been determined extensively.

However, the unpublished observations of S. I. Sollars & D. L. Hill indicate a significant GSP field development by P10, whereas CT field development is immature at this age. Thus, the termination of GSP axons in the NTS most likely precedes that of the CT nerve. In a relatively later stage of NTS development, IX fibers enter the NTS around P10 and their terminations develop in the intermediate portion of the NTS, reaching adult-like configuration at about P45 (Lasiter, 1992).

The mature distribution of CT terminations is located primarily in the lateral NTS and is most dense in the rostral pole (Hamilton and Norgren, 1984). The mature GSP terminal field is coextensive with the CT terminal field for the most part; however, the rostral limit of the GSP is just caudal to the CT terminal field (Hamilton and Norgren, 1984). IX terminations extend more caudally than CT and GSP and also project into the dorsolateral portion of the NTS (Hamilton and Norgren, 1984). A significant anatomical organization occurs in these terminal fields in the NTS during early postnatal life as they develop into their adult configurations. For instance, a 30% reduction in the total volume of the CT terminal field occurs between postnatal day 27 and adulthood (Hill et al., 2003). The GSP and IX terminal field volumes of immature rats have not been compared to adults, however, a paring back of terminations may occur as well.

Several investigators have identified three main morphological types of neurons within the gustatory NTS: elongate (or fusiform), multipolar (or stellate), and ovoid neurons (Davis and Jang, 1988; Whitehead, 1988; Lasiter et al., 1989; King and Hill, 1993; King and Bradley, 1994). Multipolar and elongate neurons receive most of their synaptic input from primary afferent fibers (Whitehead, 1993), while ovoid neurons are

presumed interneurons (Lasiter and Kachele, 1988; Davis, 1993). These gustatory neurons are produced between E12 and E15 (Altman and Bayer, 1982), well in advance of the initial entry of taste fibers. During prenatal and early postnatal development, axons of the GSP, CT, and IX nerves migrate towards the NTS neurons that will project to the PBN. The first-order dendrites of these neurons lengthen exuberantly the first three weeks postnatal and reach mature lengths at P25 (Lasiter et al., 1989). The second-order dendrites associated with NTS neurons reach maximal lengths at P70 (Lasiter et al., 1989). The branching complexity of these gustatory neurons undergoes substantial remodeling throughout development (Renehan et al., 1997). Moreover, as demonstrated in sheep, branching complexity and spine density varies between neuron types. The number of dendritic branch points continues to increase postnatally for multipolar cells but not for elongate cells (Mistretta and Labyak, 1994). Throughout development, spine density in multipolar cells remains level, but decreases substantially in elongate cells (Mistretta and Labyak, 1994). As the afferent terminal fields develop and establish connections with gustatory neurons, these neurons project to the parabrachial nucleus (PBN) between the ages of P7-P45 (Lasiter, 1992).

Presumably, the sequence of development of the circuitry of the individual gustatory afferents in the brainstem is mirrored by the sequence of development of the respective receptor populations in the oral cavity. Indeed, the maturation of palatal taste receptor cells precedes that of fungiform and circumvallate taste buds (Harada et al., 2000). Furthermore, taste receptor cells located in circumvallate papillae become functional (i.e., contain a taste pore) well after taste receptors cells located in fungiform

papillae (Harada et al., 2000). Thus, the hierarchical pattern of innervation and terminal formation in the NTS occurs in conjunction with the morphological development of gustatory receptors.

Understanding the organization of the afferent connections of the NTS has been limited by the available methodologies employed to delineate gustatory terminal field morphology. For instance, the labeling techniques, the tracers, and the imaging process used in the studies mentioned above were not capable of simultaneously detecting the interactions among all three gustatory nerve terminal fields. Of the tract tracing studies published to date, at most two tracers have been used in a single animal to identify terminal fields. Never before have the CT and GSP nerves been differentiated in a single animal. Previous experiments have either labeled the VIIth nerve (Lasiter et al., 1989), which is composed of both the CT and GSP nerves, or these nerves were labeled individually on opposing sides of the brain (Hamilton and Norgren, 1984). Furthermore, these studies have not always been performed in living animals and have used horseradish peroxidase, which may not efficiently transport to the NTS as more modern anterograde tracers. Finally, these fields were observed and reconstructed using transmitted light microscopy. Therefore, the three-dimensional relationship among the CT, GSP, and IX terminal fields in the same rat has yet to be visualized. Thus, a refinement of these current techniques is necessary in order to enhance the understanding of the organization of the NTS and provide a clearer picture how the gustatory fields occupy the NTS and relate to each other.

Plasticity of the Gustatory Terminal Fields within the NTS

Repeatedly, researchers have demonstrated the development of the NTS to be highly susceptible to modification. Much of the research in the developing gustatory NTS has focused on the unique plasticity of the CT terminations in response to early environmental manipulations. Environmental manipulations have been accomplished in either one of two approaches: altering dietary sodium or altering taste receptor function. The dorsal most portion of the CT field in the rostral pole of the NTS is extremely plastic in response to alteration of dietary sodium during early embryonic development. That is, in rats fed a low sodium diet (0.03% NaCl) from at least E3-E12 the dorsal most portion of the CT field expands caudally to over twice the size of controls (fed a 1.0% NaCl diet) while overall volume of the NTS remains unchanged (Krimm and Hill, 1997). Similar dietary manipulations result in reduced neurophysiological responses of the CT to sodium salts that can be reversed by repletion with a 1.0% NaCl diet (Hill, 1987; Hill and Przekop, 1988). However, upon restoration of 1.0% NaCl in the diet, the morphological alterations in the CT terminal field do not recover to normal volumes but rather, terminal field volumes increase even more dramatically to 3-fold the volume of control and restricted rats (King and Hill, 1991). Rats fed a diet high (6% NaCl) in dietary sodium throughout development also display an enlarged dorsal CT terminal field (Pittman and Contreras, 2002). This phenomenon brought about by dietary sodium manipulation appears to be selective to the CT field, specifically in the dorsal most portions. Restriction of dietary sodium has been reported not to affect GSP and IX field morphology (King and Hill, 1991; Sollars and Hill, 2000).

Additionally, normal anatomical development of the rostral gustatory NTS is adversely affected by manipulation of gustatory receptors on the anterior tongue during early postnatal life. Receptor damage induced at P2 results in a dramatic reduction of CT terminal field volume by 30% in adulthood (Lasiter and Kachele, 1990). Similarly, restriction of orochemical stimulation from P4-P7 results in a reduction of the caudal expansion of the CT terminal field in adulthood (Lasiter and Diaz, 1992). Stimulation of receptors with 0.15 M NaCl for 3 days is sufficient to induce normal CT terminal field volumes in adulthood (Lasiter, 1995). Therefore, the NTS appears to be remarkably plastic in regard to alterations during specific critical periods of development. Furthermore, this plasticity seems unique to the dorsal-most portion of the CT field.

Plasticity of Gustatory Neurons within the NTS

In conjunction with evidence for anatomical plasticity of CT terminal fields in the gustatory NTS, alterations in the function and structure of taste neurons in the NTS have been identified as a result of environmental manipulation. Dietary sodium restriction during development selectively attenuates central gustatory responsiveness to sodium salts by as much as 50%, while responses to non-sodium salts and non-salt stimuli are not affected (Vogt and Hill, 1993). Concomitant with central morphological changes, taste responses of animals given a NaCl replete diet at adulthood after early sodium restriction exhibit a hyper-responsiveness to sodium stimuli (Vogt and Hill, 1993). Therefore, in addition to central morphological changes, early dietary manipulations of sodium have neurophysiological effects that are relatively selective for sodium-elicited taste responses.

Furthermore, early dietary sodium restriction also affects the dendritic organization of NTS neurons. Specifically, multipolar and fusiform neurons of the rostral NTS extend up to 80% longer than respective cell types in controls (King and Hill, 1993). Other cell types are not affected. Upon repletion, dendritic morphologies of cell types affected by sodium restriction remain elongated and additionally, the dendritic organization of ovoid neurons elaborate (King and Hill, 1993). Also, the packing density of neurons in the rostral NTS is greater in sodium-restricted rats than in controls (King and Hill, 1993). Both anatomical and neurophysiological alterations are permanent and occur as a result of susceptibility to environmental conditions during early development. Thus, with dramatic changes occurring both pre- and postsynaptically as a result of an early developmental dietary manipulation, the very synapses connecting these two elements may be affected as well.

Ultrastructural Organization of the NTS

Currently, the only available information regarding the afferent synaptology of the gustatory NTS is contained in a few electron micrographic studies using hamsters (Whitehead, 1986, 1993; Brining and Smith, 1996; Davis, 1998). Labeled axon terminals deriving from the VII nerve were examined throughout the rostral-caudal extent of the NTS. Studies by Whitehead (1996, 1993) revealed that primary gustatory VII nerve axons form axo-dendritic synapses with neurons contained in the CT/GSP terminal field. VII nerve axon terminals are on average 1.2 μm in diameter, contain large, clear, round vesicles and synapse with small caliber dendrites or dendritic spines. The synaptic density associated with these axon terminals is characteristic of excitatory synapses with

thicker postsynaptic membranes than presynaptic membranes (Peters et al., 1970). VII nerve axon terminals engage in complex synaptic arrangements encapsulated in glia along with other terminals, which contain either small, pleomorphic or large, round vesicles. Pleomorphic vesicles are characteristic of inhibitory synapses, while round vesicles are often associated with excitatory synapses (Peters et al., 1970). Thus, VII nerve axon terminals associate with axons of both excitatory and inhibitory neurons. The rostral NTS contains neurons of both glutamatergic and GABAergic varieties (Bradley et al., 1996; Leonard et al., 1999). In contrast, IXth nerve axon terminals, which are an average diameter of 1.8 μm, are larger than VII nerve terminals, and IX nerve terminals engage in simpler synaptic junctions than VII axon terminals, most often with dendritic spines (Brining and Smith, 1996). Thus, a dichotomy exists between VII and IX nerves in axon terminal morphology and synaptic organization. However, the studies by Whitehead (1986, 1993) did not differentiate between the CT and GSP inputs. Further morphological differences may exist among gustatory afferents, particularly those that comprise the VII nerve. Moreover, the inter-relatedness of the synaptic connections of the gustatory afferents to NTS neurons remains speculative. Therefore, many questions regarding the synaptic organization of the first afferent relay of the NTS remain unanswered.

Convergence of Gustatory Afferents onto NTS Neurons

Given the proximity of the three gustatory terminal fields to each other in the NTS and their often overlapping patterns of termination, convergence of the synaptic inputs from the three gustatory nerves is likely to occur on the same postsynaptic cells.

Electrophysiological studies show single NTS neurons are responsive to taste stimuli applied to different receptor populations throughout the oral cavity. For example, taste stimulation of the anterior tongue and nasoincisor duct, or of the soft palate and posterior tongue elicit responses in single NTS neurons (Travers et al., 1986; Sweazey and Smith, 1987; Sweazey and Bradley, 1989). The multiplicity of responsiveness shown by these neurons is likely due to the convergence of separate gustatory nerves onto NTS neurons. Thus, individual NTS neurons probably receive synaptic input from more than one gustatory afferent; however, convergence at this level has yet to be demonstrated anatomically.

Conclusion

The connectivity of the central gustatory system develops and matures in a sequential manner in synchrony with the onset of peripheral taste receptor cell function. While the experimental findings described above collectively establish a basic knowledge of central gustatory structure and function and its developmental time course, many details remain undetermined. For example, it is unclear to what extent terminal fields of the three gustatory nerves interact with each other in the NTS, since individual terminal fields have not been visualized concurrently in a single animal. Further, the synaptic patterns of the three gustatory afferents onto the relay neurons of the NTS have not been sufficiently identified. Therefore, the existence of converging synapse formation onto NTS neurons by the three gustatory afferents is not known. Plasticity is widely characterized to occur in the NTS; however, the effects of this phenomenon on the interactions of the terminal fields of the three gustatory afferents in the NTS and on the

establishment of synaptic connections with NTS neurons are also largely unknown. The experiments described in the following chapters were designed to begin to address these issues, which beyond refining the current knowledge of the gustatory system have broader implications in the establishment of basic sensory afferent circuitry, the influence of environmental alterations on those connections, and the anatomical correlates of functional and behavioral responses.

LITERATURE CITED

Ables MF, Benjamin RM. 1960. Thalamic relay nucleus for taste in albino rat. J Neurophysiol 23:376-382.

Altman J, Bayer SA. 1982. Development of the cranial nerve ganglia and related nuclei in the rat. Adv Anat Embryol Cell Biol 74:1-90.

Benjamin RM, Pfaffmann C. 1955. Cortical localization of taste in albino rat. J Neurophysiol 18:56-64.

Bradley RM, King MS, Wang L, Shu X. 1996. Neurotransmitter and neuromodulator activity in the gustatory zone of the nucleus tractus solitarius. Chem Senses 21:377-385.

Brining SK, Smith DV. 1996. Distribution and synaptology of glossopharyngeal afferent nerve terminals in the nucleus of the solitary tract of the hamster. J Comp Neurol 365:556-574.

Contreras RJ, Beckstead RM, Norgren R. 1982. The central projections of the trigeminal, facial, glossopharyngeal and vagus nerves: an autoradiographic study in the rat. J Auton Nerv Syst 6:303-322.

Davis BJ. 1993. GABA-like immunoreactivity in the gustatory zone of the nucleus of the solitary tract in the hamster: light and electron microscopic studies. Brain Res Bull 30:69-77.

Davis BJ. 1998. Synaptic relationships between the chorda tympani and tyrosine hydroxylase-immunoreactive dendritic processes in the gustatory zone of the nucleus of the solitary tract in the hamster. J Comp Neurol 392:78-91.

Davis BJ, Jang T. 1988. A Golgi analysis of the gustatory zone of the nucleus of the solitary tract in the adult hamster. J Comp Neurol 278:388-396.

Hamilton RB, Norgren R. 1984. Central projections of gustatory nerves in the rat. J Comp Neurol 222:560-577.

Harada S, Yamaguchi K, Kanemaru N, Kasahara Y. 2000. Maturation of taste buds on the soft palate of the postnatal rat. Physiol Behav 68:333-339.

Hill DL. 1987. Susceptibility of the developing rat gustatory system to the physiological effects of dietary sodium deprivation. J Physiol 393:413-424.

Hill DL, Przekop PR, Jr. 1988. Influences of dietary sodium on functional taste receptor development: a sensitive period. Science 241:1826-1828.

Hill DL, Sollars SI, May OL. 2003. Plasticity of the developing central gustatory brainstem. Chem Senses 28:J3.

King CT, Hill DL. 1991. Dietary sodium chloride deprivation throughout development selectively influences the terminal field organization of gustatory afferent fibers projecting to the rat nucleus of the solitary tract. J Comp Neurol 303:159-169.

King CT, Hill DL. 1993. Neuroanatomical alterations in the rat nucleus of the solitary tract following early maternal NaCl deprivation and subsequent NaCl repletion. J Comp Neurol 333:531-542.

King MS, Bradley RM. 1994. Relationship between structure and function of neurons in the rat rostral nucleus tractus solitarii. J Comp Neurol 344:50-64.

Krimm RF, Hill DL. 1997. Early prenatal critical period for chorda tympani nerve terminal field development. J Comp Neurol 378:254-264.

Lasiter PS. 1992. Postnatal development of gustatory recipient zones within the nucleus of the solitary tract. Brain Res Bull 28:667-677.

Lasiter PS. 1995. Effects of orochemical stimulation on postnatal development of gustatory recipient zones within the nucleus of the solitary tract. Brain Res Bull 38:1-9.

Lasiter PS, Diaz J. 1992. Artificial rearing alters development of the nucleus of the solitary tract. Brain Res Bull 29:407-410.

Lasiter PS, Kachele DL. 1988. Organization of GABA and GABA-transaminase containing neurons in the gustatory zone of the nucleus of the solitary tract. Brain Res Bull 21:623-636.

Lasiter PS, Kachele DL. 1990. Effects of early postnatal receptor damage on development of gustatory recipient zones within the nucleus of the solitary tract. Brain Res Dev Brain Res 55:57-71.

Lasiter PS, Wong DM, Kachele DL. 1989. Postnatal development of the rostral solitary nucleus in rat: dendritic morphology and mitochondrial enzyme activity. Brain Res Bull 22:313-321.

Leonard NL, Renehan WE, Schweitzer L. 1999. Structure and function of gustatory neurons in the nucleus of the solitary tract. IV. The morphology and synaptology of GABA-immunoreactive terminals. Neuroscience 92:151-162.

Mistretta CM, Labyak SE. 1994. Maturation of neuron types in nucleus of solitary tract associated with functional convergence during development of taste circuits. J Comp Neurol 345:359-376.

Norgren R. 1976. Taste pathways to hypothalamus and amygdala. J Comp Neurol 166:17-30.

Norgren R. 1978. Projections from the nucleus of the solitary tract in the rat. Neuroscience 3:207-218.

Peters A, Palay SL, Webster HdF. 1970. The fine structures of the nervous system. New York: Harper and Row.

Pittman DW, Contreras RJ. 2002. Dietary NaCl influences the organization of chorda tympani neurons projecting to the nucleus of the solitary tract in rats. Chem Senses 27:333-341.

Renehan WE, Massey J, Jin Z, Zhang X, Liu YZ, Schweitzer L. 1997. Developmental changes in the dendritic architecture of salt-sensitive neurons in the nucleus of the solitary tract. Brain Res Dev Brain Res 102:231-246.

Sollars SI, Hill DL. 2000. Lack of functional and morphological susceptibility of the greater superficial petrosal nerve to developmental dietary sodium restriction. Chem Senses 25:719-727.

Sweazey RD, Bradley RM. 1989. Responses of neurons in the lamb nucleus tractus solitarius to stimulation of the caudal oral cavity and epiglottis with different stimulus modalities. Brain Res 480:133-150.

Sweazey RD, Smith DV. 1987. Convergence onto hamster medullary taste neurons. Brain Res 408:173-184.

Travers SP, Pfaffmann C, Norgren R. 1986. Convergence of lingual and palatal gustatory neural activity in the nucleus of the solitary tract. Brain Res 365:305-320.

Vogt MB, Hill DL. 1993. Enduring alterations in neurophysiological taste responses after early dietary sodium deprivation. J Neurophysiol 69:832-841.

Vogt MB, Mistretta CM. 1990. Convergence in mammalian nucleus of solitary tract during development and functional differentiation of salt taste circuits. J Neurosci 10:3148-3157.

Whitehead MC. 1986. Anatomy of the gustatory system in the hamster: synaptology of facial afferent terminals in the solitary nucleus. J Comp Neurol 244:72-85.

Whitehead MC. 1988. Neuronal architecture of the nucleus of the solitary tract in the hamster. J Comp Neurol 276:547-572.

Whitehead MC. 1993. Distribution of synapses on identified cell types in a gustatory subdivision of the nucleus of the solitary tract. J Comp Neurol 332:326-340.

Zhang LL, Ashwell KW. 2001. The development of cranial nerve and visceral afferents to the nucleus of the solitary tract in the rat. Anat Embryol (Berl) 204:135-151.

CHAPTER II

Gustatory Terminal Field Organization and Developmental Plasticity in the Nucleus of the Solitary Tract Revealed through Triple Fluorescent Labeling.

INTRODUCTION

Neural plasticity has been widely studied as a way to not only examine the brain's compensatory strategies, but to also characterize normal developmental processes. Some of the most dramatic and widely cited examples of neural plasticity involve higher-order cortical processing and associated circuitry in sensory systems (Hubel and Weisel, 1970; Henderson et al., 1992; Buonomano and Merzenich, 1998; Catalano and Shatz, 1998; Rauschecker, 1999; Fox et al., 2002; Katz and Crowley, 2002; Yan, 2003). However, unlike other systems, the gustatory system shows a remarkable amount of developmental plasticity at the first synaptic relay in the brainstem, in the nucleus of the solitary tract (NTS).

Much of the research in the developing gustatory NTS has focused on the unique plasticity of chorda tympani (CT) nerve terminations in response to early environmental manipulations (Lasiter and Kachele, 1990; King and Hill, 1991; Lasiter and Diaz, 1992; Lasiter, 1995; Krimm and Hill, 1997; Pittman and Contreras, 2002). In rats fed a low sodium diet (0.03% NaCl) from at least E3-E12, the dorsal most portion of the CT field expands caudally, exceeding twice the size of controls (King and Hill, 1991; Krimm and Hill, 1997). The morphological alterations in the CT terminal field are permanent in that the effects are not reversible by age or by sodium repletion. In fact, feeding a sodium replete diet at adulthood to developmentally sodium-restricted rats exaggerates the effects (King and Hill, 1991). This phenomenon, brought about by dietary sodium manipulation, appears selective to the CT field and does not affect other gustatory nerve terminal fields

(e.g., the glossopharyngeal (IX) and greater superficial petrosal (GSP) nerves (King and Hill, 1991; Sollars and Hill, 2000).

While previous tract tracing studies of gustatory projections to the NTS have provided the foundation for an understanding of the gross organization of gustatory terminations (Contreras et al., 1982; Hamilton and Norgren, 1984; Lasiter et al., 1989; Lasiter, 1992), the detailed organization of multiple gustatory terminal fields have not been examined simultaneously in a single animal. Of the tract tracing studies previously published, at most two tracers have been used in an individual animal to identify terminal fields. Previous experiments have either labeled the facial (VII) nerve (Lasiter et al., 1995), which is composed of both CT and GSP, or individual gustatory nerves were labeled on opposing sides of the animal (Hamilton and Norgren, 1984). Furthermore, these studies have either not been performed in living animals or they used horseradish peroxidase, both of which compromise the fidelity of the terminal field label. Finally, terminal fields were observed and reconstructed using transmitted light microscopy and not confocal laser microscopy. Therefore, it is difficult to precisely identify and measure the zones of overlapping fields.

In order to fully explore the plasticity of gustatory terminal fields in the brainstem, we developed a triple fluorescent labeling technique that could be used with confocal laser microscopy. The present study used these techniques to uncover unexpected and dramatic relationships among three gustatory terminal fields in developmentally sodium-restricted and control rats.

MATERIALS AND METHODS

All animal procedures were done in accordance with NIH guidelines for humane handling of animals, and all protocols were approved by the Institutional Animal Care Committee at the University of Virginia.

Animals

Eighteen adult (50-60 days old), female Sprague-Dawley rats (Harlan, Indianapolis, Indiana) maintained on either a control (n=9) or sodium-restricted (n=9) diet were used to simultaneously visualize the three gustatory terminal fields in the NTS. Sodium restriction was established by feeding pregnant rats a 0.03% NaCl diet (ICN Biomedicals, Aurora, OH) and distilled water ad libitum from three days postconception through weaning at 21 days postnatal. Once pups born to these mothers were weaned, they were maintained on the same dietary regimen through adulthood. Control rats were the offspring of dams maintained on the standard 1% NaCl rat chow and tap water ad libitum. Control pups were then weaned to the standard diet at 21 days postnatal.

Triple Fluorescent Anterograde Labeling

In order to examine the arrangement of the gustatory terminal fields within the NTS, the CT, GSP, and IX nerves projecting to the right NTS were consecutively labeled with one of three anterograde neural tracers (Fig. 1). Rats were anesthetized with a 100 mg/kg injection of ketamine, i. m. Supplementary injections were given as needed, and body temperature was maintained at 36°C using a water-circulating heating pad. Upon placement in a non-traumatic head holder (Erickson, 1966), a ventral approach, modified from Sollars and Hill (2000), was taken to expose the GSP and CT nerves in the right tympanic bulla. A longitudinal incision in the ventro-medial portion of the neck was

made and the masseter muscle and the posterior belly of the digastricus muscle were retracted. A small hole was made in the ventral aspect of the tympanic bulla to gain access to the CT and the GSP. First the GSP and then the CT nerve was cut and labeled near the geniculate ganglia. After a brief application (approximately 20 seconds) of dimethyl sulfoxide (DMSO), crystals of 3 kD Biotinylated Dextran Amine (Molecular Probes, Inc., Eugene, OR) and 3 kD Tetramethylrhodamine Dextran Amine (Molecular Probes) were carefully placed on the proximal cut ends of the GSP and CT, respectively (Fig. 1). Petroleum jelly was applied over the cut ends of each nerve to hold dye crystals in place, and a piece of parafilm was placed over the opening created in the tympanic bulla. Next, the IX nerve was approached in the ventral side of the neck medial to the tympanic bulla. The nerve was cut and the proximal stump was teased onto a section of parafilm. Crystals of 3 kD Cascade Blue Dextran Amine (Molecular Probes) were applied to the proximal cut end after a short application of DMSO (Fig. 1). Petroleum jelly and a layer of parafilm were placed on top of the nerve to secure dye placement. The incision was then sutured, and the rat remained on the heating pad until it recovered from the anesthetic. The optimal time for transport of the three neural tracers was determined through pilot data to be approximately 24 hours. Rats were sacrificed after 24 hours and were perfused transcardially with Krebs (pH 7.3) followed by 8% paraformaldehyde (pH 7.0).

Tissue preparation

Brains were removed and postfixed in 8% paraformaldehyde overnight. After removal of the cerebellum, the medulla was blocked and sectioned on a vibratome

horizontally at 50 μm through the entire NTS. This allowed visualization of the entire rostral-caudal and medial-lateral extent of the terminal fields (Davis, 1988; Whitehead, 1988; Lasiter et al., 1989). Tissue sections were collected in 0.1 mM phosphate buffered saline (PBS; pH 7.4) and remained free floating at room temperature throughout the remainder of the tissue preparation. Sections were incubated for 1 hour in 0.2% Triton X in PBS with a mixture of Streptavidin Alexa Fluor 488 (Molecular Probes) at 1:500 to visualize GSP terminals labeled with Biotinylated Dextran Amine and rabbit Anti-Cascade Blue (Molecular Probes) at 1:500 to ultimately enable visualization of IX terminals labeled with Cascade Blue (Fig. 1). Sections were rinsed in PBS and subsequently incubated for 30 minutes in 0.2% Triton X and goat anti-rabbit Cy5 (Jackson ImmunoResearch Laboratories, Inc., West Grove, PA) at 1:500 to visualize IX terminals (Fig. 1). Sections were rinsed again in PBS and stored at 4° C until imaged. These fluorescent dyes were selected specifically for their particular emission wavelengths to avoid crossover of visible fluorescence. That is, each fluorochrome used had a distinct enough range of excitation that did not overlap significantly with the emission curves of the other two dyes, allowing visualization of each field with a confocal laser microscope.

Confocal Microscopy and Data Collection

Terminal fields were imaged using an Olympus IX70 inverted microscope equipped with an argon-ion laser that excites at 488 nm and emits in the blue spectral range (used to visualize the GSP terminal field), a helium-neon laser that excites at 543 nm and emits in the green spectral range (used to visualize the CT terminal field), and a

helium-neon laser that excites at 633 nm and emits in the red spectral range (used to visualize the IX terminal field; Fig. 1). The system was run with FluoView 3.3 software (Olympus America Inc., Melville, NY). Each 50 μm section containing terminal field label was mounted between coverslips with a 9:1 mixture of glycerol and PBS, and optical images were captured every 3 μm for a total of approximately 17 images per section. Initially, for each 50 μm physical section, the GSP and CT fields were imaged with sequential passes of the blue and green lasers and collected as separate channels (Figs. 2A, B, D, E). Then, using the same parameters set for the initial scan, the IX field was imaged with the red laser and saved as a third channel (Figs. 2C, F). Finally, using FluoView, all three channels were merged to create a composite view (Fig. 3).

Terminal field volume and corresponding volumes of overlap among all three terminal fields and between individual terminal fields (Fig. 3) were quantified using Neurolucida software version 4.34 (MicroBrightField, Inc., Colchester, VT). Briefly, the perimeter of each labeled terminal field and the overlap among these fields was outlined and the area was calculated for each 3 μm optical section. Subsequently, the volume of each 50 μm physical section was calculated by summing the areas of each optical section and multiplying by 3 μm, the thickness between optical sections. Total terminal field volumes and volumes of overlap with other fields were determined by summing the volumes of each 50 μm section. For figure plates, Fireworks (Macromedia, Inc., San Francisco, CA) and Photoshop (Adobe Systems, San Jose, CA) were used to compose images. Digital images were only enhanced by contrast and brightness.

Control Measures

A variety of control measures were taken to verify that each fluorescent tracer labeled only the intended nerve. First, the geniculate ganglion, which contain cells whose axons comprise either the GSP or the CT nerve (never both; Fig. 1), were removed from three triple-labeled control and three sodium-restricted rats, sectioned on a cryostat, reacted as described above, and examined with the confocal laser microscope for the presence of double labeling. Since the tracer was applied peripheral to the ganglia these cells were labeled as well. Therefore, double-labeled geniculate ganglion cells would indicate a contamination of one nerve label with the other label carried out in the bulla (e.g., contamination of the GSP label with the CT label). In all cases, no double-labeled ganglion cells were observed. The labeling site of the IX nerve was distant from the tympanic bulla; therefore, petrosal ganglia were not examined.

Secondly, in addition to labeling afferent fibers that terminate in the NTS, each fluorescent tracer is effective in retrogradely labeling the respective salivatory nucleus cells (Contreras et al., 1980). These cells can be seen closely apposed medially to the intermediate and ventral zones of the NTS (Figs. 3B, C, D, G, H) and send outputs through only one nerve. We examined these retrogradely labeled cells for the presence of single or multiple fluorescent labels in every animal in which terminal field data were collected. Again, double-labeled cells indicates that a single tracer would inadvertently label more than one nerve. Upon every observation of the labeled terminal fields, the retrogradely labeled salivatory neurons never contained a double label.

NTS volume

To gain a perspective of the extent of terminal field distributions within the solitary nucleus, a myelin stain was used to determine total NTS volume. A separate group of adult control (n=4) and sodium-restricted (n=4) rats aged 40-60 days were perfused and brains were sectioned horizontally at 25 μm on a vibratome as described above. Sections were mounted on slides, delipidated in a graded series of alcohol and chloroform, and stained using a mixture of chromoxane cyanine R and 0.21M ferric chloride (Kiernan, 1984). With the exception of the solitary tract, the NTS is a myelin-poor area whose surrounding structures are myelin-rich. The darkly stained myelin allows the boundary of the NTS to be visualized throughout its dorsal-ventral extent (Fig. 4). To quantify NTS volumes, the visible perimeter of the right NTS was outlined in each section and the corresponding areas were calculated using Neurolucida software. Total volume of the right NTS was determined by summing the areas of each section that contained terminal field (~ 22) and multiplying by 25 μm (the thickness of each section).

Ganglion Cell Quantification

In order to determine the effects of sodium-restriction on the survival of primary taste neurons, a separate group of control (n=10) and sodium-restricted (n=10) rats were used to count individual cell numbers in the geniculate and petrosal ganglia. The CT, GSP, and IX nerves were each labeled individually in separate rats as described above, except, Microruby (Molecular Probes) was used as the anterograde tracer. Microruby was used over other tracers because of its superior quality in labeling cells and imaging whole ganglia. Each rat was perfused as described above. Ganglia were removed and postfixed in 8% paraformaldehyde overnight. Each ganglia was then dissected from

either the VII or IX nerve and the intact ganglia was imaged on the confocal microscope at 2 μm intervals using the green laser, generating an average of 50 optical sections through each ganglia. All labeled neurons were physically counted with the aid of Neurolucida software.

Statistical Analysis

Mean total terminal field volume for each nerve and terminal field overlap volumes among nerves were compared statistically between control and sodium restricted adults by analysis of variance (ANOVA). Mean volumes of dorsal, intermediate, and ventral portions (see Results for definitions of these zones) were also calculated, compared between control and sodium-restricted rats, and analyzed using ANOVA. In addition, ANOVAs were used to analyze statistical differences in NTS volumes and total ganglion cell numbers between control and sodium-restricted rats. All values are expressed as mean ± standard error. Statistical results with an alpha level less than 0.05 were reported as significant.

RESULTS

Total Terminal Field Volumes

Controls

Figure 5 shows the mean total volumes of terminal fields for the GSP, CT, and IX nerves. In control rats, the GSP terminations occupied the largest proportion of the NTS with a mean (± SEM) total terminal field volume of 77.3 (± 11.9) × 10^6 μm^3. Total mean CT terminal field volume was 31.0 (± 3.0) × 10^6 μm^3 and IX terminals occupied a mean volume of 67.2 (± 14.5) × 10^6 μm^3. In controls, GSP terminations began more dorsal

than did CT terminals and GSP terminal fields extended more ventral than the CT (Figs. 3A-D). IX projections terminated even more dorsally than GSP and extended ventrally to the dorsal-most portion of CT field (Figs. 3A, B), with the densest portions occupying the medial NTS. Therefore, the sequence of terminal fields in the control NTS in order of terminations from dorsal to ventral was IX, GSP, and then CT.

These three individual fields overlapped extensively with each other. CT and GSP fields overlapped widely within the rostral pole of the NTS (Figs. 3B-D) with a mean (± SEM) overlap volume of 27.2 (± 2.0) × 10^6 μm^3 (Fig. 5). This represents approximately 88% of the CT field overlapping with the GSP field. A greater absolute amount of overlap occurred between GSP and IX fields (41.8 (± 8.6) × 10^6 μm^3) than for CT and IX fields (8.6 (± 2.4) × 10^6 μm^3; Fig. 5); however, the percentage of overlap that the GSP field had with the IX field and the percentage of overlap the CT field had with the IX field were not as extensive as was the percentage of overlap between the CT and the GSP fields (62% for GSP and IX overlap and 28% between CT and IX). The ventral-most extension of the IX field did not extend much beyond the dorsal-most boundary of the CT field, whereas the dorsal-most boundary of the GSP field invaded the ventral portion of the IX terminal field (Figs. 3A-B). The total mean volume for the overlap among all three fields was 8.5 (± 2.3) × 10^6 μm^3 (Fig. 5). This overlap was essentially the amount found for the CT field overlap with the GSP (Fig. 5).

Sodium-restricted Rats

Developmental dietary sodium restriction resulted in profound alterations in the topography and distribution of gustatory terminal fields. Early dietary sodium restriction

resulted in a significantly enlarged mean (± SEM) CT field (53.6 (± 6.7) × 10^6 μm^3) compared to controls (P = 0.005; Fig. 5). This nearly 2X enlargement occurred in the dorsal-most portion of the CT terminal field, as it expanded caudally into the territories of the GSP and IX fields (Figs. 2E, 3F). The GSP terminal field in sodium-restricted rats was similar to controls (70.7 (± 7.0) × 10^6 μm^3; P = 0.7; Fig. 5). Finally, the total IX field volume was over 2X greater than controls (140.9 (± 17.5) × 10^6 μm^3; P = 0.01; Fig. 5). The IX field extended dorsally, ventrally, caudally, and laterally, well past the control IX field (Figs. 3E-H).

The amount of overlap occurring among fields was also different than in controls. As the CT and IX terminal fields increased in size, they expanded beyond the areas normally occupied in controls. Indeed, the volume of the mean (± SEM) CT-GSP field overlap was significantly greater than in controls (46.0 (± 5.6) × 10^6 μm^3; P = 0.004; Fig. 5). Furthermore, the increase in overlapping volume was proportionate to the increase in volume of the CT field in sodium-restricted animals and did not differ between groups (88% vs. 86% of the CT field overlapped with the GSP field in controls and restricted rats, respectively). The overlap between the CT and IX fields also significantly increased with the dietary manipulation (35.8 (± 7.7) × 10^6 μm^3; P = 0.007; Fig. 5), and was reflected in a larger proportion of the CT field overlapping with the IX field (28% vs. 67%). However, there were no group-related differences in the IX-GSP field overlap (57.6 (± 10.7) × 10^6 μm^3; P = 0.3; Fig. 5), although the percent of GSP field contained within the IX field was slightly larger in restricted rats (62% vs. 82%). This indicates that the CT and IX fields extended past territory occupied in controls, into neighboring

terminal fields. Finally, there was a significant increase in the volume in which all three terminal fields were common (36.7 (± 8.1) × 10^6 μm^3; P = 0.007; Fig. 5), again due primarily to the increased size of the CT field.

Zonal Distribution of Terminal Fields

In order to localize regions especially susceptible to the dietary effects of plasticity and to be consistent with our previous studies of CT terminal field in the NTS (King and Hill, 1991; Krimm and Hill, 1997), the NTS was divided into dorsal, intermediate, and ventral zones based on the characteristics of the chorda tympani terminal field. The dorsal zone, the largest of the three zones, encompassed almost the entire IX terminal field. In controls, this field typically ranged in size from 200-250 μm, included the presence of the solitary tract at the lateral edge, and was distinguished by the rounded shape of the CT terminal field (Figs. 2B & 3B). The next 100 μm of tissue was designated the intermediate zone. Here the CT terminal field appeared more oval in shape (Fig. 3C). The final 100-200 μm of tissue was defined as the ventral zone and contained a much smaller and more compact CT terminal field (Fig. 3D). Dividing the fields in this manner highlights the vastly different distribution of terminations along the dorsal-ventral aspect of the NTS and more narrowly defines specific regions of anatomical change. Compartmentalizing terminal fields into zones also demonstrates the similar characteristics and contiguous and overlapping arrangement of the three afferent terminal zones

Dorsal Zone Terminal Field Volume

The dorsal zone of the NTS underwent the most substantial plasticity compared to other regions of the NTS. Consistent with previous findings (King and Hill, 1991; Krimm and Hill, 1997), the mean (± SEM) volume of the CT field was over twice as large in the sodium-restricted animals (32.0 (± 5.9) × 10^6 μm^3) compared to controls (15.6 (± 2.0) × 10^6 μm^3; $P = 0.02$; Fig. 6A). The labeled fibers in restricted rats appeared more densely packed and extended more caudally than in controls (Figs. 2B, E, 3A-B, E-F). The corresponding portion of the GSP field was not significantly different between groups (restricted: 57.4 (± 10.7) × 10^6 μm^3 v. control: 72.0 (± 13.5) × 10^6 μm^3; $P = 0.4$; Figs. 2A, D; 6A). However, the volume of the IX field underwent a significant expansion in sodium-restricted rats compared to controls (131.8 (± 20.0) × 10^6 μm^3 v. 67.0 (± 14.3) × 10^6 μm^3; $P = 0.03$; Fig. 6A). The expansion of the IX field in the dorsal region extended further lateral, caudal, and ventral than in control animals (Figs. 2C, F; 3A, B, E, F).

Such differences in the patterns of gustatory terminations in the dorsal NTS were also reflected in the proportions of the overlapping fields. The dorsal CT field overlapped completely within the GSP field, and this volume of overlap was significantly greater in restricted rats compared to controls (28.3 (± 5.6) × 10^6 μm^3 v. 14.9 (± 2.0) × 10^6 μm^3; $P = 0.04$; Figs. 3B, F; 6A). In fact, the increase in overlap between the two fields was directly related to the increase in volume of the CT field, since the overlap increased proportionally to the increase in CT terminal field size. There was also a significant increase in the overlap between the CT and IX fields when comparing restricted to control rats (28.7 (± 5.2) × 10^6 μm^3 v. 8.6 (± 2.4) × 10^6 μm^3; $P = 0.007$;

Figs. 3B, F; 6A). This increase was also due to the expansion of both the CT and IX fields past their normal boundaries. However, there was no significant difference in the volume of the overlapping regions of the GSP and IX fields (restricted: 49.9 (± 9.2) × 10^6 μm^3 v. control: 41.7 (± 8.5) × 10^6 μm^3; $P = 0.5$; Figs. 3B, F; 6A). Finally, the volume of the region in which of all three terminal fields overlapped also increased significantly (restricted: 28.2 (± 5.6) × 10^6 μm^3 v. control: 8.4 (± 2.3) × 10^6 μm^3; $P = 0.009$; Figs. 3B, F; 6A).

Intermediate Zone Terminal Field Volume

A different pattern of terminal field organization between groups was also evident in the intermediate zone of the NTS. Here, the CT terminal fields in both groups had a more compact oval configuration than in dorsal regions (Figs. 3C, G). In the intermediate zone, the volume of CT terminal field label in restricted animals was not significantly different from controls (12.7 (± 1.0) × 10^6 μm^3 v. 9.4 (± 1.1) × 10^6 μm^3; $P = 0.07$; Fig. 6B). Furthermore, the GSP field volumes in this zone were also similar between groups (restricted: 17.4 (± 2.4) × 10^6 μm^3 v. control: 17.5 (± 1.1) × 10^6 μm^3; $P = 0.9$; Fig. 6B). However, the IX field in sodium-restricted rats showed robust expansion into the intermediate portion of the NTS, extending ventrally beyond the boundaries of the control field; in controls, the IX field was not present in the intermediate NTS (Figs. 3C, G). Specifically, sodium restriction yielded a 40-fold increase in volume compared to controls (7.4 (± 3.0) × 10^6 μm^3 v. 0.2 (± 0.2) × 10^6 μm^3 $P = 0.03$; Fig. 6B).

Despite no significant changes in the total volume of CT and GSP terminal fields in the intermediate NTS, there was a significant increase in the volume of overlap

between the GSP and CT fields in restricted rats compared to controls (11.1 (± 0.6) × 10^6 μm^3 v. 8.7 (± 0.7) × 10^6 μm^3; $P = 0.04$; Figs. 3C, G; 6B). Additionally, both the volume of the overlapping field between the CT and IX fields and between the GSP and IX fields in restricted rats increased proportionally with an increase in the IX terminal field volume (CT-IX restricted: 5.6 (± 2.5) × 10^6 μm^3 v. control: 0.004 (± 0.004) × 10^6 μm^3; $P = 0.04$) (IX-GSP restricted: 6.1 (± 2.7) × 10^6 μm^3 v. control: 0.1 (± 0.1) × 10^6 μm^3; $P = 0.04$; Fig. 6B). Thus, in restricted rats, the IX terminal field in the intermediate zone of the NTS intersected with both the GSP and CT terminal fields. This is also evident in the significantly increased volume of the overlapping portion of all three terminals fields (restricted: 7.0 (± 2.8) × 10^6 μm^3 v. control: 0.004 (± 0.004) × 10^6 μm^3; $P = 0.03$; Figs. 3C, G; 6B)

Ventral Zone Terminal Field Volume

The ventral portion of the NTS contained the least volume of gustatory terminal fields. Both CT and GSP terminal fields were sparse and were not reliably different between diet conditions ($P = 0.07$ and $P = 0.05$, respectively; Fig. 6C). In two of the nine sodium-restricted rats, a small portion of the IX field extended into the ventral NTS; this extension occurred in none of the control rats (Figs. 3D, H). However, there was not a significant difference in the volume of the IX field in sodium-restricted rats compared to controls ($P = 0.2$; Fig. 6C).

In addition, the terminal field volume overlap between CT-IX and IX-GSP were not significantly different between groups ($P = 0.2$ and $P = 0.2$, respectively; Fig. 6C). However, there was a significant increase in the overlap of the GSP and CT terminal

fields in sodium-restricted rats compared to controls ($P = 0.04$; Figs. 3D, H; 6C). Finally, the overlap among all three terminal fields was not significantly different ($P = 0.2$; Fig. 6C).

In summary, the three gustatory terminal fields in control rats were arranged in an ordered, yet overlapping, fashion such that IX terminals began most dorsally and spread rostrally, caudally, laterally and ventrally into the GSP terminal field. As the IX field reached its ventral-most extent, the CT field began and overlapped almost completely with the GSP terminal field. The GSP field began more dorsally than the CT field, but both the GSP and CT fields extended to the same ventral boundary of the NTS. Sodium restriction dramatically altered the topography of the CT and IX terminal fields of the NTS, without affecting the distribution of the GSP terminal field. For the CT terminal field, this plasticity was most evident in the dorsal portion of the CT field. The effects on the IXth terminal field were more widespread, whereby IX fields extended further dorsally, ventrally, caudally and laterally throughout the NTS. The three terminal fields overlapped more extensively in sodium-restricted compared to control rats, indicating that all three gustatory nerves converge onto larger areas in the NTS of restricted than in controls.

Total NTS volume

Since sodium-restricted rats are much smaller than controls at adulthood (Hill et al., 1986), we measured the total NTS volume in sodium-restricted and control rats to examine the relative size of the terminal fields within the NTS. The mean total volume of the right NTS was 10.2 ($\pm$ 0.5) $\times$ 10^8 μm^3 in control and 7.2 ($\pm$ 0.2) $\times$ 10^8 μm^3 in

restricted rats. This represented a significant 29.2% decrease in total volume of NTS in sodium-restricted rats compared to controls (P = 0.001; Fig. 7A). These totals were consistent with the total NTS volumes reported by King and Hill (1991). When individual nerve terminal field volumes were standardized to their respective NTS volumes, the group-related differences were magnified. The CT and IX terminal fields and their respective overlapping portions occupied a significantly larger percentage of the nucleus relative to controls while the GSP terminal field did not differ significantly between groups. The CT terminal field occupied 7.4% of the total NTS in sodium-restricted rats compared to 3% of the NTS in control rats (P = 0.0001; Fig. 7B). The IX terminal field occupied 19.5% of the total NTS in sodium-restricted rats compared to 6.6% of the NTS in control rats (P = 0.002; Fig. 7B). The GSP terminal field occupied 9.8% of the total NTS in sodium-restricted rats compared to 7.6% of the NTS in control rats (P = 0.2; Fig. 7B). The corresponding overlap between the individual fields and among all three fields also increased significantly (GSP-CT, P = 0.0001; CT-IX, P = 0.004; IX-GSP, P = 0.04; Fig. 7B). Therefore, the differences in the larger absolute volumes for the CT and IX fields in sodium-restricted rats compared to controls were exaggerated when expressed relative to the smaller NTS.

Ganglion cell number

Ganglion cell numbers were counted to address the hypothesis that the increase in terminal field volumes in sodium-restricted rats was due to an increased number of primary afferents terminating in the NTS. That is, a diet-related increase in neuron number may result in an increase in the volume of afferent projections to the NTS.

However, sodium restriction did not alter total number of ganglion cells for any of the three taste nerves. Figure 8 shows that there were no significant differences between control and sodium-restricted ganglion cell numbers for the CT (P = 0.1), GSP (P = 0.07), or IX nerves (P = 0.9).

DISCUSSION

Through the use of a novel triple fluorescent labeling procedure, this study demonstrated specific and dramatic plastic anatomical changes in afferent terminal fields in the gustatory medulla. The total volume of the CT and IX nerve terminal fields were expanded at least two times their normal size in developmentally sodium-restricted rats, while the GSP was unaffected by the dietary manipulation. Moreover, the change in terminal field volumes impacted the way nerves project into the NTS and overlapped with other fields. These effects were even more dramatic when considering that the total volume of the NTS in restricted rats was smaller than in controls. Furthermore, this plasticity could not be accounted for by sheer increases in innervating afferent fibers because sodium restriction did not alter the survival of geniculate or petrosal ganglion cells.

A clear advantage of our triple labeling approach is that, for the first time, the relative relationships among the terminal fields of three distinct gustatory nerves could be examined in the medulla of controls and experimental animals. Figure 9 depicts this organization in both control and sodium-restricted rats. In control rats, the IX terminates dorsal to the other two terminal fields and projects ventrally to overlap with the dorsal portion of the GSP field. The IX field extends more rostrally at the dorsal GSP zone and

terminates more laterally in the NTS than was previously reported (Hamilton and Norgren, 1984). The ventral portion of the IX field abuts the dorsal-most portion of the CT field. CT and GSP fields nearly overlap completely within the rostral pole of the NTS. Contrary to previous results, the coextensive CT and GSP fields within the rostral NTS not only occupy the lateral portions of the NTS, but both extend medially as well (Hamilton and Norgren, 1984). Importantly, there is a relatively small region where all three nerves terminate.

In sodium-restricted rats, the dorsal portion of the CT terminal field expands caudally outside its normal boundaries into GSP and IX field territory. The IX field extends dorsally, caudally, laterally, and ventrally, well past the apparent boundary of control IX field. Consequently, the overlap occurring among adjacent fields also increases.

Comparisons with previous studies

Consistent with King and Hill (1991) and Krimm and Hill (1997), we found anatomical changes induced by early dietary sodium restriction in the dorsal portion of the CT terminal field. It is within this zone where changes in terminal fields are also affected developmentally by limited taste experience (Lasiter and Diaz, 1992; Lasiter, 1995), taste receptor cell damage (Lasiter and Kachele, 1990), and high salt diets (Pittman and Contreras, 2002). Thus, a variety of experimental procedures show this zone to be especially susceptible to environmental alterations.

However, our triple label experiments show that plasticity is not exclusive to the CT terminal field as previously demonstrated (King and Hill, 1991), but also includes the

IX terminal field. Furthermore, in contrast to previous reports that dietary sodium restriction does not change the absolute volume of the CT terminal field but changes the distribution of the terminal field in the NTS (King and Hill, 1991), we found that the dietary manipulation also increases the absolute CT terminal field volume. We believe these differences are partially due to the relatively high sensitivity of labeling terminal fields with fluorescent tracers and to viewing fields with a confocal laser microscope.

Speculations on plasticity mechanisms

Since sodium taste elicited activity is a major component of the electrophysiological response of the CT nerve, hypotheses that center around CT activity shaping terminal field development have been attractive. Indeed, dietary NaCl restriction during early development produces a selective reduction in the taste response of the CT nerve to sodium salts but not to other taste stimuli (Hill, 1987; Hill and Przekop, 1988). Our data indicate, however, that terminal field plasticity is no longer unique to the CT field. In fact, compared to the CT, sodium restriction produces much more dramatic changes in the terminal field of the IX. However, the sensitivity of the IX nerve taste responses to sodium salts is insubstantial compared to responses of the CT nerve (Formaker and Hill, 1991; Kitada et al., 1998). Furthermore, the processes that determine the abnormal terminal fields in the NTS induced by dietary sodium restriction appear to be accomplished before taste receptor cells are present on the tongue. Restricting maternal dietary sodium during only a brief critical period from E3-E12 is sufficient to cause an enlarged CT terminal field (Krimm and Hill, 1997). Thus, the parameters allowing plasticity to occur are established well before sodium taste stimuli are

transduced through functional taste receptor cells, suggesting that an activity-dependent mechanism may not be the only explanation for alterations in terminal field development as a result of sodium restriction. Dietary sodium restriction must influence gustatory nerve terminal field development by additional, non-activity dependent mechanisms as well.

Prenatal dietary manipulations have a range of physiological consequences that extend beyond the gustatory system and may play a role in gustatory terminal field development. For example, reduction of sodium intake affects hormonal levels like aldosterone (Kifor et al., 1991; Lehoux et al., 1994) and early dietary restriction paradigms influence growth factor levels such as IGF1 (Fliesen et al., 1989). Indeed, IGF1 has significant effects on NTS development (Eustache et al., 1994; Dentremont et al., 1999). Thus, the anatomical rearrangement occurring within the NTS may not be directly related to taste function but may result from nonspecific effects of early sodium restriction. That is, the boundaries and subsequent molecules associated with boundary formation for the CT and IX field (e.g., axonal pathfinding) may be altered through early dietary sodium restriction, independent of neural activity.

Some selectivity must still be present, however, because the GSP terminal field is not affected. It is possible that the effects of early dietary manipulation may be expressed after processes that determine GSP field development are solidified. That is, the processes resulting from our dietary manipulation may exist after the GSP field is determined but before the molecular cues associated with the formation of CT and IX terminal fields are organized.

Given the development of the three terminal fields, it is possible that the GSP field may shape the formation of other gustatory fields in the NTS, especially the CT. Facial nerve axons, which include both CT and GSP, terminate in the rostral NTS at P1 and develop to approximately P25 (Lasiter, 1992). IX fibers enter the NTS around P10 and develop to approximately P45 (Lasiter, 1992). This chronological pattern of innervation and terminal field formation in the NTS occurs in conjunction with the morphological development of gustatory receptors. The maturation of palatal taste receptor cells precedes that of fungiform and circumvallate taste receptor cells (Harada et al., 2000). Furthermore, preliminary data from our lab indicate a significant GSP field development by P10, whereas CT field development is immature at this age (S. I. Sollars & D. L. Hill, unpublished observations). Given this sequence of individual terminal field development, we propose that the GSP terminations arrive first in the NTS and establish their boundaries before the effects of the plasticity-inducing diet are realized. As the GSP terminal field becomes established, the CT terminal field termination pattern is subject to the milieu organized by the pioneering GSP field. Indeed, the restricted CT terminal field pattern mirrors that of the GSP nerve, as they overlap almost entirely within the rostral pole of the NTS. As an aside, this would predict that disruption in GSP field development would correspondingly disrupt CT field development. Finally, the IX fibers, perhaps due to influences from other nerves, expand to where the boundary cues are apparently grossly disrupted.

Potential functional and behavioral effects

As a result of the disruption of individual terminal field boundaries, gustatory afferents from the three nerves likely converge anatomically more onto NTS neurons than in controls. Such convergence may have a corresponding functional basis. In addition to the selective decrease in taste responses from NTS neurons driven by stimulation of the anterior tongue in sodium-restricted rats (i.e., CT stimulation; Vogt and Hill, 1993), functional alterations may also be evident in NTS neurons receiving unique combinations of two or three afferent inputs. Our data indicate NTS neurons in sodium-restricted rats would likely receive inputs from receptive fields not normally found in controls (Travers et al., 1986). As a corollary to the unusual synaptic inputs in restricted rats, the morphology of NTS neurons and associated synaptic structures would also likely be affected. Indeed, gross changes in dendritic length and number occur in sodium-restricted rats (King and Hill, 1993). This potential anatomical and functional convergence may also be reflected behaviorally by altering taste-related behaviors, including sodium appetite. Therefore, the striking alterations occurring in the NTS both pre- and postsynaptically as a result of developmental dietary manipulation have important implications on central processing of taste stimuli and on behavior.

LITERATURE CITED

Buonomano DV, Merzenich MM. 1998. Cortical plasticity: from synapses to maps. Annu Rev Neurosci 21:149-186.

Catalano SM, Shatz CJ. 1998. Activity-dependent cortical target selection by thalamic axons. Science 281:559-562.

Contreras RJ, Beckstead RM, Norgren R. 1982. The central projections of the trigeminal, facial, glossopharyngeal and vagus nerves: an autoradiographic study in the rat. J Auton Nerv Syst 6:303-322.

Contreras RJ, Gomez MM, Norgren R. 1980. Central origins of cranial nerve parasympathetic neurons in the rat. J Comp Neurol 190:373-394.

Davis BJ. 1988. Computer-generated rotation analyses reveal a key three-dimensional feature of the nucleus of the solitary tract. Brain Res Bull 20:545-548.

Dentremont KD, Ye P, D'Ercole AJ, O'Kusky JR. 1999. Increased insulin-like growth factor-I (IGF-I) expression during early postnatal development differentially increases neuron number and growth in medullary nuclei of the mouse. Brain Res Dev Brain Res 114:135-141.

Erickson R. 1966. Nontraumatic headholders for mammals. Physiol Behav 1:97-98.

Eustache I, Seyfritz N, Gueritaud JP. 1994. Effects of insulin-like growth factors on organotypic cocultures of embryonic rat brainstem slices and skeletal muscle fibers. Brain Res Dev Brain Res 81:284-292.

Fliesen T, Maiter D, Gerard G, Underwood LE, Maes M, Ketelslegers JM. 1989. Reduction of serum insulin-like growth factor-I by dietary protein restriction is age dependent. Pediatr Res 26:415-419.

Formaker BK, Hill DL. 1991. Lack of amiloride sensitivity in SHR and WKY glossopharyngeal taste responses to NaCl. Physiol Behav 50:765-769.

Fox K, Wallace H, Glazewski S. 2002. Is there a thalamic component to experience-dependent cortical plasticity? Philos Trans R Soc Lond B Biol Sci 357:1709-1715.

Hamilton RB, Norgren R. 1984. Central projections of gustatory nerves in the rat. J Comp Neurol 222:560-577.

Harada S, Yamaguchi K, Kanemaru N, Kasahara Y. 2000. Maturation of taste buds on the soft palate of the postnatal rat. Physiol Behav 68:333-339.

Henderson TA, Woolsey TA, Jacquin MF. 1992. Infraorbital nerve blockade from birth does not disrupt central trigeminal pattern formation in the rat. Brain Res Dev Brain Res 66:146-152.

Hill DL. 1987. Susceptibility of the developing rat gustatory system to the physiological effects of dietary sodium deprivation. J Physiol 393:413-424.

Hill DL, Mistretta CM, Bradley RM. 1986. Effects of dietary NaCl deprivation during early development on behavioral and neurophysiological taste responses. Behav Neurosci 100:390-398.

Hill DL, Przekop PR, Jr. 1988. Influences of dietary sodium on functional taste receptor development: a sensitive period. Science 241:1826-1828.

Hubel DH, Wiesel TN. 1970. The period of susceptibility to the physiological effects of unilateral eye closure in kittens. J Physiol 206:419-436.

Katz LC, Crowley JC. 2002. Development of cortical circuits: lessons from ocular dominance columns. Nat Rev Neurosci 3:34-42.

Kiernan JA. 1984. Chromoxane cyanine R. II. Staining of animal tissues by the dye and its iron complexes. J Microsc 134 (Pt 1):25-39.

Kifor I, Moore TJ, Fallo F, Sperling E, Menachery A, Chiou CY, Williams GH. 1991. The effect of sodium intake on angiotensin content of the rat adrenal gland. Endocrinology 128:1277-1284.

King CT, Hill DL. 1991. Dietary sodium chloride deprivation throughout development selectively influences the terminal field organization of gustatory afferent fibers projecting to the rat nucleus of the solitary tract. J Comp Neurol 303:159-169.

King CT, Hill DL. 1993. Neuroanatomical alterations in the rat nucleus of the solitary tract following early maternal NaCl deprivation and subsequent NaCl repletion. J Comp Neurol 333:531-542.

Kitada Y, Mitoh Y, Hill DL. 1998. Salt taste responses of the IXth nerve in Sprague-Dawley rats: lack of sensitivity to amiloride. Physiol Behav 63:945-949.

Krimm RF, Hill DL. 1997. Early prenatal critical period for chorda tympani nerve terminal field development. J Comp Neurol 378:254-264.

Lasiter PS. 1992. Postnatal development of gustatory recipient zones within the nucleus of the solitary tract. Brain Res Bull 28:667-677.

Lasiter PS. 1995. Effects of orochemical stimulation on postnatal development of gustatory recipient zones within the nucleus of the solitary tract. Brain Res Bull 38:1-9.

Lasiter PS, Diaz J. 1992. Artificial rearing alters development of the nucleus of the solitary tract. Brain Res Bull 29:407-410.

Lasiter PS, Kachele DL. 1990. Effects of early postnatal receptor damage on development of gustatory recipient zones within the nucleus of the solitary tract. Brain Res Dev Brain Res 55:57-71.

Lasiter PS, Wong DM, Kachele DL. 1989. Postnatal development of the rostral solitary nucleus in rat: dendritic morphology and mitochondrial enzyme activity. Brain Res Bull 22:313-321.

Lehoux JG, Bird IM, Rainey WE, Tremblay A, Ducharme L. 1994. Both low sodium and high potassium intake increase the level of adrenal angiotensin-II receptor type 1, but not that of adrenocorticotropin receptor. Endocrinology 134:776-782.

Pittman DW, Contreras RJ. 2002. Dietary NaCl influences the organization of chorda tympani neurons projecting to the nucleus of the solitary tract in rats. Chem Senses 27:333-341.

Rauschecker JP. 1999. Auditory cortical plasticity: a comparison with other sensory systems. Trends Neurosci 22:74-80.

Sollars SI, Hill DL. 2000. Lack of functional and morphological susceptibility of the greater superficial petrosal nerve to developmental dietary sodium restriction. Chem Senses 25:719-727.

Travers SP, Pfaffmann C, Norgren R. 1986. Convergence of lingual and palatal gustatory neural activity in the nucleus of the solitary tract. Brain Res 365:305-320.

Vogt MB, Hill DL. 1993. Enduring alterations in neurophysiological taste responses after early dietary sodium deprivation. J Neurophysiol 69:832-841.

Whitehead MC. 1988. Neuronal architecture of the nucleus of the solitary tract in the hamster. J Comp Neurol 276:547-572.

Yan J. 2003. Canadian Association of Neuroscience Review: development and plasticity of the auditory cortex. Can J Neurol Sci 30:189-200.

FIGURE LEGENDS

Figure 1. The anatomical organization of the peripheral gustatory system and the first central synaptic relay in the nucleus of the solitary tract (NTS). The chorda tympani (CT) nerve innervates taste buds in fungiform and foliate papillae on the anterior tongue. The greater superficial petrosal (GSP) nerve innervates taste buds in the nasoincisor duct, the geschmacksstreifen (GS), and the soft palate. Both nerves comprise the VIIth cranial nerve and have cell bodies in the geniculate ganglia. The glossopharyngeal (IX) nerve innervates taste buds in foliate and circumvallate papillae on the posterior tongue, and has cell bodies in the petrosal ganglia. All three nerves terminate bilaterally in the NTS; the glossopharyngeal nerve is shown on the left side only for illustrative purposes. The respective fluorescent markers used to detect each terminal field are noted in parentheses. See methods for a detailed description.

Figure 2. Fluorescent photomicrographs of separated channels of the GSP (green: A, D), CT (red: B, E), and IX (blue: C, F) terminal fields in the dorsal zone of NTS (perimeter marked by dotted line) in control (A-C) and sodium-restricted (D-F) rats. Note the enlarged appearance of the CT and IX terminal fields in sodium-restricted rats compared to controls. See figure 3B, F for corresponding merged images of these separate channels. R, rostral; L, lateral. Scale bar in A equals 100 μm.

Figure 3. Composite, fluorescent photomicrographs comparing the triple labeled terminal fields in horizontal sections of the NTS (perimeter marked by dotted line) in control (A-D) and sodium-restricted (E-H) rats. The CT and IX terminal fields in the dorsal zone of restricted rats (E & F) are more expansive than controls (A & B). In the

intermediate zone, the appearance of terminal fields in sodium-restricted rats (G) is also different from controls (C). Often, the IX terminal field in restricted rats extends into the ventral zone (H); however, this does not occur in controls (D). Retrogradely labeled salivatory nuclei are indicated by arrows (B-D, G & H). Refer to the color key in A to identify individual fields and respective overlap among different terminal fields. R, rostral; L, lateral. Scale bar in E equals 100 μm.

Figure 4. Horizontal section through the rat medulla stained for myelin allowing visualization of the bilateral NTS, which flanks the IVth ventricle. Note the heavily myelinated solitary tract (arrows) coursing from rostral to caudal through the lateral portion of the nucleus. The perimeter of the right lateral half of the NTS, shown by a dashed line, was traced to determine volume. R, rostral; L, lateral. Scale bar equals 500 μm.

Figure 5. Mean (± SEM) total terminal field volumes of the GSP, CT, and IX nerves and corresponding overlap (e.g., GSP-CT) in the NTS of control (solid bars) and sodium-restricted (open bars) rats. In restricted rats, the CT and IX fields are larger than that of controls. This expansion results in corresponding increases in the overlap among terminal fields. GSP field size does not change. Asterisks indicate $p < 0.05$.

Figure 6. Zonal distribution of mean (± SEM) terminal field volumes of the GSP, CT, and IX nerves and corresponding overlap in the NTS of control (solid bars) and restricted (open bars) rats. **A.** Dorsal zone. The largest proportion of the respective terminal fields is contained in the dorsal zone. Also, the greatest increases in terminal field volume occur in this zone in restricted rats compared to controls. **B.** Intermediate

zone. Terminal field volumes are distributed differently in this zone compared to others. Dietary manipulation affects only the IX field and resulting overlap of the IX field with CT and GSP. **C.** Ventral zone. This zone contains the least volume of terminal fields. The significance in CT-GSP overlap in restricted rats is attributed to a difference in how the GSP and CT fields are distributed within the NTS. Asterisks indicate $p < 0.05$.

Figure 7. A. Total mean volume of the right half of the NTS in control (solid bars) and restricted (open bars) rats. The NTS volume of restricted rats is significantly smaller than controls. **B.** Mean volume of GSP, CT, and IX terminal fields and their respective overlapping portions normalized to total NTS volume in control (solid bars) and restricted (open bars) rats. A greater proportion of the NTS is occupied by overlapping terminal fields in restricted rats compared to controls. Error bars denote SEM; asterisks indicate $p < 0.05$.

Figure 8. Mean ($\pm$ SEM) number of geniculate (GSP, CT) and petrosal (IX) ganglion cells in control (solid bars) and restricted (open bars) rats. The number of cells in each respective ganglia are similar in control and restricted rats. Note: petrosal ganglia contain 3X more cells than geniculate ganglia.

Figure 9. Model of terminal field organization through the dorsal-ventral extent of horizontal sections from the right NTS in control and restricted rats. Overlapping fields are represented at four levels along the dorsal-ventral axis. See results for details of the overlap among the three fields and a comparison of diet-related differences. Refer to color key to identify individual fields and respective overlap among different terminal fields.

FIGURE 1.

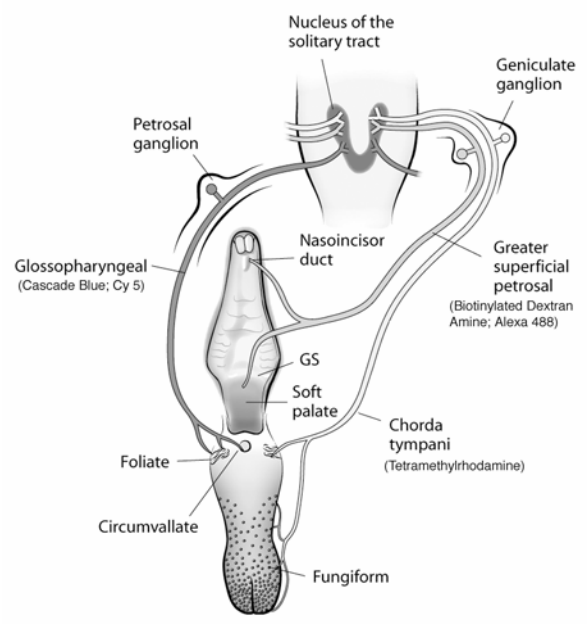

FIGURE 2.

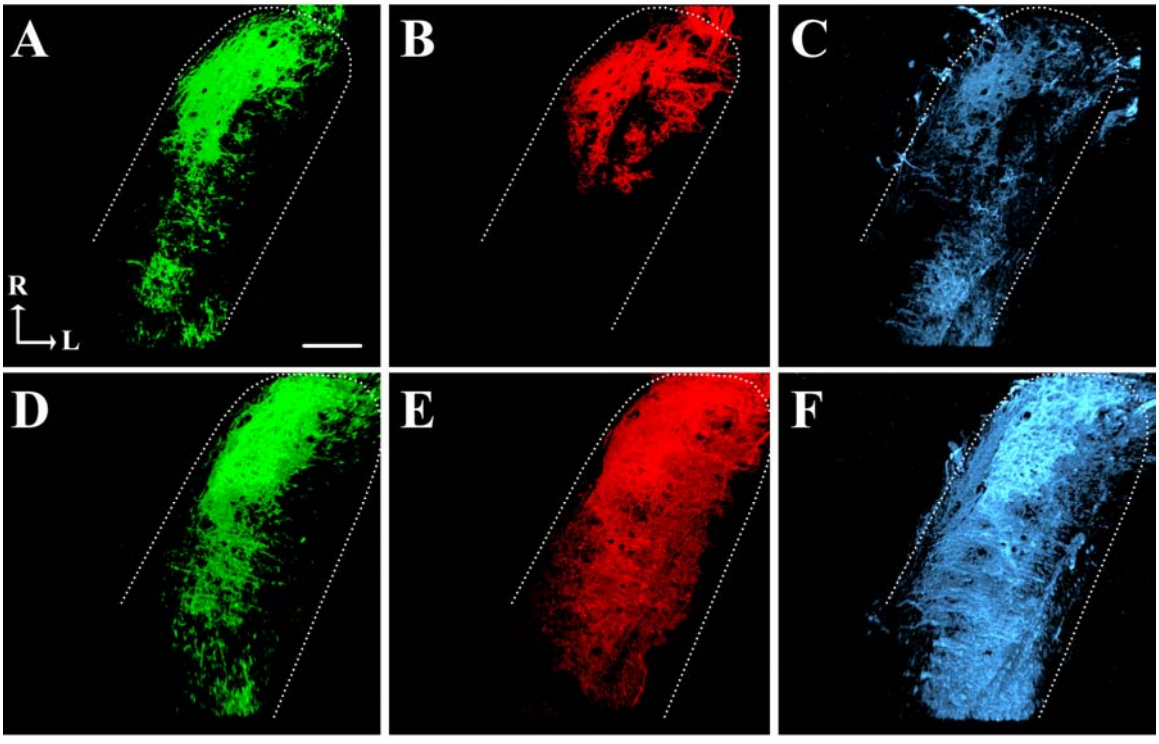

FIGURE 3.

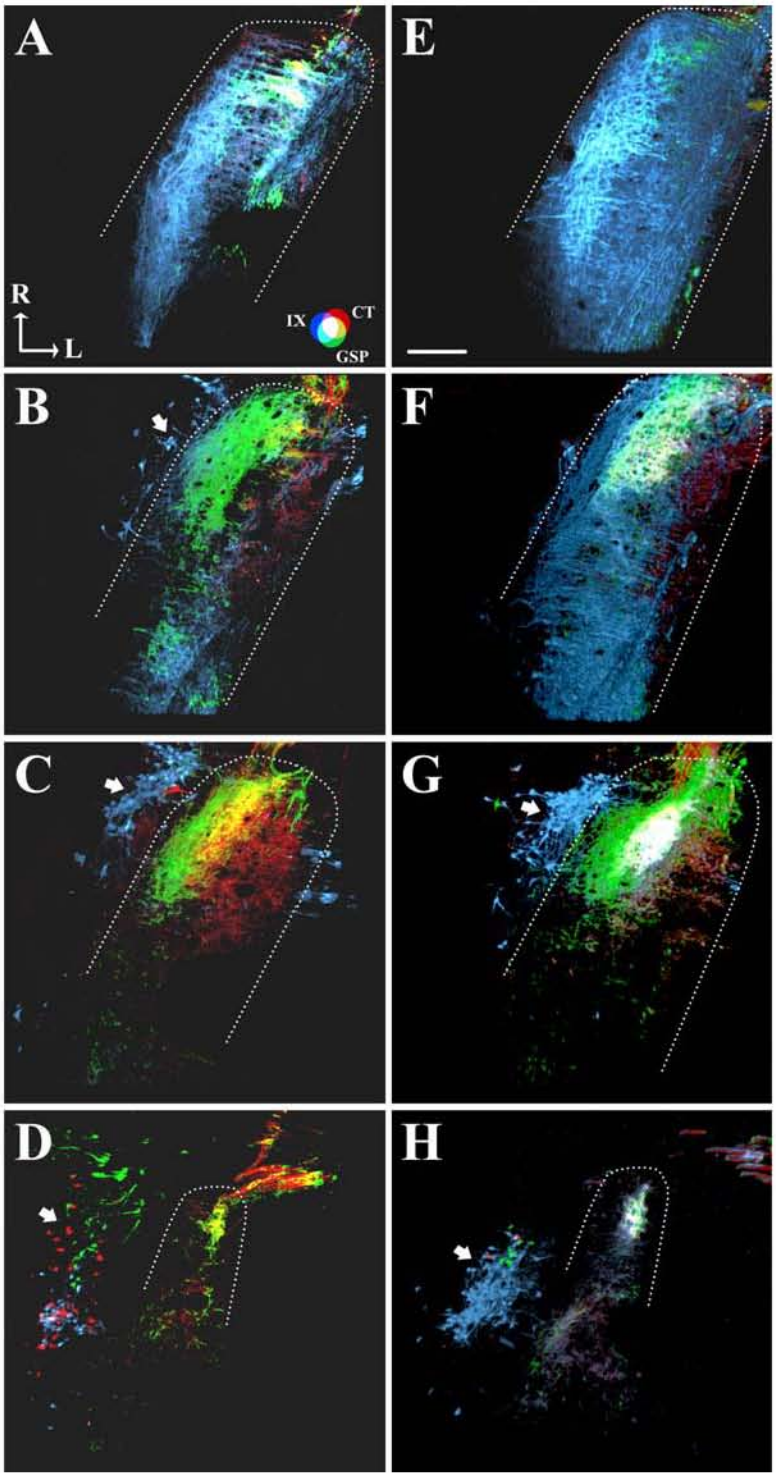

FIGURE 4.

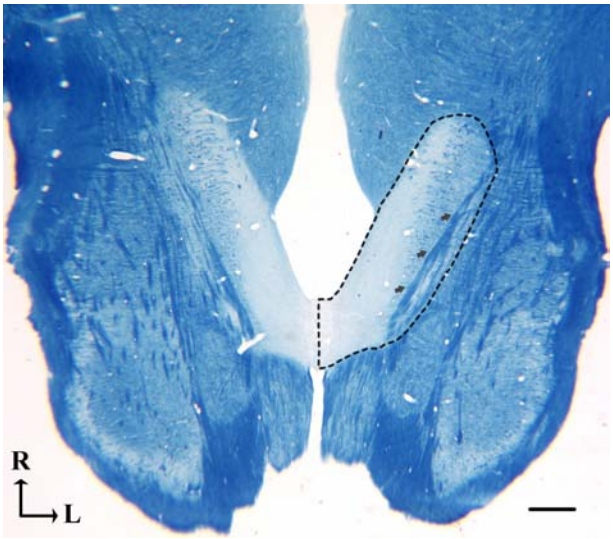

FIGURE 5.

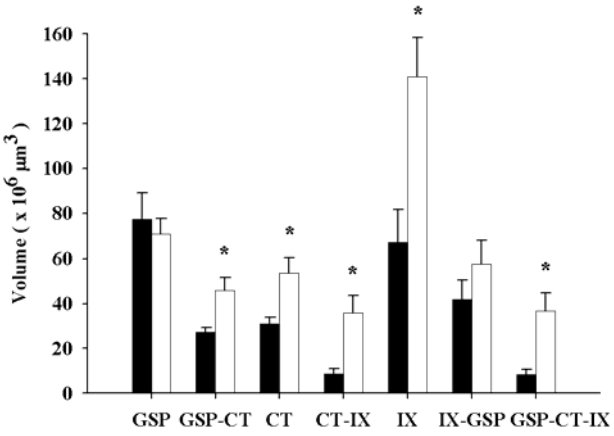

FIGURE 6.

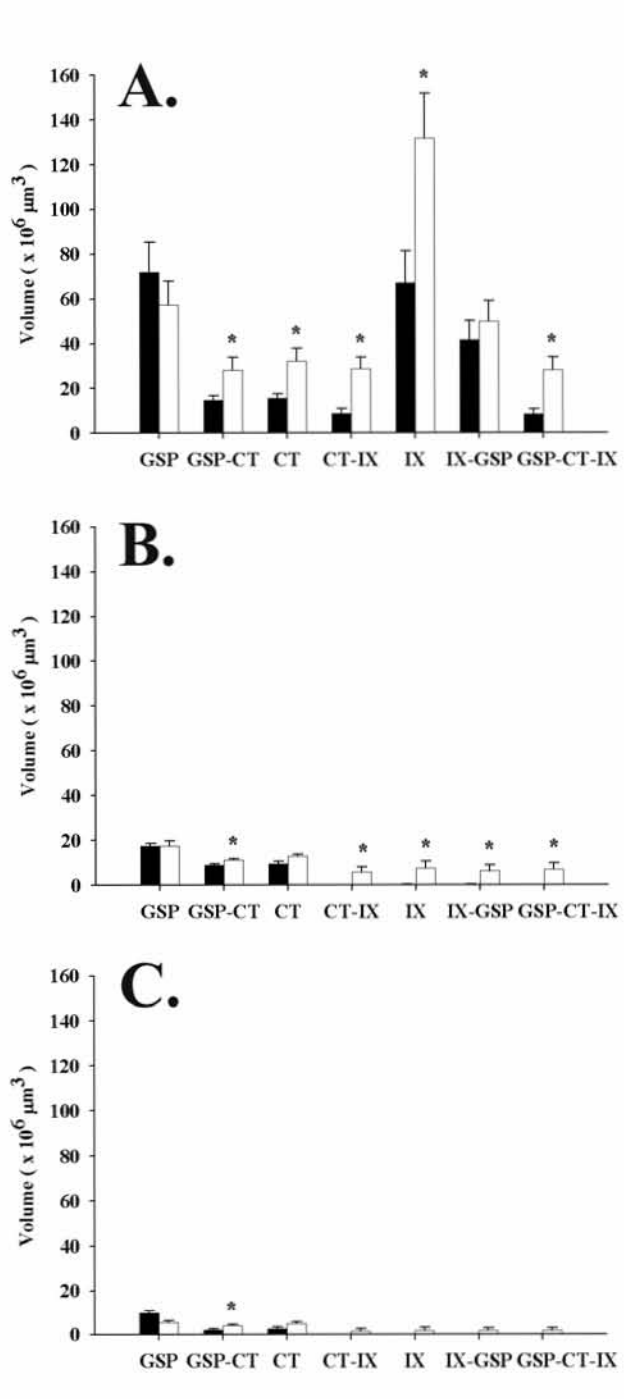
A.
B.
C.
Volume (x 10^6 µm^3)
0
20
40
60
80
100
120
140
160
GSP
GSP-CT
CT
CT-IX
IX
IX-GSP
GSP-CT-IX
*

FIGURE 7.

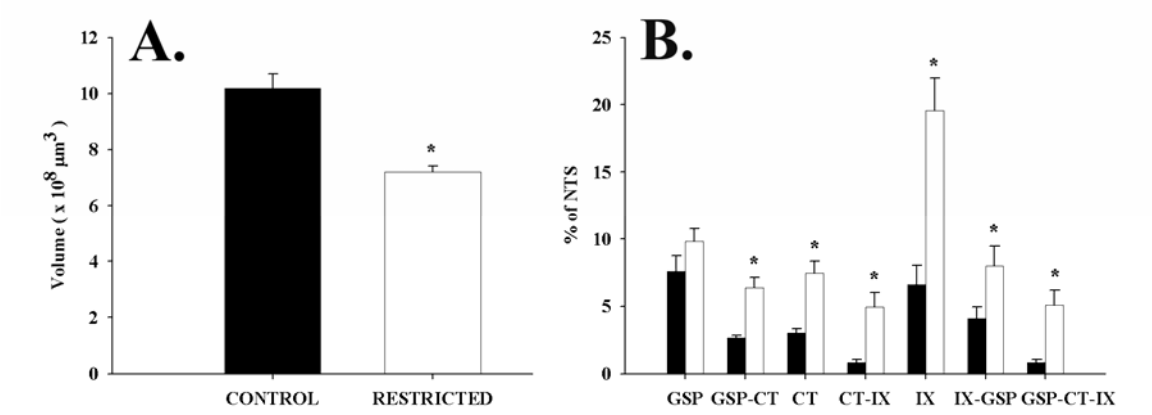

FIGURE 8.

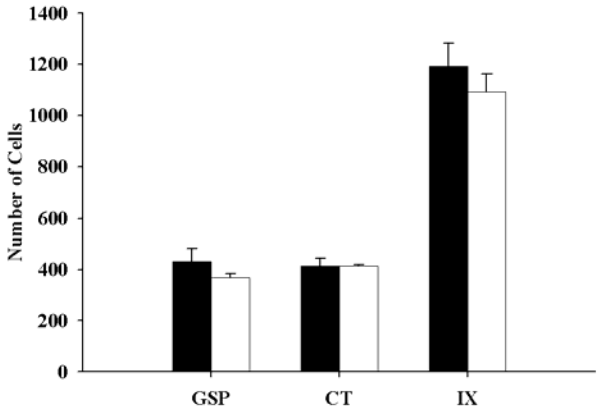

FIGURE 9.

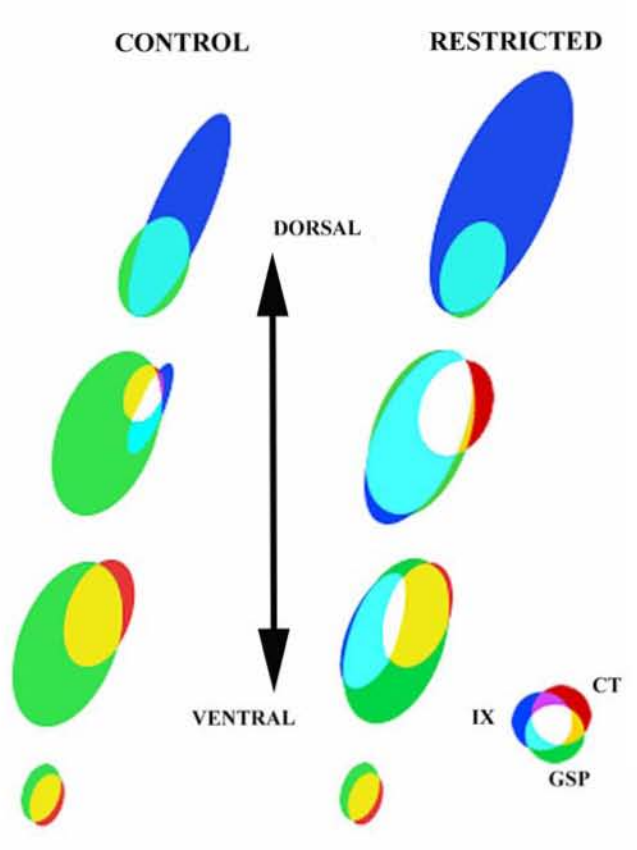

CHAPTER III

The Ultrastructure of Primary Afferent Terminals and Synapses in the Rat Nucleus of the Solitary Tract: A Comparison Among the Greater Superficial Petrosal, Chorda Tympani, and Glossopharyngeal Nerves.

INTRODUCTION

The nucleus of the solitary tract (NTS) is the first-order afferent relay of the central gustatory system (Contreras et al., 1982). This nucleus receives gustatory input from three different nerves: the chorda tympani (CT) nerve, which innervates taste receptor cells located in the anterior tongue; the greater superficial petrosal (GSP) nerve, which innervates taste receptor cells located in the soft palate; and the glossopharyngeal (IX) nerve, which innervates taste receptors on the posterior tongue. An analysis of the morphological characteristics of these individual inputs and their putative synaptic patterns onto gustatory relay (or projection) neurons in the NTS is fundamental to understanding the circuitry of the central gustatory system.

The bulk of what is known regarding the synaptic anatomy of the gustatory system centers on the peripheral connection of the primary sensory neurons to taste receptor cells (Miller and Chaudhry, 1976; Kinnamon et al., 1985; Delay and Roper, 1988; Kinnamon et al., 1988; Royer and Kinnamon, 1988, 1994), while little research has been devoted to the central connections. Currently, the only available information regarding the afferent synaptology of the gustatory NTS is contained in a few electron micrographic studies using hamsters (Whitehead, 1986, 1993; Brining and Smith, 1996; Davis, 1998). In these studies, labeled terminals deriving from the VIIth nerve and the IXth cranial nerves were examined separately throughout the rostral-caudal extent of the NTS. While establishing a strong foundation for the synaptic organization of the NTS, two branches of the VIIth nerve, the CT and GSP nerves were not differentiated (Whitehead, 1986, 1993). Given that the CT and GSP nerves innervate separate receptor

populations in the oral cavity and display distinct taste response properties when these receptors are stimulated (Beidler et al., 1955; Frank et al., 1983; Nejad, 1986; Sollars and Hill, 1998), corresponding differences in the connectivity of these nerves with neurons in the NTS may also exist. Furthermore, peripheral electrophysiology and central terminal field anatomy are markedly different in hamster from that of rat (Hill, 1988; Stewart et al., 2004; Stewart et al., 2005). Therefore, as a corollary to the physiological and anatomical species differences, ultrastructural differences between the morphology of the gustatory terminals in the NTS of hamster and rat may be present as well.

With the aid of triple fluorescence labeling and confocal microscopy, we have recently begun to characterize afferent projections into the rat gustatory NTS. We described the terminal field patterns of the three gustatory nerves and their overlapping fields along the dorsal-ventral axis of the NTS (May and Hill, submitted). The IX, GSP, and CT nerves project rostro-caudally in the solitary tract and send off branches medially that terminate in the solitary nucleus in an ordered, yet extensively overlapping array. All three terminal fields overlap considerably in the dorsal portion of the rostral pole of the NTS. This high degree of convergence of these primary afferent terminal fields in the NTS gives rise to the question of whether synaptic convergence of these afferents occurs on individual NTS cells or whether primary afferents remain segregated through the NTS. To start addressing these questions, the current study sought to determine the ultrastructural properties that characterize these individual terminal fields and their synapses onto postsynaptic targets in adult rats. To this aim, we labeled the three

gustatory nerves individually and examined their axon terminals in the zone in the NTS where these three gustatory nerves converge.

MATERIALS AND METHODS

All animal procedures were in accordance with NIH guidelines for humane handling of animals, and all protocols were approved by the Institutional Animal Care Committee at the University of Virginia.

Animals and Tissue Preparation

Nine adult (50-60 days old), female Sprague-Dawley rats (Harlan, Indianapolis, Indiana) maintained on standard rat chow and tap water ad libitum were used to examine the ultrastructural morphology of GSP, CT, and IX nerve axon terminals. The CT, GSP, and IX nerves were labeled individually in separate adult animals resulting in three different groups: CT (n=3), GSP (n=3), and IX (n=3). Animals were anesthetized with medetomadine hydrochloride (IM; 0.2 mg/kg) followed by ketamine (IM; 20 mg/kg) and placed on a water-circulating heating pad to maintain body temperature at 36°C. Upon placement in a non-traumatic head holder (Erickson, 1966), a ventral approach, modified from Sollars and Hill (2000) was taken to expose either the GSP or CT nerve in the right tympanic bulla or the IXth nerve in the ventral side of the neck medial to the tympanic bulla. A longitudinal incision in the ventro-medial portion of the neck was made, and the masseter muscle and the posterior belly of the digastricus muscle were retracted. A small hole was made in the ventral aspect of the tympanic bulla to gain access to the CT and the GSP nerves, and the IXth nerve was exposed dorsal to the hypoglossal nerve. Each nerve was cut peripheral to the ganglia. After a brief application (approximately 20 seconds) of

dimethyl sulfoxide (DMSO), crystals of 3 kD Biotinylated Dextran Amine (BDA) (Molecular Probes, Inc., Eugene, OR) were carefully placed on the proximal cut ends of the nerves, and petroleum jelly was applied over the proximal stump to hold dye crystals in place. A piece of parafilm was used to cover the opening created in the tympanic bulla, or a layer of parafilm and petroleum jelly sandwiched the IXth nerve to secure dye placement. The incision was then sutured, and animals were injected with atipamezole, (IM; 1 mg/kg) to reverse the effects of medetomadine HCl. The rats were allowed to recover from the anesthetic on a heating pad. From previous work (May and Hill, submitted), the optimal time for anterograde transport of the BDA to the medulla was determined to be approximately 24 hours.

Animals were perfused transcardially for 10-30 minutes with a Krebs solution that contained 1% heparin followed by a mixture of 4% paraformaldehyde and 1% gluteraldehyde in 0.1M phosphate buffer (PB, pH 7.4). Brains were removed and postfixed in 4% paraformaldehyde overnight. The medulla was blocked and sectioned on a vibratome horizontally at 50 μm through the entire NTS. Tissue sections were collected in 0.1 mM PBS at pH 7.4. To stop the cross-linking action of residual fixative in the tissue, the sections were treated with 3% sodium borohydride for 30 minutes and then rinsed 10 minutes in phosphate buffer. Tissue sections were then reacted in a 1:100 avidin-biotinylated peroxidase complex in PBS overnight at 4° C, and rinsed in PBS 3 times for 3 minutes. The sections were then incubated in 1% Diaminobenzidine (DAB) and 0.0003% H_2O_2 for 5-8 minutes.

Embedding

In preparation for examination on the electron microscope, the sections were postfixed with osmium tetroxide and embedded using standard procedures (Hayat, 2000). DAB-stained sections were washed in 0.1M PB and then placed in 1% osmium tetroxide diluted in PB for 1 hour. Sections were then washed in PB three times for 3 minutes, and dehydrated sequentially in 50% ethanol (ETOH) for 3 minutes, filtered 4% uranyl acetate in 70% ETOH for 1 hour, 70% ETOH for 1 minute, 90% ETOH for 5 minutes, and 100% ETOH three times for 5 minutes. Next, the sections were rinsed with acetone three times for 10 minutes. The final acetone rinse was replaced with a 1:1 mixture of acetone and EPON for 2-4 hours or overnight. This 1:1 acetone-EPON solution was replaced with full EPON for 2-4 hours or overnight. Finally, the sections were flat embedded between sheets of ACLAR and placed in a 60°C oven overnight.

Light microscopy was used to identify the dorsal boundary of the rostral pole of the NTS. To locate tissue sections that contained this portion of the NTS, the outlines of the NTS, DAB-stained terminal fields, and landmarks, such as the fourth ventricle, myelinated axon bundles, and blood vessels, in individual sections were drawn on a camera lucida and compared to individual terminal fields characterized in May and Hill (submitted). The sections to be examined were placed on the bottom of BEEM capsules. The capsules were filled with EPON and placed in a 60°C oven overnight to polymerize. Ultrathin sections were cut at 90 nm through the dorsal NTS, collected on 200 mesh copper grids, and viewed with a JEOL 1010 electron microscope. Photographs were taken using either an analog film camera, or a 16Mpixel SIA-12C digital camera (Scientific Instruments and Applications, Inc., Duluth, GA), using MaxIm DL CCD

software (Diffraction Limited, Ottawa, Ontario, Canada). Photographic film was developed, digitized at 600 dpi with an Epson Perfection 1200 Photo Scanner, and examined at a final 30,000X-50,000X magnification on a computer monitor.

Quantitative analysis

Ultrathin sections were examined at the densely labeled region of the dorsal NTS. The copper grids, upon which these sections were placed, provided a means to arbitrarily divide dorsal NTS sections into small squares of tissue. A sample area is illustrated in Figure 1. For each selected sample, a series of overlapping pictures were taken at a relatively low power (1500X) of magnification to cover an entire grid square. Using Photoshop 7.0 (Adobe Systems, San Jose, CA), a montage of these pictures was created in order to reconstruct each selected square of the grid. The area of the sample was computed using imaging and quantification software (Image Pro Plus, v4.5; Media Cybernetics, Inc., Silver Spring, MD) by tracing the perimeter of the square, excluding any blood vessels or EPON patches (Fig. 1). Typically, each area constructed in this manner averaged (± SEM) $6.3 \pm 0.2\ \mu m^2$.

Each selected grid square was systematically reexamined with the electron microscope for the presence of any DAB-labeled profiles. When a profile was encountered, a photograph was taken at 10,000X magnification. We collected images from every labeled profile within each predetermined sample area, regardless of whether the labeled profile contained a synapse. Three animals were labeled for each individual afferent nerve (IX, GSP, or CT), and within each animal, three grid squares were

examined, resulting in a total of nine grid squares quantified for each nerve [IX (n=9), GSP (n=9), and CT (n=9)].

On initial examination, the labeled GSP terminals observed in the individual grids of the GSP nerve group were sparse, and the morphologies of the GSP terminals were statistically variable within the population; therefore, photomicrographs of twenty additional labeled terminals were analyzed beyond the parameters of each original grid square to increase the total population for this group. Measurements of these additional terminals were only included for measurements such as extrapolated synapse frequency, and not for measurements in which the area of the grid square was a variable (i.e., volumetric density of synapses and areal axon density).

Photographs of each labeled profile were evaluated for both the presence of a synapse and the type of postsynaptic profile, (e.g., dendrite or spine). Synapses were recognized by the existence of 1) a parallel alignment of a segment of the presynaptic membrane to the postsynaptic membrane, 2) at least three vesicles in a profile, and 3) at least one vesicle in the presynaptic profile in contact with the presynaptic membrane (Colonnier, 1968). For all identified synapses, the postsynaptic profile was classified as a spine, a dendritic shaft, an axon terminal, or a cell soma. A dendritic shaft was identified by the presence of microtubules, either organized in parallel or cut perpendicular to their axis, or by the presence of mitochondria. Axon terminals were identified as having synaptic vesicles. Cell bodies were identified by the presence of an endoplasmic reticulum, subsynaptic cisterna, a Golgi apparatus, or a nucleus. Profiles that did not fit into any of these categories were classified as spines.

Several measurements were taken using Image Pro Plus. 1) *Synapse length:* The length of the postsynaptic density along the parallel pre- and postsynaptic membranes of the profiles was traced. 2) *Synaptic terminal area*: The perimeter of labeled axonal segments that contained a synapse was outlined and the area inside the outline was calculated. 3) *Long and short calibers:* The *feret minimum* and *feret maximum* features of Image ProPlus were used to calculate the long and the short caliber of every labeled terminal. These measurements represented the maximum length and width of the outlined terminal. 4) *Postsynaptic profile area, and long and short calibers:* The perimeters of the postsynaptic profiles of the labeled synaptic terminals were outlined and the area inside the outline as well as the length and width of the outlined postsynaptic object were computed to determine the relative caliber of the postsynaptic target.

Using these measurements, the length of labeled axons, the synapse frequency of labeled axons, and the volumetric density of synapses onto labeled axons were calculated. *Density of labeled axons*: The axon density represented by all labeled profiles was determined by using a formula that assessed the short caliber (C_s) and the long caliber (C_l) of the profile as well as the section thickness (t) (Erisir and Dreusicke, 2005). This formula was based on the assumption that the shape of an axon was cylindrical. Hence, the short caliber (C_s) represents the diameter of the axon, which in 3D forms a right angle with the long caliber (C_l). The hypotenuse of the right angle formed by these two measures would, therefore, represent the length of the axis of the cylinder that axonal profile spanned, which determined the extrapolated length of the axon of each labeled profile. Then, the total density of axon measured in a grid was calculated by summing the

extrapolated length of each labeled profile in each sample grid square of tissue, correcting for section thickness, and standardizing that total by the measured area of the grid square (*a*), which is represented by the following formula:

$$Areal\ axon\ density\ (\mu m/mm^2) = \frac{\sum\left(\sqrt{C_l^2 - C_s^2}\right) + t}{a}$$

This allowed a computation of the total length of the observed axon, reported relative to the area of the sample grid.

Synapse frequency of labeled axons: To estimate the frequency of synapses along labeled axons, we first calculated the percentage of labeled profiles that contained a synapse. However, this measure is subject to a sampling bias due to the variation in the size of the synapses and the caliber of the axons. To account for any bias in our sampling, we used the following stereological formula (Beaudet and Sotelo, 1981):

$$Extrapolated\ synapse\ frequency\ (\%) = \frac{\left(\frac{p_s \times 100}{p}\right)}{\left[\left(\frac{l_s}{D} \times \frac{2}{\pi}\right) + \frac{t}{D}\right]}$$

In this formula, p_s equals the number of labeled profiles (p) that contained a synapse. D equals the mean diameter of axons, which was calculated as the average of the long and short axes of each labeled profile. l_s equals the average length of the synapse. t equals the section thickness (~ 90nm). Umbriaco et al. (1994) have shown this extrapolation approach to be consistent in estimating synapse frequency on 3D reconstructed axon segments.

Volumetric density of synapses: In order to calculate the volumetric density (N_V) of labeled synapses, we used the formula $N_V = N_A$/ average synapse length (Colonnier and Beaulieu, 1985; DeFelipe et al., 1999). N_A is the number of labeled synapses per area. This calculation was based on the assumption that the shape of a typical synapse was a circular disk. Hence, the average length of synapses from all the synaptic profiles examined in a selected area also represented the average diameter of the synapses. Therefore, synapse length could be used to predict the average depth, perpendicular to the plane of the section, of the volume of a region represented in two-dimension. Colonnier and Beaulieu (1985) found this formula to be the most accurate in estimating the number of synapses contained within a unit of volume.

Photomicrograph production

Electron photomicrographs were produced by digitizing negative films at a resolution of 1600dpi to yield enlargements at 400dpi without resampling the image. In addition, images captured using a 16Mbyte digital camera were displayed at 400-600dpi and resampled to reduce the size of the electronmicrograph to the same magnification as the digitized negatives. Photoshop 7.0 was used to compose and label the plates. Minimal brightness and contrast adjustments were performed.

Statistical Analysis

Mean axon terminal area, synapse length, and postsynaptic target caliber were compared among the GSP, CT, and IX afferent terminals and analyzed statistically using non-parametric Mann-Whitney U tests. An alpha level of 0.05 was considered significant. Postsynaptic target preference, estimated total axon density, synapse frequency, and

volumetric density of synapses were also compared among the GSP, CT, and IX afferent terminals and analyzed statistically using a priori comparisons. For this statistical analysis, the alpha level of 0.05 was adjusted to reflect the number of comparisons among nerves (0.05/3 comparisons).

RESULTS

Based on anatomical characteristics, the horizontal plane of the gustatory NTS has been divided into three distinct regions: dorsal, intermediate, and ventral (May and Hill, submitted). We chose to focus our characterization of the ultrastructure of the gustatory NTS on only the dorsal aspect of the rostral NTS, because all three nerve terminal fields are present in this plane. Unlike the GSP and CT terminal fields, the IX field does not extend into the more ventral regions of the NTS (May and Hill, submitted). Furthermore, of the three divisions of the NTS, the dorsal region undergoes the most restructuring during normal development (Hill et al., 2003) and is the most susceptible to plasticity-inducing environmental manipulations (e.g., King and Hill, 1991; May and Hill, submitted). Thus, by examining the dorsal alone, we could compare how labeled axon terminals from each nerve all occupy the same region within the NTS.

Qualitative properties of labeled terminals

At the light microscopic level, DAB-labeled fibers densely terminated in the dorsal portion of the rostral NTS (Fig. 2A). The termination patterns of each gustatory nerve were reminiscent of the fluorescent-labeled gustatory terminal fields characterized in May and Hill (submitted). The orientation of DAB-labeled fibers did not vary between animals for each gustatory nerve. Axon arbors coursed in all directions with no single

orientation or trajectory (Fig. 2B). The terminal endings of each gustatory afferent appeared as swellings along the axons like beads on a string. Terminal boutons were also observed (Fig. 2B). However, finer details regarding those terminations were better revealed at the ultrastructural level.

General appearance of afferent axon terminals

At the electron microscopic level, DAB labeled profiles appeared dark and densely filled. The intensity of the label did not obscure cellular membranes, postsynaptic densities, vesicles, or organelles, allowing qualitative and quantitative evaluation of intracellular organelles. Gustatory afferent terminals were generally unmyelinated, medium to large in size (0.1 μm^2 to 7.6 μm^2), and contained round clear vesicles and dark mitochondria (Figs. 3-9). Synaptic contacts were made with dendrites, spines, and axons either in a simple pattern in which one terminal formed synapses with only one postsynaptic target (e. g., Figs. 3C, 5A) or in more complex patterns in which an axon terminal formed synapses upon multiple postsynaptic targets (e. g., Figs. 3A, 4A). Primary afferent terminals were not observed forming synapses directly with cell soma in this study. Labeled terminals often appeared in glomerular arrangements in which glial membranes enveloped a collection of profiles that included dendrites, spines, and unlabeled vesicle-filled profiles (Figs. 3B, 4A & B, 5A). Postsynaptic unlabeled vesicle-filled profiles were observed to form either symmetric or asymmetric synapses onto other profiles (Fig. 4B). Although infrequent, afferent terminals also engaged in triadic arrangements, where a labeled terminal formed a synapse with a target, which in turn made a synapse with another profile that was also postsynaptic to the original labeled

terminal. Configurations such as these were typically enclosed in glia. All synapses formed by labeled terminals were asymmetric (i.e., displaying a thicker density on the postsynaptic side) corresponding to Gray's Type I excitatory classification (Peters et al., 1970).

Occasionally, inclusions or unlabeled, membrane-bound patches appeared in labeled terminals creating a hole-punched appearance of the terminals (Figs. 3C, 4B, 5A & 6-9). These were caused by spinules, protrusions of dendrites or dendritic spines, which were completely enveloped by the axon terminal (Tarrant and Routtenberg, 1977). Therefore, upon sectioning through a labeled terminal perpendicular to the spine protrusion, the cross section of the terminal appeared punched out by the spinule. Unlabeled terminals were also sometimes included inside of labeled axon terminals (Fig. 3C). Also, perforations or interruptions in synaptic densities (Peters and Kaiserman-Abramof, 1969; Figs. 3B & C, 4B, 5B, 6-7, 9) occurred for terminals of all three gustatory nerves.

Quantitative analysis of afferent axon terminals

In order to detect ultrastructural differences among gustatory afferents, several morphometric parameters were quantified for GSP, CT, and IX afferent terminals.

Terminal area: In order to determine differences in terminal size among the different afferents, the terminal area of each labeled synaptic profile was measured. The distribution of the area of GSP, CT, and IX axons revealed significant size differences in the terminal endings of IX axons compared to the terminal endings of GSP and CT axons (Fig. 10A). The average size of GSP and CT axon terminals was not significantly

different (P = 0.2; Fig. 10B). The mean area (± SEM) of GSP terminals was 1.0 ± 0.1 μm^2 and ranged in size from 0.1–3.3 μm^2, and the mean area (± SEM) of CT terminals was 1.1 ± 0.1 μm^2 and ranged in size from 0.1–4.4 μm^2. However, IX terminals were significantly larger than both GSP (P = 0.0001) and CT terminals (P = 0.004; Fig. 10B). The mean area (± SEM) of IX terminals was 1.6 ± 0.1 μm^2 and ranged in size from 0.2–7.6 μm^2.

Synapse length: The extent of the active zone provides one indication of the efficacy of the synaptic contacts associated with axon terminals (Pierce and Lewin, 1994). Therefore, to quantify the size of the active zone, synapse length was measured. The lengths of synapses on CT, GSP, and IX terminals varied among nerve terminals, but all synapses measured ranged in size from 0.1 to 1.0 μm (Fig. 11A). With a mean length (± SEM) of 0.4 ± 0.02 μm, synapses on CT terminals were significantly longer than synapses on both GSP and IX terminals whose mean lengths (± SEMs) were 0.3 ± 0.01 μm (P = 0.0001) and 0.3 ± 0.01 μm (P = 0.001), respectively (Fig. 11B). The mean length of synapses associated with GSP and IX terminals were not significantly different from each other (Fig. 11B).

Postsynaptic target preference: In order to determine differences in the postsynaptic targets of GSP, CT, and IX terminals, the percentage of the total number of synapses that occurred on dendrites, spines, and axons was assessed for each afferent terminal. For GSP terminals, 75% of the total number of synapses occurred on dendrites and 21% of synapses occurred on spines. The remaining 4% of synapses occurred on

unlabeled axon terminals. Similarly for CT terminals, 76% of synapses occurred on dendrites, 18% of synapses occurred on spines, and 6% of synapses occurred on axons. There were no significant differences in the target preferences of GSP and CT afferents; both formed synapses most often on dendritic shafts ($P = 0.9$; Fig. 12A). However, there was a significant nerve-related difference in the postsynaptic targets of IX terminals. Specifically, 37% of synapses from IX terminals occurred on dendrites and 54% of synapses from IX terminals occurred on spines. The remaining 9% of synapses occurred on axons. Thus, IX terminals formed synapses significantly more often with spines and significantly less often with dendrites compared to that of GSP terminals ($P = 0.0001$) and CT terminals ($P = 0.001$; Fig. 12A).

To further assess differences in the postsynaptic target of these afferent terminals, the relative caliber of the postsynaptic dendrites was measured. This measurement served as an estimate of the distance where the axodendritic synapse occurred relative to the soma. Since dendritic shafts are presumably conical in shape, tapering away from the soma, the closer a dendrite was to the soma, the larger in diameter it would appear. The calibers of the dendrites observed were compared relative to GSP, CT, and IX related synapses. There were no significance differences in the caliber of the dendrites postsynaptic to GSP and CT terminals ($P = 0.9$). GSP terminals formed synapses on dendrites with a mean diameter (± SEM) of 1.1 ± 0.1 μm and ranged in size from 0.3-3.7 μm. CT terminals formed synapses on dendrites with a mean diameter (± SEM) of 1.2 ± 0.1 μm and ranged in size from 0.3-4.1 μm (Fig. 12B). The dendrites on which IX terminals formed synapses were similar in caliber compared to those related to GSP ($P =$

0.2) and CT (P = 0.2) terminals. They had a mean diameter (± SEM) of 0.9 ± 0.04 μm and ranged in size from 0.3-2.2 μm (Fig. 12B), respectively.

Unlabeled inclusions and perforated synapses: Spinules and perforations of synapses are both morphological features of axon terminals that indicate the dynamic and transient nature of synapses (Sorra et al., 1998). In NTS neuropil, unlabeled inclusions, with ultrastructural properties of spines, dendrites, or vesicle containing profiles, were observed inside of GSP, CT, and IX terminals (Figs. 3C, 4B, 5A, 7-9), but occurred significantly more frequently in IX terminals. On average, 7.9 ± 1.5% of labeled IX terminals observed within the dorsal NTS were invaginated by spinules and other unlabeled inclusions (Fig. 13A). This is a significant increase in incidence compared to the less frequent occurrence of the various unlabeled inclusions invaginating CT terminals (P = 0.002); 2.1 ± 0.5% of CT terminals contained spinules and other unlabeled inclusions (Fig. 13A). GSP terminals also contained less unlabeled inclusions than IX terminals. This trend was marginally significant by our alpha level of 0.02 (P = 0.02). That is, 3.3 ± 1.0% of GSP terminals were observed to contain unlabeled inclusions (Fig. 13A). The difference in the frequency of unlabeled inclusions observed in CT and GSP terminals was not significant (P = 0.3).

Infrequently, axon terminals from all three gustatory nerves displayed perforated postsynaptic densities (Figs. 3B & C, 4B, 5A, 6-7, 9). On average, 1.3 ± 0.4% of the synapses of IX terminals were perforated. A similar low percentage of the synapses of CT terminals (2.3 ± 0.7%) and of GSP terminals (1.8 ± 0.7%) were also perforated.

Thus, there were no significant differences in the occurrence of these perforated synapses among the different nerve terminals (*P*s > 0.2; Fig. 13B).

Areal axon density: To gain a perspective of the density of axons present in the dorsal NTS, the total axon length was estimated and expressed relative to the area of the NTS region that was examined. The average total density of labeled GSP and CT axons in the dorsal NTS was not significantly different ($P = 0.8$). GSP axons occupied an average length (± SEM) of 13.2 ± 1.6 μm/ mm^2, and CT axons occupied an average length of 12.5 ± 1.9 μm/ mm^2 (Fig. 14A). However, labeled IX axons were significantly denser compared to GSP axons ($P = 0.003$) and CT axons ($P = 0.003$). IX axons had an average length (± SEM) of 40.3 ± 7.6 μm/ mm^2 (Fig. 14A).

Synapsing frequency of axons: How often synapses occur on an axon provides one indication of the strength in connectivity that axon has with its postsynaptic target. In order to determine the frequency at which the axons of GSP, CT, and IX afferents formed synapses, the probability of a synapse appearing on an axon segment was calculated. A 100% frequency probability score would indicate that every labeled axon segment observed made one synapse. A probability score higher than 100% would be interpreted that each observed axon segment formed more than one synapse (e.g., 200% indicates two synapses per axon segment). A probability score lower than 100% would indicate that not every axon segment contained a synapse (e.g., 50% indicates a synapse forms on every other axon segment encountered). Synapses occurred significantly more frequently with IX axons than with CT axons ($P = 0.001$). The frequency of synapses on IX axons occurred at a rate of 197.3 ± 20.7% synapse. Synapses occurred less frequently on CT

axons at a rate of 106.9 ± 11.4% (Fig. 14B). Additionally, synapses occurred on GSP axons at a rate of 204.7 ± 39.2%. This frequency was not significantly different from the frequency of synapses occurring with IX axons (P = 0.9; Fig. 14B). While the synapse frequency of GSP axons appeared higher than the synapse frequency of CT axons, this difference was close to significance by our stringent alpha level of 0.02 (P = 0.03). Additional GSP axons were analyzed beyond the original parameters of this calculation to accommodate for the high variability, and a trend existed for individual GSP axons to engage in more synaptic contacts than individual CT axons.

Volumetric density of synapses: The relative density of synapses of labeled axons contained within a measured volume of the dorsal NTS was also compared among GSP, CT, and IX afferents. For unit volume of the NTS region examined, there was a significantly higher density of synapses associated with IX axons compared to the density of synapses associated with GSP axons (P = 0.001) and CT axons (P = 0.001). An average of 22.0 ± 4.1 synapses/ mm^3 were found for IX axons versus an average (± SEM) of 4.4 ± 0.8 synapses/ mm^3 for GSP axons and an average of 4.9 ± 0.9 synapses/ mm^3 for CT axons (Fig. 14C). The difference in the volumetric density of synapses associated with GSP axons and with CT axons was not significant (P = 0.7).

DISCUSSION

The results of our analyses reveal for the first time the morphological characteristics of identified GSP, CT, and IX afferent terminals in the dorsal zone of the rat NTS. An understanding of the synaptic arrangements of this particular zone is integral to determining how the three gustatory afferents are integrated at the first

synaptic relay of the gustatory circuitry because of its unique anatomical features (i.e., overlapping terminal fields, susceptibility to environmental manipulations, age-related reorganization). In this zone, all three primary afferents display similar characteristics in vesicular shape and asymmetry of synaptic contacts, which are typical of excitatory nerve terminals. However, distinct differences in the morphology and synaptic arrangements exist among the terminals of these three gustatory afferents.

Presynaptic Terminal Size and Postsynaptic Target Differences: The most salient difference among gustatory afferents was the dichotomy in presynaptic terminal area. IX axons displayed larger terminal endings than GSP and CT axons, while GSP and CT axon terminals were similar in size. These results are consistent with Whitehead (1986) and Brining and Smith (1996). It is not surprising that CT and GSP nerves have similarly sized terminals, since both nerves are branches of the facial nerve and both have soma in the geniculate ganglia. Thus, the disparity of IX axon terminal size compared to CT and GSP axon terminals could be a reflection of the differences associated with the identity of the cranial nerve.

Another prominent feature that distinguished IX terminations from GSP and CT terminations was the postsynaptic target of these afferents. Synapses from GSP and CT axons occurred most frequently on dendritic shafts, while synapses on IX axons occurred more readily on dendritic spines. This result may also reflect differences related to the identity of the cranial nerve and their developmental time courses. Specifically, individual gustatory afferents and their postsynaptic targets develop in separate stages. Geniculate ganglia cells are born on embryonic day 11 (E11), while petrosal ganglion

(IXth nerve) cells are born at E14 (Altman and Bayer, 1982). VII afferents are present in NTS at P1 and terminal fields reach mature size at P25, while IX afferents enter the NTS at P10 and the terminal field matures at P45 (Lasiter et al., 1989; Lasiter, 1992). Furthermore, first order dendrites of NTS cells reach mature lengths at P25 and second order dendrites reach maximal lengths at P70 (Lasiter et al., 1989). Thus, the earlier projecting CT and GSP terminals may preferentially synapse on first order dendrites as they enter the NTS. As IX terminals arrive in the NTS later in development, they may be relegated to available dendritic spines. Alternatively, there may be nerve-specific mechanisms that match the respective nerve with its target.

Aberrations in Morphology: An additional, noticeable dissimilarity between the VII and IX afferent terminals was the presence of dendritic spinules. These spine protrusions invaginated IX axon terminals markedly more often than GSP or CT axon terminals. Spinules, similar to those observed in this study, have been described in detail in other brain regions including area CA 1 of the hippocampus (Spacek and Harris, 2004), the dentate gyrus of the hippocampus (Tarrant and Routtenberg, 1977), the cerebellum (Eccles et al., 1967), frontal cortex (Cadete-Leite et al., 1986), sensorimotor cortex (Bozhilova-Pastirova and Ovtscharoff, 1999), and visual cortex (Erisir and Dreusicke, 2005), suggesting a commonality of excitatory input throughout the brain. While the function of the spinule remains speculative (Spacek and Harris, 2004), the existence of these protuberances in the NTS neuropil increases the postsynaptic surface area available with which IX terminals can make synaptic contacts. Moreover, the presence of larger IX terminals having a majority of their synaptic input occurring on

spines in conjunction with the presence of spinules elevates the likelihood for IX terminals to engulf their postsynaptic spines.

Despite understanding the exact functional significance of spinules, these spine protrusions provide substantial evidence for spine motility in the NTS neuropil. CNS neurons have a basal level of spine motility, which presumably enables spines to extend filopodia to probe for axon terminals with which to contact (Dunaevsky et al., 1999). Although spine motility does not ensure synaptic contact (Dunaevsky et al., 2001), it may mediate the formation of synapses from IX terminals with spines on NTS cells. That is, spines may selectively attract (or seek out) IX terminals preferentially over GSP and CT terminals.

Density and frequency differences: The synaptic arrangements of each gustatory afferent in the dorsal NTS, quantified by synapse frequency and density measurements, also distinguished the axonal input of each nerve (Fig. 15). Substantially more synapses were associated with IX axons than with GSP and CT axons. That is, an average of two synapses appeared with each IX and GSP axon terminal, but synapses occurred less frequently with CT axon terminals. (While on average each GSP axon terminal contained two synapses, fewer GSP axon terminals were encountered in the NTS neuropil than IX axon terminals.) Within a given volume of the dorsal NTS, synapses on IX axons were four times as dense than synapses on GSP and CT axons. Also, the estimated total density of IX axons was four-fold denser than both CT and GSP axons; CT and GSP axons terminated in the dorsal zone in similar proportions. Hence, IX axons occupied more volume in the dorsal zone of the NTS compared to CT and GSP axons, and the IX axon

terminals engaged in more synaptic contacts with their postsynaptic targets (Fig. 15). Compared to GSP and CT terminals, this disproportionate distribution of synaptic junctions on IX axon terminals is most likely related to physical capacity. The relatively larger size of the IX terminal has more surface area with which to engage in synaptic contacts. Furthermore, the formation of synapses on spines by these large IX terminals increases the packing density of synaptic contacts that would not be achieved by formation of synapses directly onto dendritic shafts. Both the size and postsynaptic target of IX terminals enable these terminals to make more synaptic contacts with NTS neurons. Therefore, in comparing the density and distribution of synaptic contacts upon afferent terminals, the majority of synaptic junctions in the dorsal zone of the NTS are associated with the IXth nerve. This distribution of synapses in the dorsal zone, however, would not be sustained in more intermediate and ventral portions of the NTS since the terminal field of the IXth nerve does not extend into these zones (May and Hill, submitted).

Comparison of Species

The morphological properties of GSP, CT, and IX terminals characterized by these results are similar to the ultrastructure described by Whitehead (1986) and Brining and Smith (1996). However, the synapse frequency and density measurements of each individual afferent included in the current study were not examined previously by Whitehead (1986) or Brining and Smith (1996). As in rat, hamster primary gustatory axons formed mostly axodendritic synapses that were asymmetric. In both species, synaptic endings were typically ovoid profiles, filled with round clear vesicles, and abutted by surrounding processes that made synaptic connections. Hamster VIIth nerve

terminals were on average 1.2 μm in diameter and engaged often in complex glomerular-type arrangements involving both small caliber dendrites or spines and unlabeled terminals. (Whitehead, 1986). IXth nerve terminals were larger with an average 1.8 μm diameter and engaged in simpler synaptic junctions, most often with dendritic spines (Brining and Smith, 1996). We found similar size differences between VII and IX terminals in rat and observed both simple (Figs. 3C, 5A) and glomerular arrangements (Figs. 3B, 4A, 5A) of these terminals. In fact, the morphological characteristics of the IXth nerve terminals of rat appeared similar to that of hamster. However, we also observed significant differences in the synaptic properties of the two branches of the VIIth nerve that were not available for comparisons in Whitehead (1986).

Differences between CT and GSP Nerve Terminals In Rat

In rat, differences in synapse properties distinguished CT terminals from GSP terminals morphologically. Specifically, the synaptic junctions on CT axon terminals were significantly longer than GSP terminals, and CT axon terminals made synapses with their postsynaptic targets less frequently than GSP terminals. These differences between CT and GSP terminals point to alternate strategies each afferent adopts in contacting postsynaptic targets and potentially reflect differences in synapse efficacy. Ultrastructural features including both synapse number and synapse length are presumed correlates of the potential strength of synaptic contacts (Pierce and Lewin, 1994). Therefore, measurable differences in morphological properties exist between CT and GSP terminals. These measurements not only reveal noticeable differences in the patterns of synaptic contact among the three gustatory nerves, but they also yield insight to the

complexity of the connectivity of each individual afferent with NTS neurons and, in turn, provide a means for speculation of how those connections are formed.

Evidence for Convergence

GSP, CT, and IX nerves all terminate in an overlapping pattern onto the rostral NTS (May and Hill, submitted), presumably converging on the relay neurons. This portion of the NTS also receives overlapping projections from the lingual branch of the trigeminal nerve (V), which provides somatosensory innervation (Hamilton and Norgren, 1984). Given the proximity of these inputs to each other, convergence of these inputs onto the same postsynaptic cells is likely. Indeed, electrophysiological studies show single NTS neurons are responsive to taste stimuli applied to different receptor populations throughout the oral cavity (Travers et al., 1986; Sweazey and Smith, 1987). From the results of the current study it is evident that each afferent terminal synapses onto dendritic shafts with similar caliber. Therefore, the proximal distance of each afferent input from the postsynaptic cell soma is similar, which is consistent with the hypothesis that different gustatory nerves are contacting (and possibly competing for) similar postsynaptic targets. However, these results do not delineate from which soma the dendritic branches originate. That is, even if the gustatory nerve terminals are contacting dendritic shafts at similar distances away from NTS cell somas, it is not known if these nerve terminals are forming synapses with dendrites of the same NTS cell. Therefore, despite the postsynaptic targets having similar morphological features, we cannot definitively say that the same cell population is being contacted or that axons are terminating onto separate relay neurons. Dual-labeling experiments designed to

simultaneously examine the synaptology of gustatory afferents would aptly address this matter.

Moreover, the majority of the synaptic contacts of IX afferents were on dendritic spines. The scope of this study, however, did not assess the location of the dendrite from which these spines originated or, subsequently, their proximity from the soma. Therefore, even if IX terminals formed synapses with the same NTS cells as GSP and CT terminals, the results of this study cannot delineate if they interact with each other on the same dendrite or at proximal locations on a single dendrite. Spines are disproportionately distributed along dendrites of NTS neurons. For single neurons, one or two dendrites contain a large number of spines while the remaining dendrites do not have spines (Lasiter et al., 1989). Furthermore, spines are found most often on the distal segments of dendrites (Lasiter et al., 1989). Thus, IX terminals may contact the same postsynaptic target as CT and GSP terminals, but they could be sorted to separate dendritic arbors or separate portions of the same dendritic branch of that target.

Our observations of NTS neuropil, however, did not rule out the possibility of convergence among the different afferents. Unlabeled terminals that display excitatory morphologies do synapse in the vicinity of labeled terminals (Figs. 3B, 4B, 5A, 6, 8-9). Because these unlabeled terminals display characteristics similar to labeled terminals they most likely originate from another gustatory nerve (although alternatively they could derive from V input). For example, large terminals, some of which were larger than the largest CT and GSP terminals encountered, were observed among labeled CT terminals (Fig. 6) and GSP terminals. Since the population of IX terminals contained profiles larger

than the range observed in the population of GSP and CT terminals, these unlabeled terminals could potentially be IX terminals. Additionally, labeled afferent terminals were observed to synapse on unlabeled axon terminals with excitatory characteristics (Fig. 4B). This suggests that in addition to an interaction of separate gustatory afferents on single NTS neurons, gustatory afferents may also modulate each other through direct contact of terminal endings. Ultimately, the morphological identity of synaptic convergence can only be confirmed by multiple labeling of afferent terminals and by examining serial sections through the NTS neuropil.

If the gustatory primary afferents converge onto single NTS cells, such organization would set this system apart from other sensory systems where sensory information is carried in segregated pathways. Primary afferents in these systems are organized in parallel. They relay sensory information from separate receptive fields and occupy the same area of the brain while maintaining distinct synaptic characteristics. For example, in the visual system, the lateral geniculate nucleus receives excitatory input from two physiologically and morphologically distinct classes of retinal ganglion cells (X cells and Y cells), which each innervate separate classes of geniculate relay cells (relay X and Y cells) (Kemp and Sillito, 1982; Sherman and Spear, 1982). The synaptic patterns of these two cells are different in that the terminations of X cells are often involved in complex glomerular structures, while the terminations of Y cells engage in simpler synaptic connections (Wilson et al., 1984; Erisir et al., 1997). Hence, specific patterns of synaptic organization exist for functionally different relay cells that maintain the segregation of two distinct retinal inputs. Segregation of primary afferent input is also

evident in the somatosensory system. Two parallel C fiber primary afferent pathways with distinct cytochemical and synaptic relationships carry similar nociceptive information to different layers of the dorsal horn (Hunt and Rossi, 1985). Specifically, peptide-containing C fibers terminate superficially within the dorsal horn and directly contact spinothalamic projection neurons, while non-peptide containing C fibers terminate deeper within the dorsal horn in glomerular-like synaptic arrangements. As a final example, axons of olfactory receptor neurons that share the same odorant receptor(s) segregate in the olfactory bulb by terminating on a few distinct glomeruli (Ressler et al., 1994; Vassar et al., 1994; Mombaerts et al., 1996). Our data provides evidence for the possible presence of multiple primary excitatory inputs within the same glomerulus engaging in synaptic contact (Fig. 4B). This is different than the glomerular structures observed in all other sensory relay nuclei, where the only postsynaptic vesicle-filled profiles are the dendritic appendages of interneurons (Guillery and Sherman, 2002). Thus, the converging synaptic organization of the gustatory system makes this system unique from other sensory systems where primary afferent inputs are segregated into parallel pathways.

Functional Significance

The conspicuous differences in morphology and synaptology of the gustatory afferents may have functional significance. That is, the segregation of GSP and CT terminals to dendrites and IX terminals to spines could be related to differences in the processing of taste stimuli received from individual gustatory nerves. In rat, the CT nerve responds well to NaCl and HCl and much less so to sucrose and quinine HCl

(Beidler et al., 1955; Frank et al., 1983); the GSP nerve responds better to sucrose and NaCl then quinine (Nejad, 1986; Sollars and Hill, 1998); the IX nerve responds to quinine better than any other stimulus (Yamada, 1966; Frank, 1975). Therefore, in addition to differences related to the developmental properties of individual gustatory nerves and differences in receptive field properties, physiological factors that differentiate gustatory nerves may relate to the dichotomy in terminal morphology.

The partitioning of the synaptic junctions of GSP, CT, and IX terminals onto dendrites and spines may also have implications on the processing of taste information. GSP and CT terminals form synapses with dendrites that are sometimes engaged in complex glomeruli configurations. However, IX terminals form more simple synaptic arrangements. This difference in connectivity coincides with the differences in the peripheral responsivity of the receptive fields of each nerve. Both the GSP and CT nerves are sensitive to stimuli that are appetitive to rats (i.e., NaCl, HCl, and sucrose) (Beidler et al., 1955; Frank et al., 1983; Nejad, 1986; Sollars and Hill, 1998) while the IX nerve is maximally responsive to stimuli that are aversive (i.e., QHCl) (Yamada, 1966; Frank, 1975). Although glomeruli were infrequently observed, the GSP and CT inputs that are involved in these intricate arrangements may be modulated by interneurons or other synaptic components of the glomeruli as taste information carried by each nerve is combined. By having simpler nerve-target interactions, IX axons have a more direct connection to the central target, which would establish a rapid means by which aversive stimuli could be processed. The swift transmission of aversive stimulus information is paramount for the detection and rejection of toxic substances. Indeed, the fact that IX

terminals are relatively larger than GSP and CT terminals and have a higher density and frequency of synapses, points to the necessity for efficacious active zones. While much is to be revealed about the complexity of the convergence of gustatory afferents onto NTS neurons, our results that characterize the morphology and synaptology of individual nerve terminals provides the anatomical basis for understanding how taste qualities may be modulated and perceived functionally.

LITERATURE CITED

Altman J, Bayer SA. 1982. Development of the cranial nerve ganglia and related nuclei in the rat. Adv Anat Embryol Cell Biol 74:1-90.

Beaudet A, Sotelo C. 1981. Synaptic remodeling of serotonin axon terminals in rat agranular cerebellum. Brain Res 206:305-329.

Beidler LM, Fishman IY, Hardiman CW. 1955. Species differences in taste responses. Am J Physiol 181:235-239.

Bozhilova-Pastirova A, Ovtscharoff W. 1999. Intramembranous structure of synaptic membranes with special reference to spinules in the rat sensorimotor cortex. Eur J Neurosci 11:1843-1846.

Brining SK, Smith DV. 1996. Distribution and synaptology of glossopharyngeal afferent nerve terminals in the nucleus of the solitary tract of the hamster. J Comp Neurol 365:556-574.

Cadete-Leite A, Tavares MA, Paula-Barbosa MM, Gray EG. 1986. 'Perforated' synapses in frontal cortex of chronic alcohol-fed rats. J Submicrosc Cytol 18:495-499.

Colonnier M. 1968. Synaptic patterns on different cell types in the different laminae of the cat visual cortex. An electron microscope study. Brain Res 9:268-287.

Colonnier M, Beaulieu C. 1985. An empirical assessment of stereological formulae applied to the counting of synaptic disks in the cerebral cortex. J Comp Neurol 231:175-179.

Contreras RJ, Beckstead RM, Norgren R. 1982. The central projections of the trigeminal, facial, glossopharyngeal and vagus nerves: an autoradiographic study in the rat. J Auton Nerv Syst 6:303-322.

Davis BJ. 1998. Synaptic relationships between the chorda tympani and tyrosine hydroxylase-immunoreactive dendritic processes in the gustatory zone of the nucleus of the solitary tract in the hamster. J Comp Neurol 392:78-91.

DeFelipe J, Marco P, Busturia I, Merchan-Perez A. 1999. Estimation of the number of synapses in the cerebral cortex: methodological considerations. Cereb Cortex 9:722-732.

Delay RJ, Roper SD. 1988. Ultrastructure of taste cells and synapses in the mudpuppy Necturus maculosus. J Comp Neurol 277:268-280.

Dunaevsky A, Blazeski R, Yuste R, Mason C. 2001. Spine motility with synaptic contact. Nat Neurosci 4:685-686.

Dunaevsky A, Tashiro A, Majewska A, Mason C, Yuste R. 1999. Developmental regulation of spine motility in the mammalian central nervous system. Proc Natl Acad Sci U S A 96:13438-13443.

Eccles JC, Ito MSJ, Szentagothai J. 1967. The cerebellum as a neuronal machine. New York: Springer. p 127-130.

Erickson R. 1966. Nontraumatic headholders for mammals. Physiol Behav 1:97-98.

Erisir A, Dreusicke M. 2005. Quantitative morphology and postsynaptic targets of thalamocortical axons in critical period and adult ferret visual cortex. J Comp Neurol 485:11-31.

Erisir A, Van Horn SC, Bickford ME, Sherman SM. 1997. Immunocytochemistry and distribution of parabrachial terminals in the lateral geniculate nucleus of the cat: a comparison with corticogeniculate terminals. J Comp Neurol 377:535-549.

Frank ME. 1975. Response patterns of rat glossopharyngeal taste neurons. In: Olfaction and Taste. Denton D, Coghlan J, Eds. New York: Academic Press.

Frank ME, Contreras RJ, Hettinger TP. 1983. Nerve fibers sensitive to ionic taste stimuli in chorda tympani of the rat. J Neurophysiol 50:941-960.

Guillery RW, Sherman SM. 2002. Thalamic relay functions and their role in corticocortical communications: generalizations from the visual system. Neuron 33:163-175.

Hamilton RB, Norgren R. 1984. Central projections of gustatory nerves in the rat. J Comp Neurol 222:560-577.

Hayat MA. 2000. Principles and techniques of electron microscopy. Biological applications. New York: Cambridge University Press.

Hill DL. 1988. Development of chorda tympani nerve taste responses in the hamster. J Comp Neurol 268:346-356.

Hill DL, Sollars SI, May OL. 2003. Plasticity of the developing central gustatory brainstem. Chem Senses 28:J3.

Hunt SP, Rossi J. 1985. Peptide- and non-peptide-containing unmyelinated primary afferents: the parallel processing of nociceptive information. Philos Trans R Soc Lond B Biol Sci 308:283-289.

Kemp JA, Sillito AM. 1982. The nature of the excitatory transmitter mediating X and Y cell inputs to the cat dorsal lateral geniculate nucleus. J Physiol 323:377-391.

King CT, Hill DL. 1991. Dietary sodium chloride deprivation throughout development selectively influences the terminal field organization of gustatory afferent fibers projecting to the rat nucleus of the solitary tract. J Comp Neurol 303:159-169.

Kinnamon JC, Sherman TA, Roper SD. 1988. Ultrastructure of mouse vallate taste buds: III. Patterns of synaptic connectivity. J Comp Neurol 270:1-10, 56-17.

Kinnamon JC, Taylor BJ, Delay RJ, Roper SD. 1985. Ultrastructure of mouse vallate taste buds. I. Taste cells and their associated synapses. J Comp Neurol 235:48-60.

Lasiter PS. 1992. Postnatal development of gustatory recipient zones within the nucleus of the solitary tract. Brain Res Bull 28:667-677.

Lasiter PS, Wong DM, Kachele DL. 1989. Postnatal development of the rostral solitary nucleus in rat: dendritic morphology and mitochondrial enzyme activity. Brain Res Bull 22:313-321.

May OL, Hill DL. 2005. Gustatory terminal field organization and developmental plasticity in the nucleus of the solitary tract revealed through triple fluorescent labeling. (submitted).

Miller RL, Chaudhry AP. 1976. Comparative ultrastructure of vallate, foliate and fungiform taste buds of golden Syrian hamster. Acta Anat (Basel) 95:75-92.

Mombaerts P, Wang F, Dulac C, Chao SK, Nemes A, Mendelsohn M, Edmondson J, Axel R. 1996. Visualizing an olfactory sensory map. Cell 87:675-686.

Nejad MS. 1986. The neural activities of the greater superficial petrosal nerve of the rat in response to chemical stimulation of the palate. Chem Senses 11:283-293.

Peters A, Kaiserman-Abramof IR. 1969. The small pyramidal neuron of the rat cerebral cortex. The synapses upon dendritic spines. Z Zellforsch Mikrosk Anat 100:487-506.

Peters A, Palay SL, Webster HdF. 1970. The fine structures of the nervous system. New York: Harper and Row.

Pierce JP, Lewin GR. 1994. An ultrastructural size principle. Neuroscience 58:441-446.

Ressler KJ, Sullivan SL, Buck LB. 1994. Information coding in the olfactory system: evidence for a stereotyped and highly organized epitope map in the olfactory bulb. Cell 79:1245-1255.

Royer SM, Kinnamon JC. 1988. Ultrastructure of mouse foliate taste buds: synaptic and nonsynaptic interactions between taste cells and nerve fibers. J Comp Neurol 270:11-24, 58-19.

Royer SM, Kinnamon JC. 1994. Application of serial sectioning and three-dimensional reconstruction to the study of taste bud ultrastructure and organization. Microsc Res Tech 29:381-407.

Sherman SM, Spear PD. 1982. Organization of visual pathways in normal and visually deprived cats. Physiol Rev 62:738-855.

Sollars SI, Hill DL. 1998. Taste responses in the greater superficial petrosal nerve: substantial sodium salt and amiloride sensitivities demonstrated in two rat strains. Behav Neurosci 112:991-1000.

Sollars SI, Hill DL. 2000. Lack of functional and morphological susceptibility of the greater superficial petrosal nerve to developmental dietary sodium restriction. Chem Senses 25:719-727.

Sorra KE, Fiala JC, Harris KM. 1998. Critical assessment of the involvement of perforations, spinules, and spine branching in hippocampal synapse formation. J Comp Neurol 398:225-240.

Spacek J, Harris KM. 2004. Trans-endocytosis via spinules in adult rat hippocampus. J Neurosci 24:4233-4241.

Stewart RE, Chastain M, Selby J, Stewart JS. 2005. Extensive anatomical overlap of greater superficial petrosal (GSP) and IXth nerve terminal fields in hamster solitary nucleus (NTS). Chem Senses 30:A95.

Stewart RE, Stewart JS, Hill DL. 2004. Greater superficial petrosal nerve terminal field in hamster nucleus tractus solitarius. Society for Neuroscience abstract. San Diego, CA.

Sweazey RD, Smith DV. 1987. Convergence onto hamster medullary taste neurons. Brain Res 408:173-184.

Tarrant SB, Routtenberg A. 1977. The synaptic spinule in the dendritic spine: electron microscopic study of the hippocampal dentate gyrus. Tissue Cell 9:461-473.

Travers SP, Pfaffmann C, Norgren R. 1986. Convergence of lingual and palatal gustatory neural activity in the nucleus of the solitary tract. Brain Res 365:305-320.

Umbriaco D, Watkins KC, Descarries L, Cozzari C, Hartman BK. 1994. Ultrastructural and morphometric features of the acetylcholine innervation in adult rat parietal

cortex: an electron microscopic study in serial sections. J Comp Neurol 348:351-373.

Vassar R, Chao SK, Sitcheran R, Nunez JM, Vosshall LB, Axel R. 1994. Topographic organization of sensory projections to the olfactory bulb. Cell 79:981-991.

Whitehead MC. 1986. Anatomy of the gustatory system in the hamster: synaptology of facial afferent terminals in the solitary nucleus. J Comp Neurol 244:72-85.

Whitehead MC. 1993. Distribution of synapses on identified cell types in a gustatory subdivision of the nucleus of the solitary tract. J Comp Neurol 332:326-340.

Wilson JR, Friedlander MJ, Sherman SM. 1984. Fine structural morphology of identified X- and Y-cells in the cat's lateral geniculate nucleus. Proc R Soc Lond B Biol Sci 221:411-436.

Yamada K. 1966. Gustatory and thermal responses in the glossopharyngeal nerve of the rat. Jpn J Physiol 16:599-611.

FIGURE LEGENDS

Figure 1. Electron micrograph of a square division within a copper mesh grid used to examine ultrathin sections of the dorsal nucleus of the solitary tract (NTS). DAB-labeled terminals (arrowheads) appear dark and are dispersed throughout the square of tissue. A higher magnification of the area framed in bold lines is presented in figure 4A. Arrows point to myelinated axons. Abbreviations: bv, blood vessel; g, glia; n, nucleus. Scale bar equals 10 μm.

Figure 2. Light micrographs of DAB-labeled chorda tympani (CT) nerve terminal field in the dorsal NTS of an adult rat. **A.** A horizontal section through the brainstem displaying the densely labeled terminal field in the dorsal NTS. The border of the NTS is outlined (dotted line). The boxed area is magnified in B. R, rostral; L, lateral. **B.** Higher magnification of the periphery of the dense network of terminal field reveals individual fibers displaying frequent swellings (arrows). Terminal boutons are apparent as well (arrowheads). Scale bars in both A and B equal 10 μm.

Figure 3. Electron micrographs of DAB-labeled greater superficial petrosal (GSP) terminals in the dorsal zone of the NTS. **A.** A labeled, vesicle-filled terminal (t*) forms synapses with a dendrite (d) and a spine (s). **B.** A labeled terminal (t*) and an unlabeled terminal (t) both form perforated synapses (arrows) on a dendrite. Surrounding glia (g) suggests a glomerular structure. **C.** Another labeled terminal (t*) that forms a perforated synapse (arrows) on a dendrite (d). A spine (s) protrudes from the dendrite at the site of the synapse and into the terminal. Some unlabeled inclusions observed in labeled profiles were assumed to be cross-sections of protruding spines and, hence, were

labeled spinules (sp). Other unlabeled inclusions were identified as axon segments (t) when they contained synaptic vesicles. m, mitochondria. Scale bar in A equals 0.5 μm.

Figure 4. Electron micrographs of DAB-labeled CT terminals in the dorsal zone of the NTS. **A.** A labeled CT terminal (t*) is forming multiple synapses (arrows) on both a dendrite (d) and spines (s1, s2), some of which are protruding into the terminal. Glia (g) surrounds this structure. m, mitochondria. **B.** Another labeled terminal (t*) that contains two spinules (sp) and forms synapses (arrows) onto two dendrites (d1, d2), a spine (s1), and an unlabeled axon terminal (t1). The unlabeled terminal (t1) forms asymmetric synapses with a spine (s2) and a dendrite (d3) and it receives a synapse from an unlabeled terminal (t2). Scale bar in A equals 0.5 μm.

Figure 5. Electron micrographs of DAB-labeled CT terminals in the dorsal zone of the NTS. **A.** A small, labeled terminal (t*) that forms synapses (arrows) with two spinules (sp). An unlabeled terminal (t) forming a synapse (arrow) with a dendrite (d) is also present in the same field. **B.** A large labeled terminal (t*) in a glomerular formation forms synapses (arrows) with three dendrites (d1, d2, d3) and a spine (s) protruding from a dendrite (d3). Synapses on d2 and d3 are perforated. The structure is surrounded by glia (g). Scale bar in A equals 0.5 μm.

Figure 6. An electron micrograph of unlabeled terminals (t1, t2, t3) forming synapses in the vicinity of two small labeled CT terminals (t*). A large unlabeled terminal (t1) forms synapses (arrows) on two different spines (s1, s2). The synapse on s1 is perforated. Additional unlabeled terminals (t2, t3) form synapses (arrows) on dendrites (d1, d2). Scale bar equals 0.5 μm.

Figure 7. An electron micrograph of a large, DAB-labeled glossopharyngeal (IX) terminal in the dorsal zone of the NTS. The labeled terminal (t*) forms multiple synapses (arrows) with three separate dendritic profiles (d1, d2, d3). All synapses displayed are perforated. Inclusions (sp) were often observed in these terminals. Scale bar equals 0.5 μm.

Figure 8. An electron micrograph of a large, DAB-labeled IX terminal in the dorsal zone of the NTS. This labeled terminal (t*) is punched by spinules (sp) and forms synapses (arrows) with two separate dendritic profiles (d1, d2) as well as an unlabeled terminal (t2). One of these unlabeled terminals (t2) forms a synapse (arrow) on a spine (s). Another unlabeled terminal (t1) forms a symmetric synapse (arrow) on the same dendrite (d2) upon which the labeled terminal (t*) is forming a synapse. Scale bar equals 0.5 μm.

Figure 9. An electron micrograph of DAB-labeled IX terminals in the dorsal zone of the NTS. Two separate labeled terminals (t1*, t2*) are displayed. Terminal t1* contains a membrane bound inclusion (sp) and forms a perforated synapse (arrows) on a dendrite (d1). Terminal t2* forms synapses on two separate spines (s1, s2). Nearby, an unlabeled terminal (t3) forms a synapse with a dendrite (d2). Scale bar equals 0.5 μm.

Figure 10. Frequency distribution histogram of the terminal areas of DAB-labeled GSP, CT, and IX axons, measured on terminal cross-sections that contained a synapse. Frequencies for each nerve are displayed as a percentage of the total to allow visual comparison between groups. IX axon terminals were significantly larger than GSP and CT terminals. Median and population size (n) are indicated for each nerve. **B.** Mean

terminal areas of DAB-labeled GSP, CT, and IX axons. Error bars indicate standard error. The asterisk indicates a statistical significance of $P < 0.05$.

Figure 11. A. Frequency distribution histogram of the synapse lengths of DAB-labeled GSP, CT, and IX axon terminals. Frequencies for each nerve are displayed as a percentage of the total to allow visual comparison between groups. Synapses found on CT axon terminals were significantly longer than synapses on GSP and IX terminals. Median and population size (n) are indicated for each nerve. **B.** Mean synapse length of DAB-labeled GSP, CT, and IX axon terminals. Error bars indicate standard error. The asterisk indicates a statistical significance of $P < 0.05$.

Figure 12. A. Preference for the postsynaptic targets of DAB-labeled GSP, CT, and IX axons. Preference is indicated by the percentage of total synapses terminating on dendrites (hatched bars), spines (open bars), and axons (closed bars). The majority synapses of GSP and CT axon terminals occurred on dendrites while the majority of synapses of IX terminals occurred on spines (see Results). There were no differences among nerves in targeting unlabeled axons. Asterisks indicate a statistical significance of $P < 0.02$. **B.** Frequency distribution histogram of the caliber of the dendrites postsynaptic to GSP, CT, and IX axon terminals. Frequencies for each nerve are displayed as a percentage of the total to allow visual comparison between groups. There were no significant differences among nerves. The majority of synaptic contact from each nerve occurred on medium caliber (0.5-1.5 μm) dendrites. Median and population size (n) are indicated for each nerve.

Figure 13. A. Mean percentage of DAB-labeled GSP, CT, and IX axon terminals that were punched by unlabeled inclusions. More IX axon terminals displayed punched morphologies than GSP and CT axon terminals. **B.** Mean percentage of postsynaptic densities associated with DAB-labeled GSP, CT, and IX axon terminals that were perforated. Perforations of postsynaptic densities were rarely observed for each nerve terminal. (See Results for definitions.) Error bars indicate standard error. The asterisk indicates a statistical significance of $P < 0.02$.

Figure 14. A. Areal axon density of DAB-labeled GSP, CT, and IX axons per mm^2 of the dorsal NTS. IX axons were four-fold denser than GSP and CT axons located in the same plane. The density of GSP and CT axons were not significantly different. **B.** Extrapolated synapse frequency of DAB-labeled GSP, CT, and IX axon terminals. (See Results for interpretation.) IX axons formed synapses at a significantly higher frequency than CT axons. GSP axons also formed synapses at a higher frequency than CT axons, this difference was close to significance. **C.** Volumetric density of synapses associated with DAB-labeled GSP, CT, and IX axons. Four times as many synapses were present on IX axons than on GSP and CT axons. There was no significant difference in the density of synapses associated with GSP and CT axons. See Methods for calculations. Error bars indicate standard error. Asterisks indicate a statistical significance of $P < 0.02$.

Figure 15. Schematic of density and frequency distributions and dendrite/spine targeting of the axon terminals of the GSP, CT, and IX nerves. IX axon terminals are larger than GSP and CT axon terminals and synapse more often on dendritic spines (circles) than dendritic shafts (ellipses). Dendrites contain mitochondria (filled symbols).

(Small circles inside of axon terminals represent synaptic vesicles.) GSP and CT axon terminals synapse more often on dendritic shafts. IX axon terminals made the majority of synaptic contacts onto NTS neurons. Note, for descriptive purposes, synapses represented by this model are meant to indicate the estimated synapse density and frequency of afferent terminals in the entire dorsal NTS.

FIGURE 1.

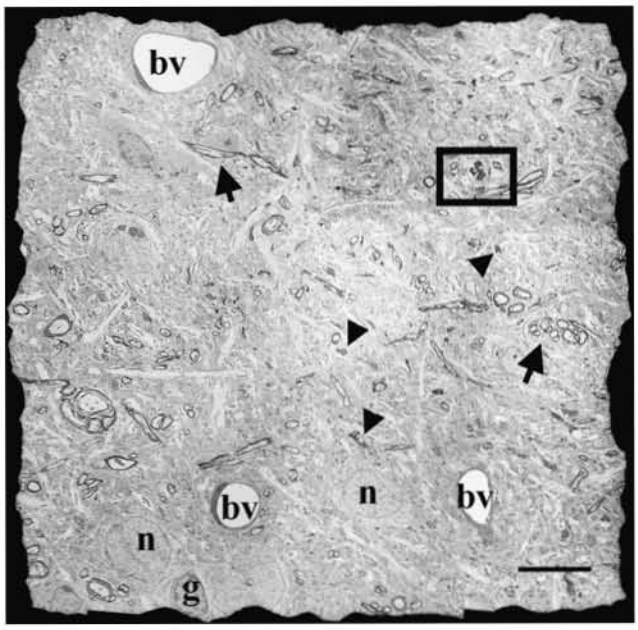

FIGURE 2.

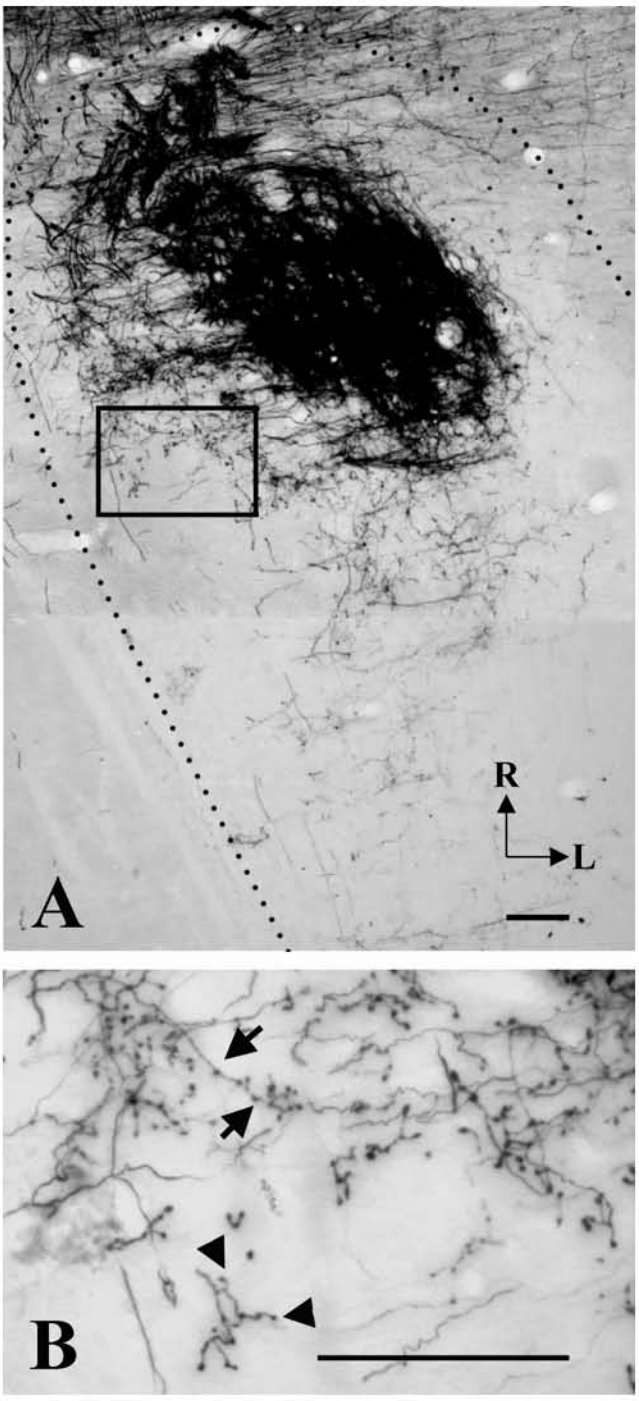

FIGURE 3.

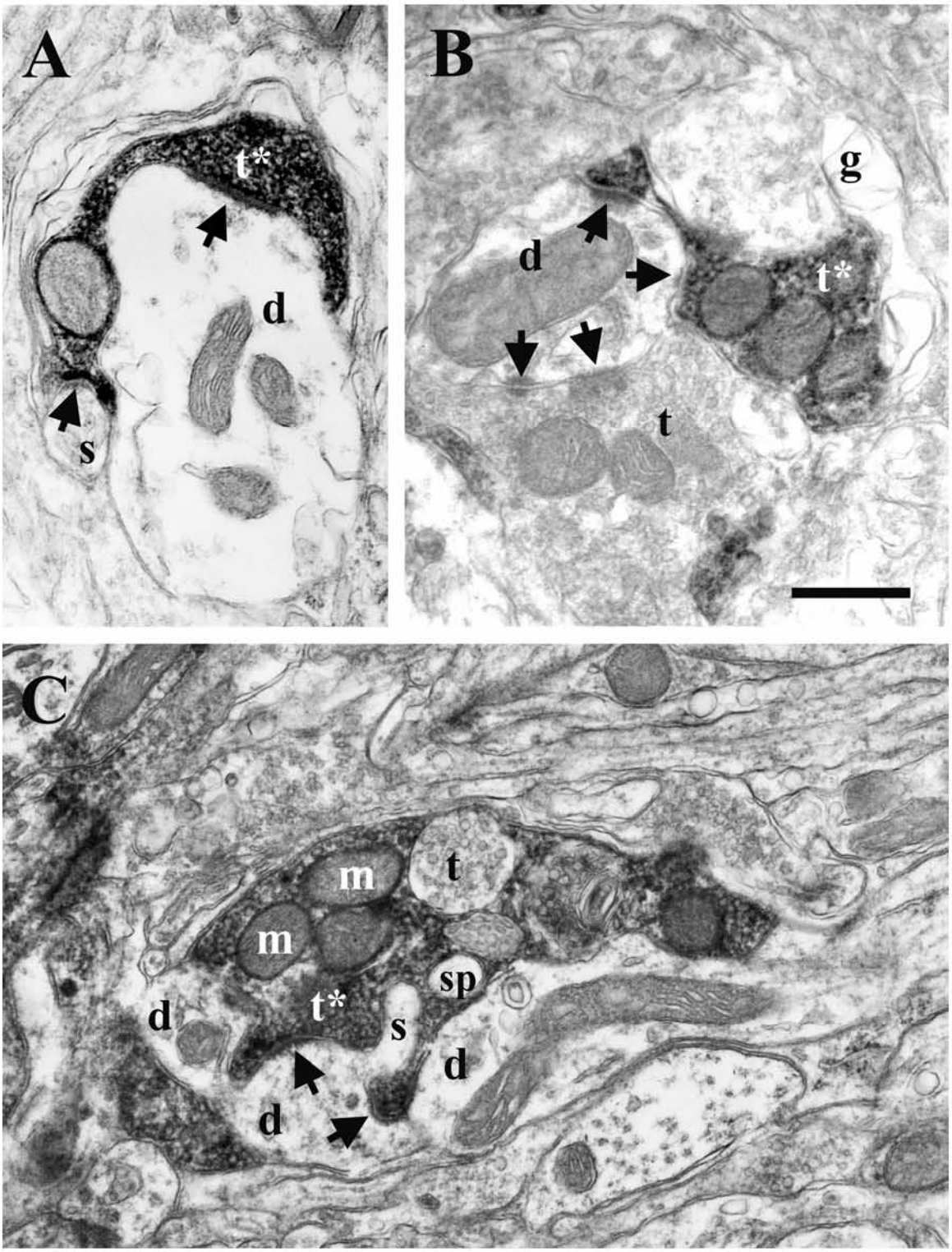

FIGURE 4.

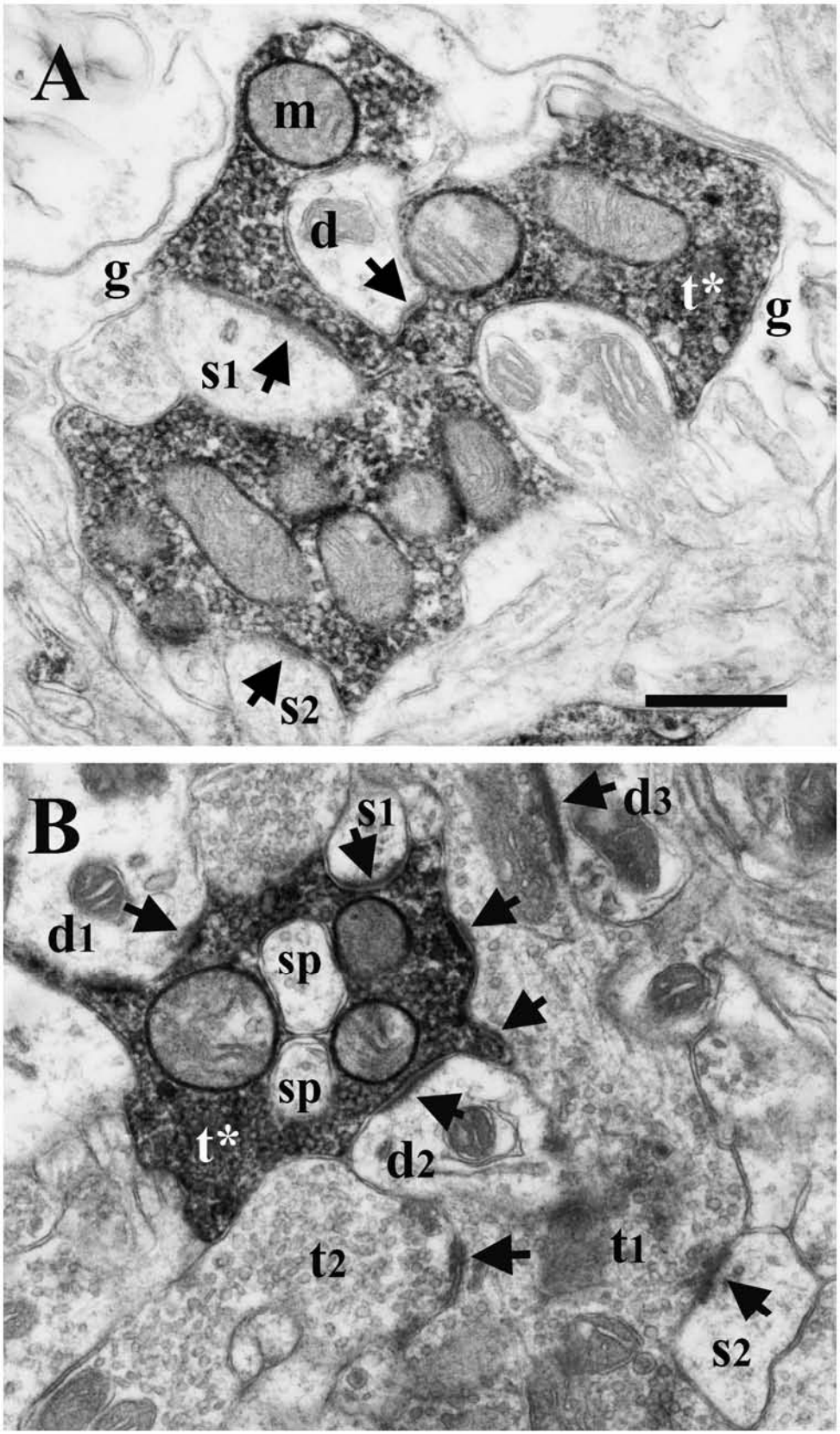

FIGURE 5.

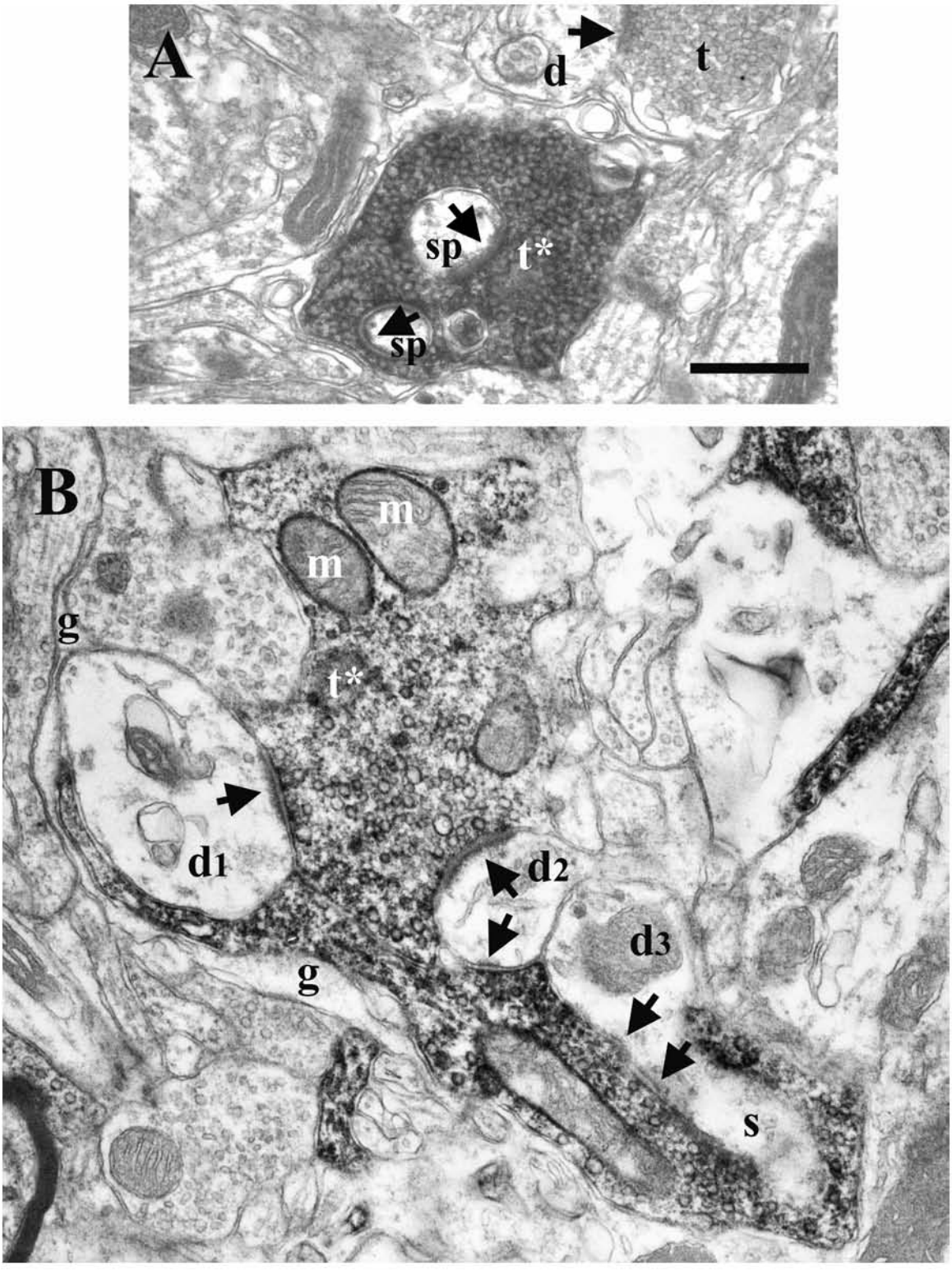

FIGURE 6.

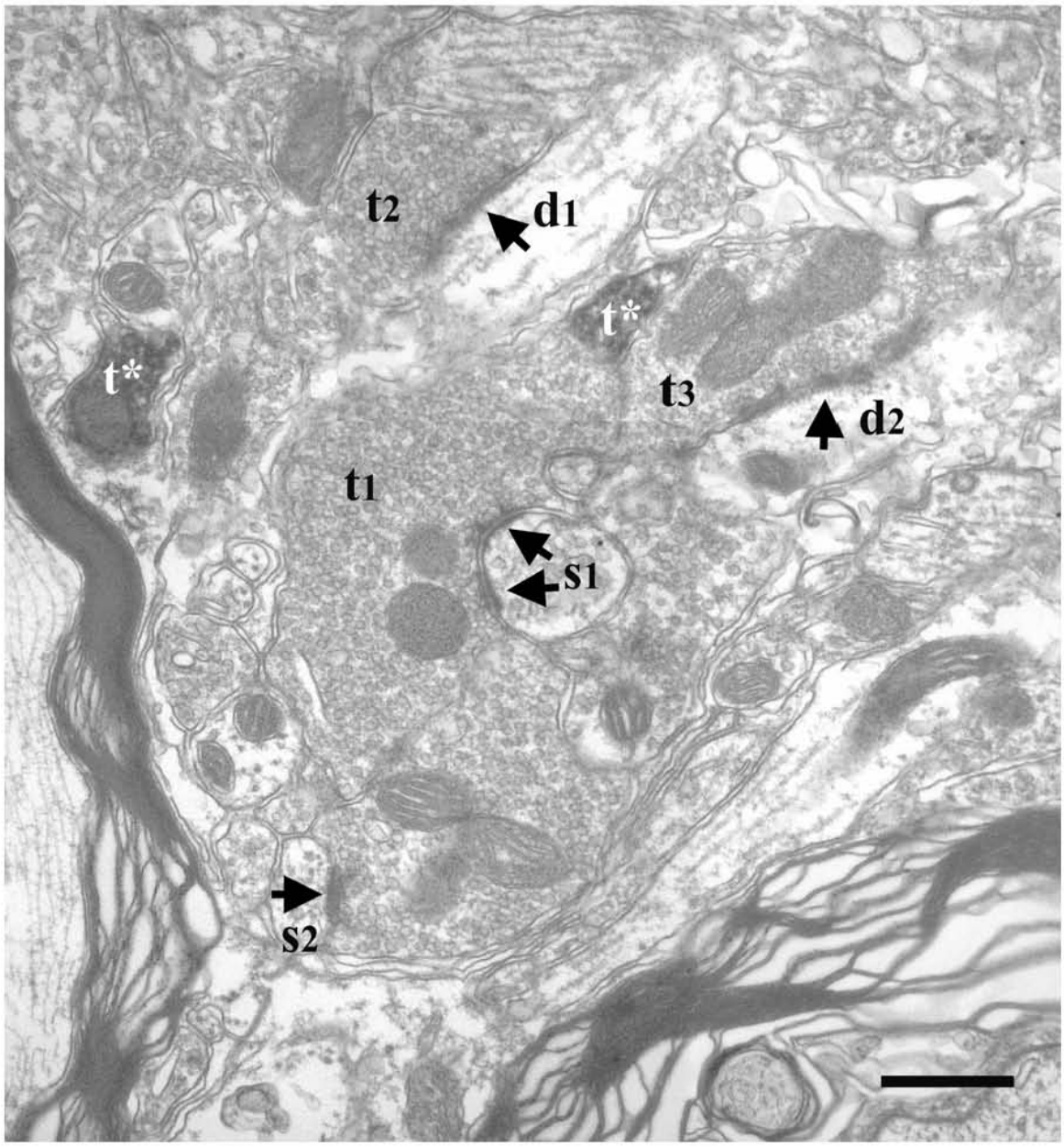

FIGURE 7.

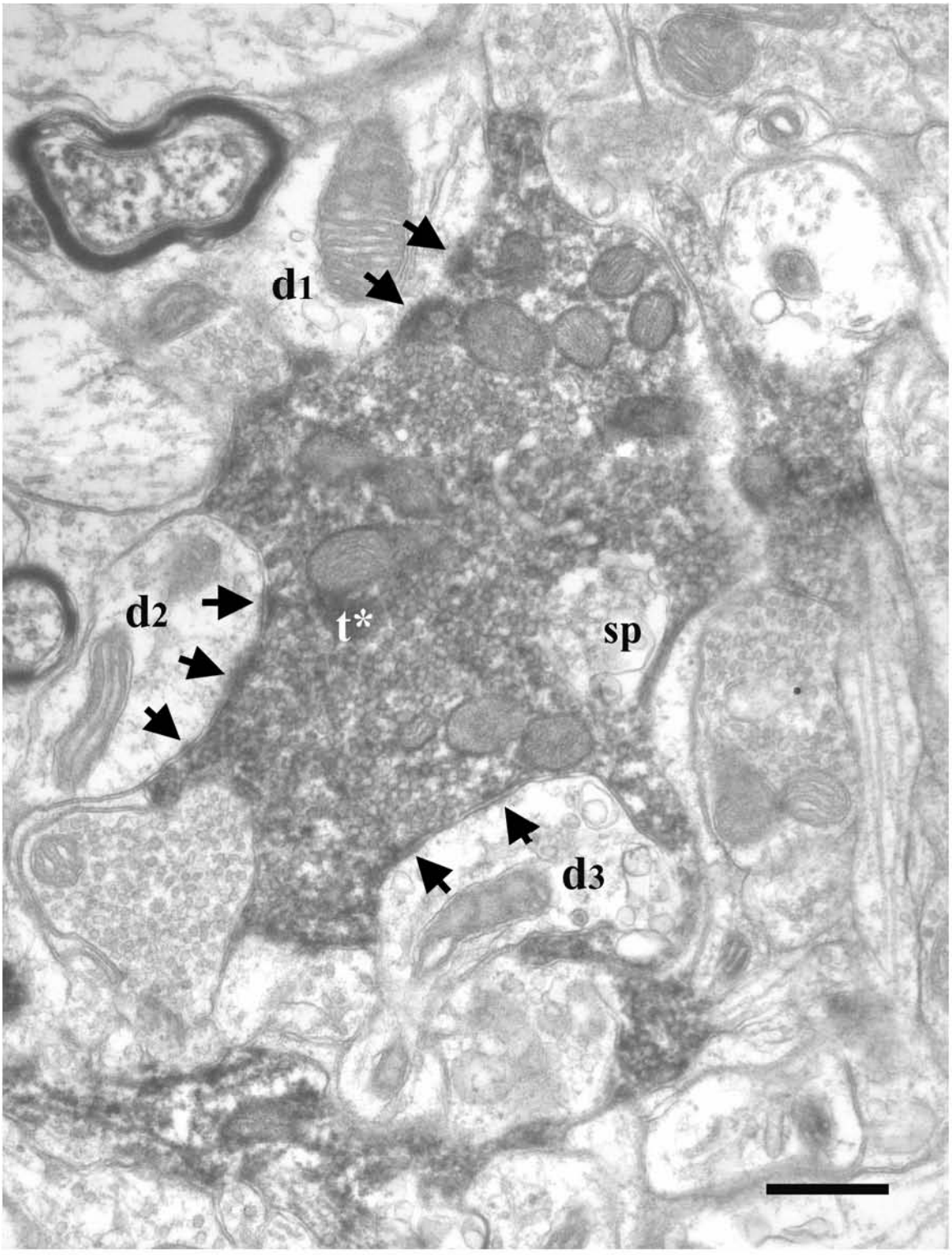

FIGURE 8.

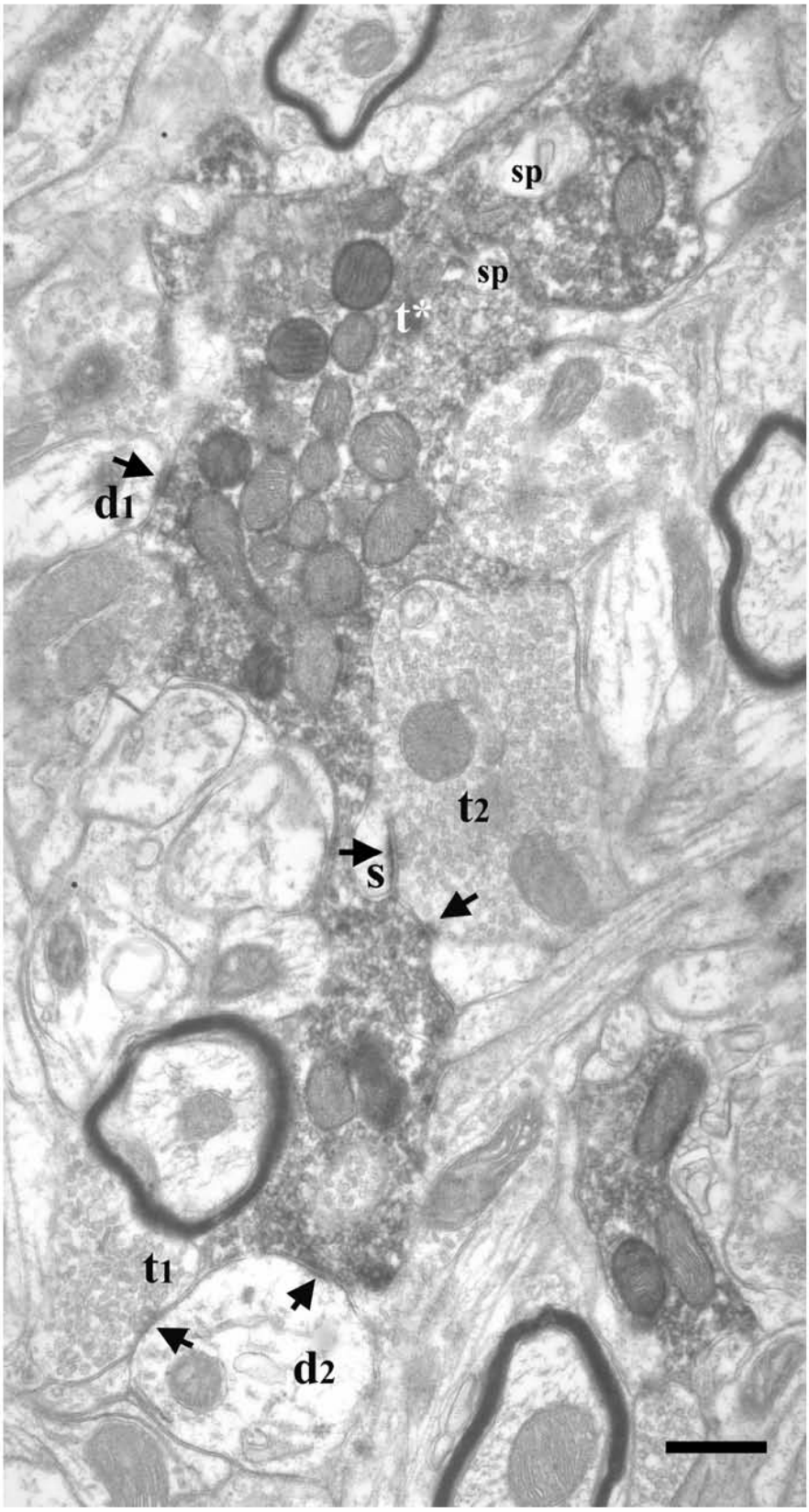

FIGURE 9.

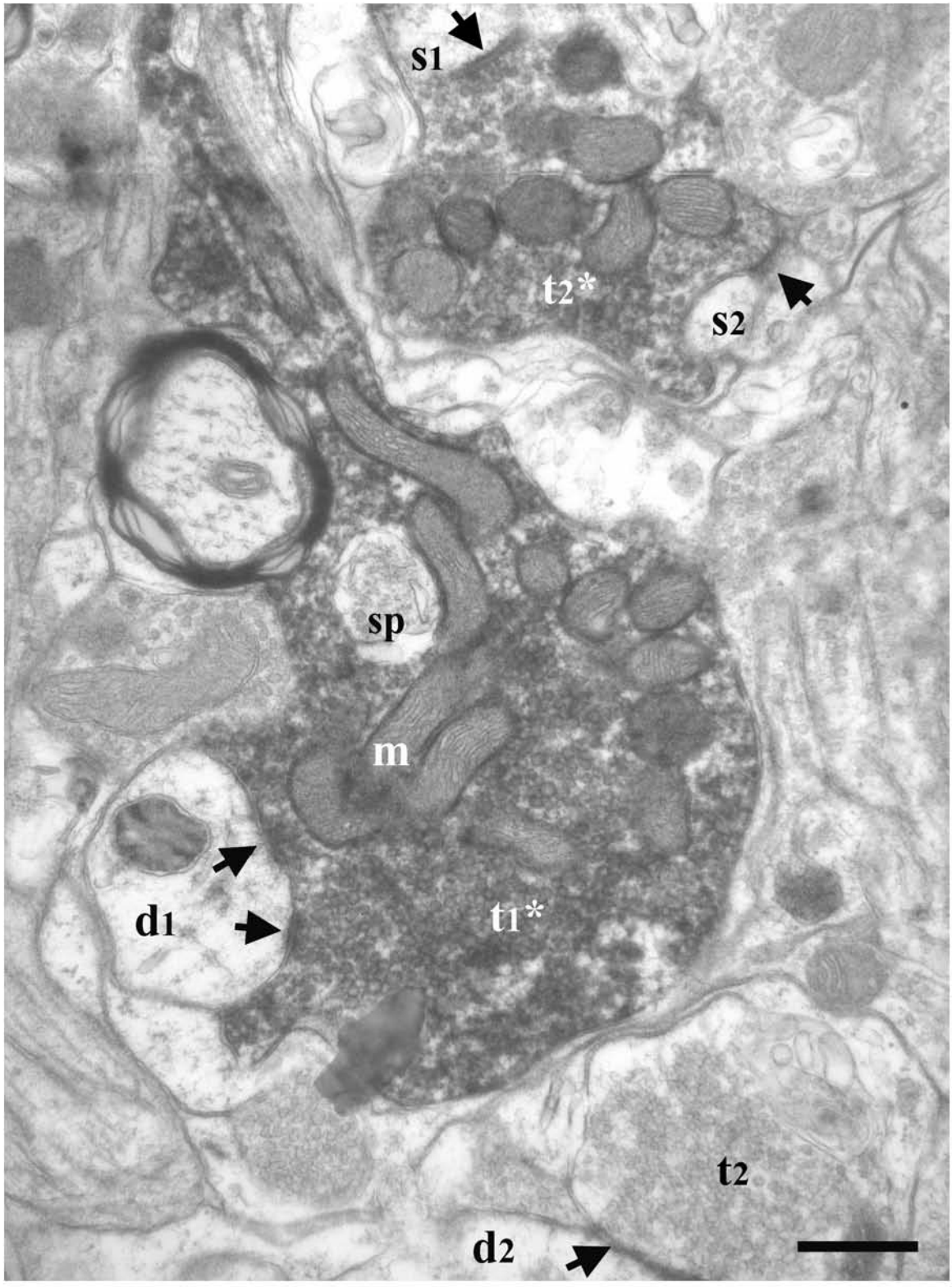

FIGURE 10.

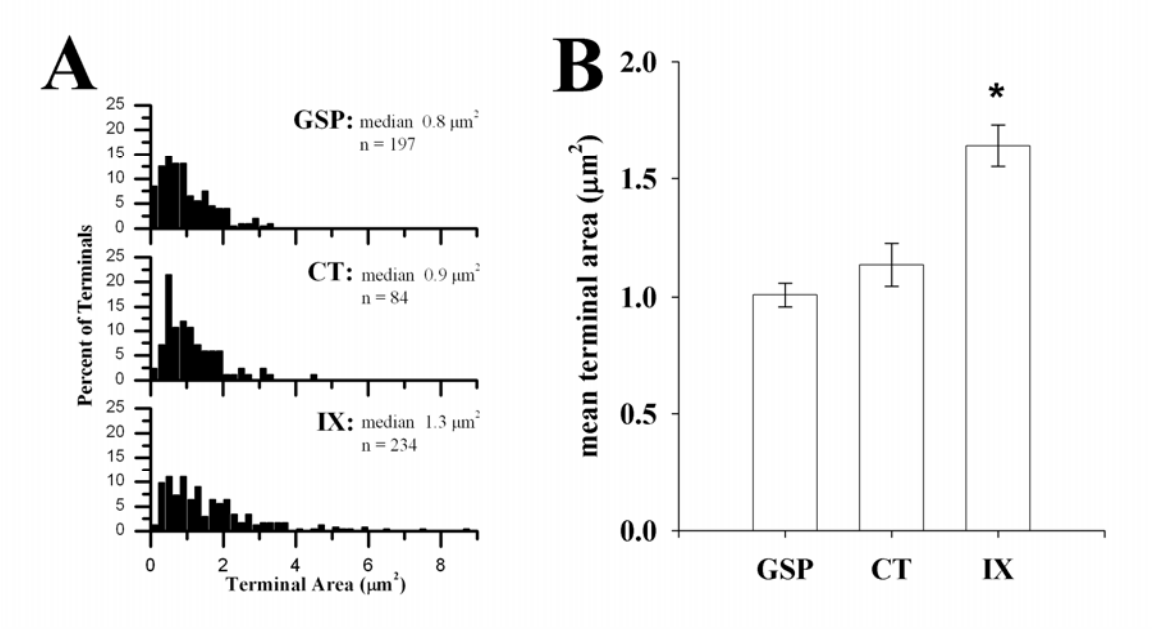

FIGURE 11.

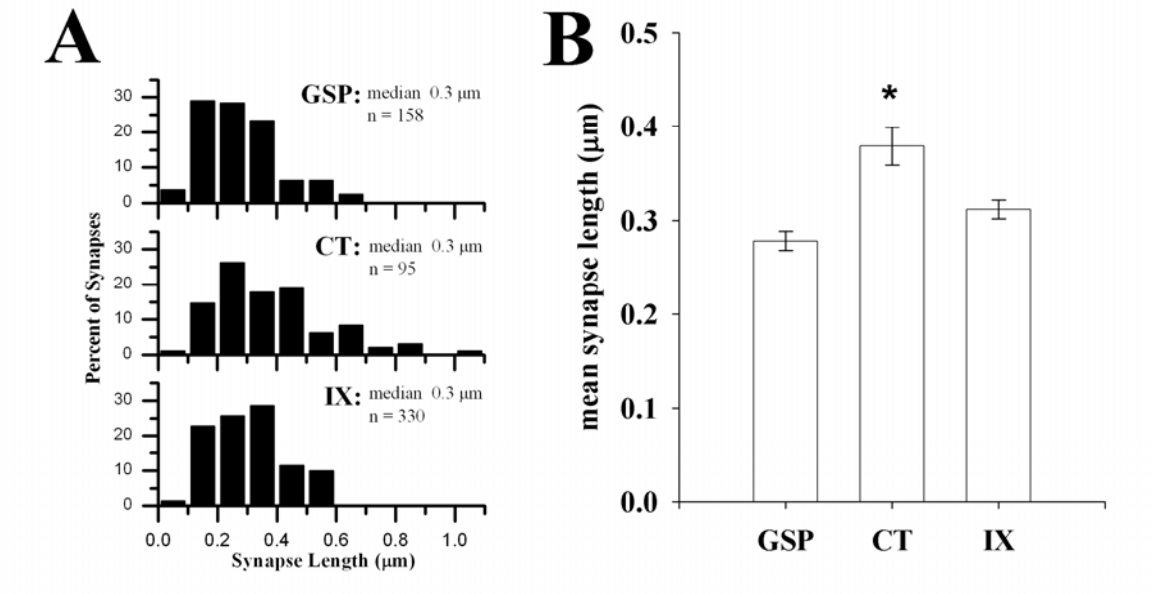

FIGURE 12.

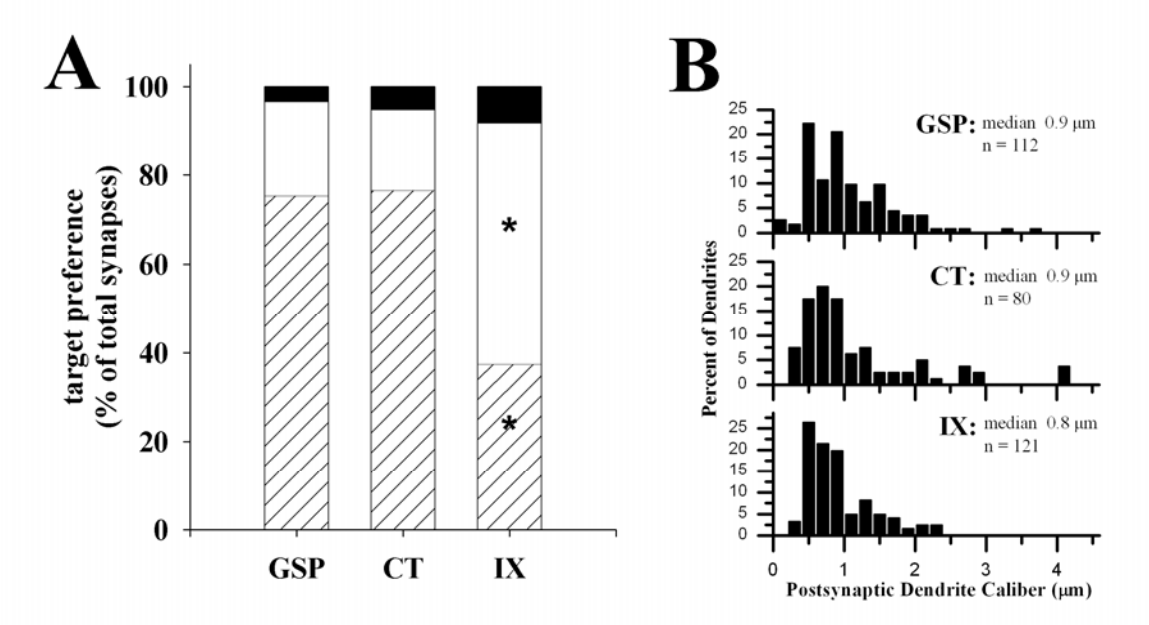

FIGURE 13.

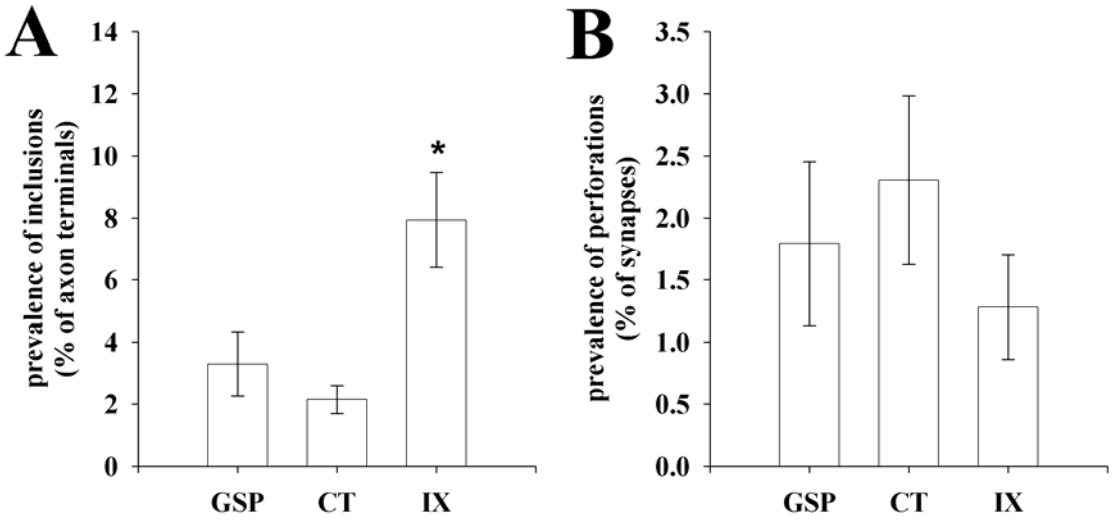

FIGURE 14.

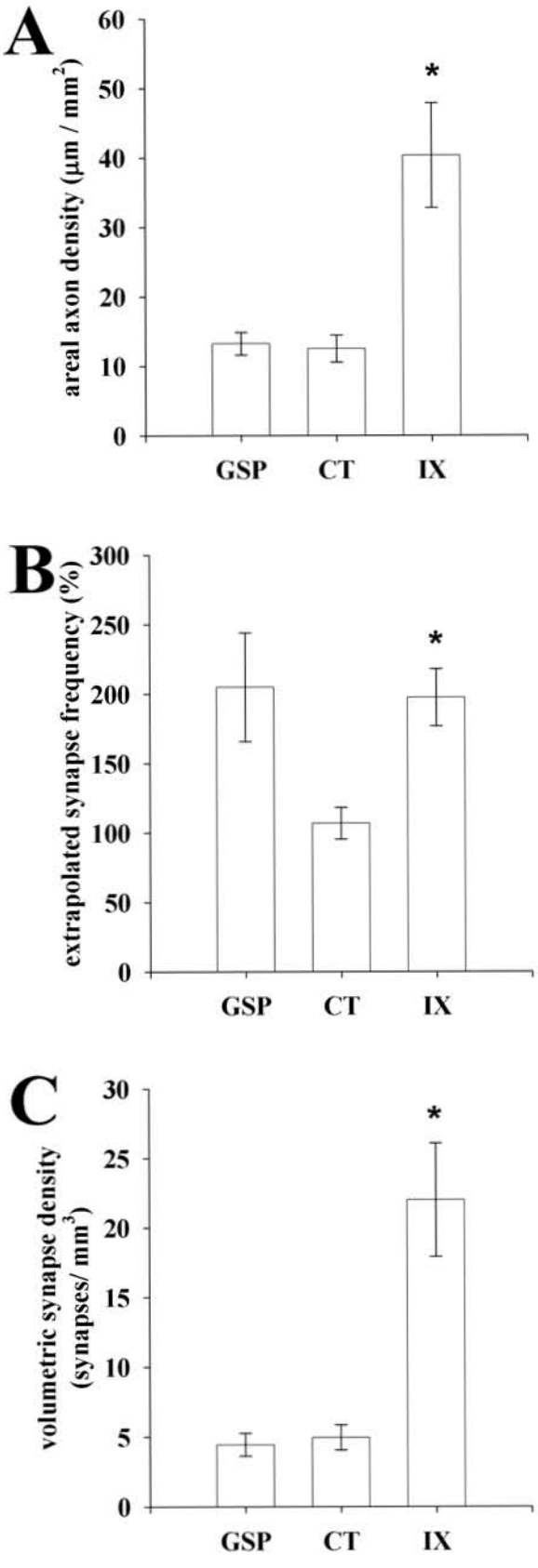
A
areal axon density (µm / mm²)
60
50
40
30
20
10
0
*
GSP
CT
IX
B
extrapolated synapse frequency (%)
300
250
200
150
100
50
0
*
GSP
CT
IX
C
volumetric synapse density (synapses/ mm³)
30
25
20
15
10
5
0
*
GSP
CT
IX

FIGURE 15.

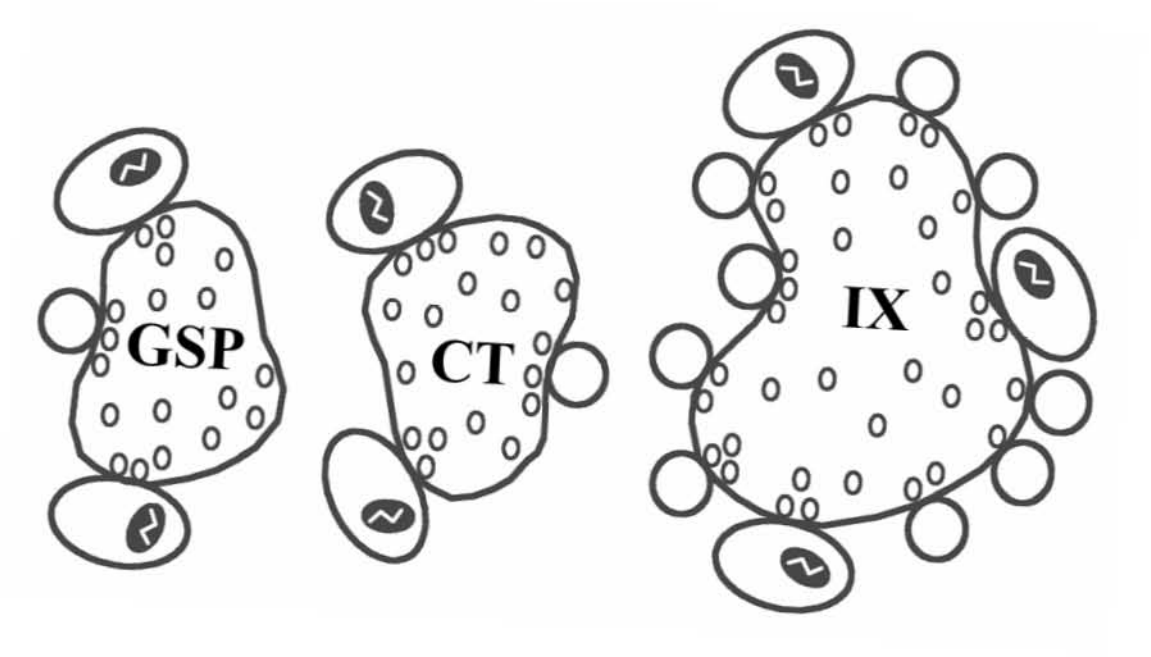

CHAPTER IV

Synaptic Plasticity of Primary Afferent Terminals in the Nucleus of the Solitary Tract of Developmentally Sodium-Restricted Rats: A Comparison Among the Greater Superficial Petrosal, Chorda Tympani, and Glossopharyngeal Nerves.

INTRODUCTION

For every sensory system, established paradigms of sensory deprivation result in a compensatory anatomical reorganization of the brain (vision: Hubel and Wiesel, 1970; somatosensation: Harris and Woolsey, 1981; audition: Smith et al., 1983; olfaction: Frazier and Brunjes, 1987; gustation: May and Hill, submitted). Mediated by plasticity of synaptic connections, such anatomical restructuring has been widely studied at both thalamic and cortical levels (Buonomano and Merzenich. 1998; Katz and Crowley, 2002; Shepherd et al., 2003). However, in the gustatory system, plasticity is evident at the first central synaptic relay in the nucleus of the solitary tract (NTS). This medullary structure receives converging sensory input from three separate nerves: the chorda tympani (CT) nerve, which innervates taste receptor cells located in the anterior tongue, the greater superficial petrosal (GSP) nerve, which innervates taste receptor cells located in the soft palate, and the glossopharyngeal (IX) nerve, which innervates taste receptors on the posterior tongue. However, the manifestations of plasticity in the gustatory NTS have not been identified anatomically at the level of the synapse (i.e., ultrastructrally).

Regionally specific anatomical alterations confined to the dorsal CT terminal field were induced during development by limiting taste experience (Lasiter and Diaz, 1992; Lasiter, 1995), damaging taste receptor cells (Lasiter and Kachele, 1990), and implementing diets low (0.03%; King and Hill, 1991; Krimm and Hill, 1997) and high (6%; Pittman and Contreras, 2002) in NaCl. More recently, May and Hill (submitted) reported that rats maintained on a 0.03% NaCl diet from early gestation showed a 2-fold increase in the volumes of both CT and IX terminal fields. The most profound effects of

this dietary manipulation occurred in the dorsal-most portion of the rostral NTS. CT and IX fields extended past their normal boundaries, significantly increasing the overlap among all gustatory terminal fields. Furthermore, this increase was selective in that the volume of the GSP terminal field was not affected (Sollars and Hill, 2000; May and Hill, submitted). This reorganization of terminal fields may reflect a concomitant alteration in terminal morphology and synaptology of the gustatory inputs into the NTS.

Recently, the ultrastructural properties that define the GSP, CT, and IX axon terminals and their synapses onto postsynaptic targets in the dorsal NTS were described in normal adult rats (May et al., submitted). While GSP, CT, and IX terminals all display similar characteristics of primary afferents (i.e., synaptic vesicle-filled terminals engaging in asymmetric synaptic junctions), these terminals are somewhat distinct in their terminal size, and in their targeting, frequency and density distribution of synapses onto NTS neurons. Most notably, primary differences occurred between IX and both CT and GSP afferents. IX terminals were larger than CT and GSP terminals, they engaged in synaptic contacts more often with dendritic spines (CT and GSP terminals contacted dendritic shafts), and they accounted for the majority of synaptic input to the NTS. Less dramatic but measurable differences in the synapse patterns were observed between CT and GSP terminals.

Since dietary sodium restriction results in specific increases in terminal field volume and increased overlap among terminal fields, corresponding, identifiable changes in synaptic arrangements may occur as well. To discern the specificity and extent of synaptic plasticity in the NTS as a consequence of sodium restriction, the ultrastructure of

labeled GSP, CT, and IX axon terminals from developmentally sodium-restricted rats were examined in dorsal zone of the NTS.

MATERIALS AND METHODS

All animal procedures conformed to NIH guidelines for humane handling of animals, and the Institutional Animal Care Committee at the University of Virginia approved all protocols.

Animals and Tissue Preparation

Nine adult (50-60 days old), female Sprague-Dawley rats raised on a sodium-restricted diet were used to examine the ultrastructural morphology of GSP, CT, and IX nerve axon terminals. Sodium restriction was established by feeding pregnant rats (breeders supplied by Harlan; Indianapolis, Indiana) a 0.03% NaCl diet (ICN Biomedicals, Aurora, OH) and distilled water ad libitum from three days postconception through weaning at 21 days postnatal. The offspring of these mothers were weaned and retained on the same dietary regimen through adulthood. Anterograde labels of the CT, GSP, and IX nerves were individually performed in separate adult animals resulting in three different groups: CT (n=3), GSP (n=3), and IX (n=3). The ultrastructure and synaptology of these experimental animals was compared to previously published data (May et al., submitted) from age-matched control animals maintained on a standard diet consisting of 1% NaCl and tap water ad libitum.

Animals were anesthetized with medetomadine hydrochloride (IM; 0.2 mg/kg) followed by an injection of ketamine (IM; 20 mg/kg) and placed on a water-circulating heating pad to maintain body temperature at 36°C. Upon placement in a non-traumatic

head holder (Erickson, 1966), a ventral approach similar to May and Hill (submitted) was taken to expose either the GSP or CT nerve in the right tympanic bulla or the IX nerve in the ventral side of the neck medial to the tympanic bulla. A longitudinal incision in the ventro-medial portion of the neck was made, and the masseter muscle and the posterior belly of the digastricus muscle were retracted. A small hole was made in the ventral aspect of the tympanic bulla to gain access to the CT and the GSP nerves, and the IXth nerve was exposed dorsal to the hypoglossal nerve. Each nerve was cut peripheral to the ganglia. After a brief application (approximately 20 seconds) of dimethyl sulfoxide (DMSO), crystals of 3 kD Biotinylated Dextran Amine (BDA) (Molecular Probes, Inc., Eugene, OR) were carefully placed on the proximal cut ends of the nerves, and petroleum jelly was applied over the proximal stump to hold dye crystals in place. A piece of parafilm was used to cover the opening created in the tympanic bulla, and a piece of parafilm and petroleum jelly sandwiched the IXth nerve to secure dye placement. The incision was then sutured, and animals were injected with atipamezole (IM; 1 mg/kg) to reverse the effects of medetomadine HCl. Rats recovered from the anesthetic on a heating pad. In accordance with May and Hill (submitted), BDA was allowed to anterogradely transport to the medulla for approximately 24 hours.

Tissue preparation for electron microscopy was identical to the procedures described in May et al. (submitted). Briefly, animals were perfused transcardially with Krebs solution that contained 1% heparin followed by a mixture of 4% paraformaldehyde and 1% gluteraldehyde in 0.1M phosphate buffer (PB, pH 7.4) for 10-30 minutes. Brains were removed and postfixed in 4% paraformaldehyde overnight. The medulla was

blocked and the entire NTS was sectioned horizontally at 50 μm with a vibratome. Tissue sections were collected in 0.1 mM PBS at pH 7.4, treated with 3% sodium borohydride for 30 minutes, and rinsed 10 minutes in phosphate buffer. Then, tissue sections were reacted for biotin by incubation in a 1:100 avidin-biotinylated peroxidase complex in PBS overnight at 4° C, and rinsed in PBS 3 times for 3 minutes. Finally, sections were incubated in 1% Diaminobenzidine (DAB) and 0.0003% H_2O_2 for 5-8 minutes until a dark reaction product was observed.

Embedding

Following postfixation with osmium tetroxide, sections were embedded using standard procedures in preparation for examination on the electron microscope (Hayat, 2000). DAB-stained sections were washed in 0.1M PB and then placed in a 1% osmium tetroxide/PB solution for 1 hour. Sections were rinsed in PB three times for 3 minutes, and dehydrated sequentially in 50% ethanol (ETOH) for 3 minutes, filtered 4% uranyl acetate in 70% ETOH for 1 hour, 70% ETOH for 1 minute, 90% ETOH for 5 minutes, and 100% ETOH three times for 5 minutes. The sections were next rinsed in acetone three times for 10 minutes. The final acetone rinse was replaced with a 1:1 solution of acetone-EPON for 2-4 hours or overnight. This 1:1 mixture was replaced with pure EPON for 2-4 hours or overnight. Finally, the sections were flat embedded between sheets of ACLAR and placed in a 60°C oven overnight.

Light microscopy was used to identify tissue sections that contained terminal field label in the same dorsal plane as sections examined in May et al. (submitted) and where the three nerves project (May and Hill, submitted; Fig. 1). To locate this area, the

outlines of the NTS, DAB-stained terminal fields, and landmarks (e.g., IVth ventricle, myelinated axon bundles, blood vessels) in individual sections were drawn on a camera lucida and compared to corresponding terminal fields characterized in May and Hill (submitted). The sections to be examined with the electron microscope were placed on the bottom of BEEM capsules. The capsules were filled with EPON and polymerized overnight in a 60°C oven. The features of embedded sections were again drawn in detail with the aid of a camera lucida. Ultrathin sections were cut at 90 nm, collected on 200 mesh copper grids, and viewed with a JEOL 1010 electron microscope. Photographs were taken either using an analog film camera, or a 16Mpixel SIA-12C digital camera (Scientific Instruments and Applications, Inc., Duluth, GA), using MaxIm DL CCD software (Diffraction Limited, Ottawa, Ontario, Canada). Photographic film was developed, digitized at 600 dpi with an Epson Perfection 1200 Photo Scanner, and examined at a final 30,000X-50,000X magnification on a computer monitor.

Quantitative analysis

The densely labeled region of the dorsal NTS examined in ultrathin sections was divided arbitrarily into small squares (or samples) by the copper grids on which the ultrathin sections were placed. The area of each sample was determined by taking a series of overlapping pictures at a 1500X magnification; Photoshop 7.0 (Adobe Systems, San Jose, CA) was used to create a montage of these electron micrographs. Each sample was reconstructed, and the area of the square was computed by tracing the perimeter of the neuropil within the grid square, excluding any blood vessels (Image Pro Plus, v4.5;

Media Cybernetics, Inc., Silver Spring, MD). Typically, areas constructed in this manner averaged (± SEM) 6.2 ± 0.3 μm^2.

Each selected grid square was then reexamined systematically with the electron microscope for the presence of DAB-labeled profiles. When a profile was encountered, a photograph was taken at 10,000X magnification. (Regardless of whether the labeled profile contained a synapse, pictures were taken of every labeled profile.) Three animals were labeled for each afferent nerve (IX, GSP, or CT). Three grid squares were examined for each animal, resulting in a total of nine grid squares quantified for each experimental group [IX (n=9), GSP (n=9), and CT (n=9)].

Images of every labeled profile were evaluated for both the presence of a synapse and the identity of the postsynaptic profile (i.e., spine, dendritic shaft, axon terminal, or soma). Synapses were defined by 1) a parallel alignment of a segment of the presynaptic membrane to the postsynaptic membrane, 2) at least three vesicles in a profile, and 3) at least one vesicle in the presynaptic profile in contact with the presynaptic membrane (Colonnier, 1968). Postsynaptic profiles were classified based on their content. A dendritic shaft contained microtubules organized either in parallel or cut perpendicular to their axis or contained mitochondria. Axon terminals contained synaptic vesicles. Cell somas contained endoplasmic reticulum, subsynaptic cisterna, a Golgi apparatus, or a nucleus. Profiles that did not contain any of these features were classified as spines.

Several ultrastructural features were measured, using Image Pro Plus. These measurements included: 1) *synapse length,* the length of the postsynaptic density along the aligned pre- and postsynaptic membranes of the profiles; 2) *presynaptic terminal*

area, the region contained within the perimeter of labeled axonal segments; 3) *long and short calibers,* the maximum length and width of the outlined terminal; 4) *postsynaptic profile area, and long and short calibers,* the region contained within the perimeter of the postsynaptic object and its respective length and width, which was used to determine the relative caliber of the postsynaptic target. These measurements were consistent with the measurements reported in May et al., (submitted).

These measurements were also used to calculate the areal density of labeled axons, the synapse frequency of labeled axons, and the volumetric density of synapses onto labeled axons.

Density of labeled axons: The total axon density represented by all labeled profiles was calculated by summing the extrapolated length of each labeled profile in each sample grid square of tissue, correcting for section thickness (t), and standardizing that total by the measured area of the grid square (a), which is represented by the following formula:

$$Areal\ Axon\ Density\ (\mu m/mm^2) = \frac{\sum\left(\sqrt{C_l^2 - C_s^2}\right) + t}{a}$$

The extrapolated length was determined by using the short caliber (C_s) and the long caliber (C_l) of each labeled profile to estimate the extent of that profile (Erisir and Dreusicke, 2005). This allowed us to compute the total length of axon observed and to report this total length relative to the area of the sample grid.

Synapse frequency of labeled axons: To determine how frequently synapses occurred along labeled axons, we used the following stereological formula (Beaudet and Sotelo, 1981):

$$\textit{Extrapolated synapse frequency (\%)} = \frac{\left(\frac{p_s \times 100}{p}\right)}{\left[\left(\frac{l_s}{D} \times \frac{2}{\pi}\right) + \frac{t}{D}\right]}$$

This formula was used to avoid errors created by the sampling bias introduced by variability in synapse length and axon terminal caliber. The variables in this formula include: the number of labeled profiles (p) that contained a synapse (p_s); the mean diameter of axons (D), which was calculated as the average of the long and short axes of each labeled profile; the average length of the synapse (l_s); the thickness of the section (t; about 90nm). Umbriaco et al. (1994) have shown this extrapolation approach to be consistent in estimating synapse frequency on 3D reconstructed axon segments.

Volumetric density of synapses: The volumetric density (N_V) of labeled synapses was calculated by the formula $N_V = N_A$/ average synapse length (Colonnier and Beaulieu, 1985; DeFelipe et al., 1999). N_A is the number of synapses per area.

Photomicrograph production

Electron photomicrographs used for figure plates were produced by digitizing negative films at a 1600dpi resolution to yield enlargements at 400dpi without resampling the image. In addition, images captured using a 16Mbyte digital camera were displayed at 500dpi and resampled to reduce the electron micrograph to the same magnification as the

digitized negatives. Photoshop 7.0 was used to compose and label the plates. Only the brightness and contrast of the electron micrographs were adjusted.

Statistical Analysis

Mean axon terminal area, synapse length, postsynaptic target preference, postsynaptic target caliber, estimated total axon density, synapsing frequency, and volumetric density of synapses of the GSP, CT, and IX afferent terminals from sodium-restricted rats were compared to GSP, CT, and IX afferent terminals from control rats whose data was previously reported in May et al. (submitted). Statistical analysis of post synaptic target preference, estimated total axon density, synapsing frequency, and volumetric density of synapses was conducted using a priori comparisons. For this statistical analysis, the alpha level of 0.05 was adjusted to reflect the number of comparisons among nerves (0.05/3 comparisons). Non-parametric Mann-Whitney U tests were used to assess significant differences in mean axon terminal area, synapse length, and postsynaptic target caliber. For this statistical analysis, results with an alpha value less than 0.05 were reported as significant.

RESULTS

Qualitative properties of sodium-restricted terminals

At the light microscopic level, DAB-labeled fibers from each gustatory nerve densely terminated in the dorsal portion of the rostral NTS (Fig. 1A). The features of DAB-labeled terminal fields of each gustatory nerve were comparable to fluorescently labeled terminal fields described in May and Hill (submitted). Furthermore, the appearance and orientation of individual axon arbors for each gustatory afferent in

sodium-restricted rats were similar to axon arbors in control rats described in May et al. (submitted). Axon arbors coursed in all directions with no single trajectory, and en passant synapses appeared as swellings along the axons (Fig. 1B). At the light level, the only noticeable difference between control and sodium-restricted DAB-labeled fibers was the density of the labeled fibers. The volume of DAB-labeled nerve fibers from sodium-restricted rats appeared denser than controls (May et al., submitted).

General appearance of sodium-restricted, afferent axon terminals

At the electron microscopic level, DAB-labeled profiles from sodium-restricted rats appeared identical to DAB-labeled profiles from control rats. Each labeled terminal was densely filled with DAB causing it to appear dark. However, the intensity of the label did not obscure cellular membranes, postsynaptic densities, vesicles, or organelles, which would interfere with qualitative and quantitative assessments. Similar to controls (May et al., submitted), gustatory afferent terminals of sodium-restricted rats were, medium to large in size (0.1 μm^2 to 12.2 μm^2), and contained round clear vesicles and dark mitochondria (Figs. 2-7). These terminals formed synapses with dendrites, spines, and other unlabeled axons. However, neuronal cell bodies were not directly contacted by these primary afferents in our observations. Sodium-restricted afferent terminals were observed engaging in both simple synaptic junctions where one terminal formed a synapse with one postsynaptic element (Figs. 2A, 3, 6 & 7) and complex glomeruli (Peters et al., 1970). These glomerular complexes consisted of glia surrounding an axon terminal that formed synapses with more than one postsynaptic target (Fig. 4A). Afferent terminals also engaged in triadic arrangements, where a labeled terminal formed a

synapse with a target, which in turn made a synapse with another profile that was also postsynaptic to the original labeled terminal (Fig. 2B). Configurations such as these were also enclosed in glia. Typical of all excitatory afferents (Peters et al., 1970), synapses associated with labeled terminals were asymmetric. That is, the density of the synaptic junction was thicker postsynaptically. Unlabeled axon terminals, with ultrastructural features similar to labeled axon terminals, were also observed forming asymmetric synapses in the vicinity of labeled axon terminals (Figs. 2B, 3, 4A). In some cases, these unlabeled, excitatory terminals were postsynaptic to labeled terminals (Fig. 2B). Occasionally, both labeled and unlabeled axon terminals contained dense-cored vesicles (Figs. 3 & 5). Spinules (Tarrant and Routtenberg, 1977) and other unlabeled inclusions, which had ultrastructural characteristics of dendrites and axons, protruded into identified GSP, CT, and IX terminals of sodium-restricted rats resulting in a hole-punched appearance of the profile (Figs. 4 & 5). Labeled terminals from all three gustatory nerves in sodium-restricted rats also occasionally displayed perforated postsynaptic densities (Peters and Kaiserman-Abramof, 1969) similar to control rats.

Quantitative analysis of sodium-restricted, afferent axon terminals

In order to detect evidence for ultrastructural plasticity in gustatory primary afferents resulting from developmental sodium restriction, several morphometric parameters were quantified.

Terminal area: In order to determine if dietary sodium restriction affects afferent terminal size, the terminal area of each labeled synaptic profile was measured and compared between control and sodium-restricted rats. The distribution of the area of

GSP, CT, and IX axon terminal endings in sodium-restricted rats was consistent with the sizes of the respective axon terminal endings in controls (Fig. 8A). The mean size (± SEM) of GSP, CT, and IX axon terminals of sodium-restricted rats were not significantly different from the respective axon terminals in controls (Fig. 8B). The mean area (± SEM) of GSP terminals in sodium-restricted rats was 1.0 ± 0.1 μm^2 (v. control: 1.0 ± 0.1 μm^2; $P = 0.6$) and ranged in size from 0.1–4.8 μm^2, and the mean area (± SEM) of CT terminals in sodium-restricted rats was 1.0 ± 0.04 μm^2 (v. control: 1.1 ± 0.1 μm^2; $P = 0.1$) and ranged in size from 0.1–4.0 μm^2. The mean area (± SEM) of IX terminals in sodium-restricted rats was 1.5 ± 0.1 μm^2 (v. control: 1.6 ± 0.1 μm^2; $P = 0.2$) and ranged in size from 0.1–12.2 μm^2. As reported for control afferent terminals, the IX terminals in sodium-restricted rats were also significantly larger than both GSP ($P = 0.0001$) and CT terminals ($P = 0.0001$), but the area of the GSP and CT terminals in sodium-restricted rats did not differ significantly ($P = 0.6$; Fig. 8B).

Synapse length: The efficacy of the synaptic contacts associated with axon terminals can be predicted by the extent of the active zone (Pierce and Lewin, 1994). Thus, in order to determine the effects of dietary sodium manipulation on the efficacy of synapses associated with gustatory afferents, synapse length was also compared between control and sodium-restricted rats among GSP, CT, and IX axons. With a mean length (± SEM) of 0.3 ± 0.01 μm and ranging in size from 0.1-0.9 μm, synapses associated with CT terminals in sodium-restricted rats were significantly shorter than synapses on CT terminals in control rats (v. controls: 0.4 ± 0.02 μm; $P = 0.005$) (Fig. 9). Conversely,

synapses associated with GSP and IX terminals in sodium-restricted rats were significantly longer than synapses with GSP and IX terminals in control rats. GSP terminals in restricted rats had mean lengths (± SEM) of 0.4 ± 0.02 μm (v. controls: 0.3 ± 0.01 μm; $P = 0.0001$) and ranged in size from 0.1-0.7 μm (Fig. 9). CT terminals in restricted rats had mean lengths (± SEM) of 0.4 ± 0.01 μm ($P = 0.0001$) and ranged in size from 0.03-1.1 μm (Fig. 9). Furthermore, CT terminals in sodium-restricted rats were significantly shorter than synapses with GSP terminals and IX terminals ($P < 0.02$ and $P = 0.0001$, respectively; Fig. 9). This result is opposite from that found in control rats (May et al., submitted); synapses on CT terminals were longer than synapses on GSP and IX terminals. Synapses on GSP and IX terminals in sodium-restricted rats did not differ significantly from each other ($P = 0.3$; Fig. 9).

Postsynaptic target preference: Differences in the postsynaptic target preference of GSP, CT, and IX terminals were assessed by determining the percentage of the total number of synapses that occurred on dendrites, spines, and axons for each terminal. There were no significant diet-related differences in the target preferences for GSP and CT terminals (Fig. 10A). For GSP terminals, 78.5 ± 4.8% (v. control: 75.3 ± 6.5%; $P = 0.7$) of the total number of synaptic junctions were formed with dendritic shafts, and 20.1 ± 4.4% (v. control: 21.3 ± 7.5%; $P = 0.9$) of synaptic junctions were formed with dendritic spines. For CT terminals, 80.1 ± 2.3% (v. control: 76.4 ± 5.0%; $P = 0.5$) of active zones were associated with dendrites and 19.0 ± 2.4% (v. control: 18.3 ± 4.6%; $P = 0.9$) of active zones were associated with spines. Both GSP and CT axon terminals in

sodium-restricted rats did not differ significantly in their preference in forming synapses most often with dendritic shafts (P = 0.8; Fig. 10A). However, as reported for controls (May et al., submitted), there was a significant difference in the postsynaptic target preference of IX terminals in sodium-restricted rats. Significantly, more IX terminals formed synapses with spines compared to that of GSP (P = 0.001) and CT (P = 0.0001) terminals (Fig. 10A). Furthermore, there were significant differences between sodium-restricted and control rats in the distribution of synapses associated with IX terminals. Specifically, 57.2 ± 3.7% (v. control: 37.4 ± 2.8%; P = 0.001) of synapses from IX terminals occurred on dendrites and 42.1 ± 3.6% (v. control: 54.3 ± 2.2%; P = 0.01) of synapses from IX terminals occurred on spines (Fig. 10A). Therefore, a significant diet-related shift in synaptic contacts from spines to dendrites occurred with IX terminals.

The relative caliber of the postsynaptic dendrites where synapses were made with GSP, CT and IX terminals were measured in order to derive the proximal distance from the postsynaptic soma. Thus, the results of this measurement may be beneficial in predicting the functional influence each afferent has on the cells of the NTS and in determining the amount of convergence of primary afferents onto these cells. Additionally, a comparison of the relative calibers of the dendrites postsynaptic to GSP, CT, and IX terminals between sodium-restricted and control rats would presumably underscore changes in synapse efficacy (measured by proximity to the cell soma) or convergence resulting from the diet manipulation.

In comparing sodium-restricted rats to controls, there was no measurable difference in the relative caliber of the postsynaptic dendrites of GSP, CT, and IX

terminals. In sodium-restricted rats, GSP terminals formed synapses on dendrites with a mean diameter (± SEM) of 1.0 ± 0.1 μm (v. control: 1.1 ± 0.1 μm; $P = 0.4$) and ranged in size from 0.3-2.4 μm (Fig. 10B). CT terminals in sodium-restricted rats formed synapses on dendrites with a mean diameter (± SEM) of 1.2 ± 0.04 μm (v. control: 1.2 ± 0.1 μm; $P = 0.1$) and ranged in size from 0.3-3.6 μm (Fig. 10B). IX terminals formed synapses on dendrites of a similar caliber to that of controls with a mean diameter (± SEM) of 0.9 ± 0.03 μm (v. control: 0.9 ± 0.4 μm; $P = 0.9$) and ranged in size from 0.3-3.1 μm (Fig. 10B). On average, all afferent terminals formed synapses on relatively medium sized dendrites. Interestingly, CT terminals in sodium-restricted rats formed synapses on slightly larger dendrites than GSP or IX terminals in restricted rats ($P = 0.008$ and $P = 0.0001$). There was not a significant difference in the calibers of dendrites targeted by GSP and IX terminals ($P = 0.7$; Fig. 10B).

Unlabeled inclusions and perforated synapses: In various areas of the brain, an increased presence of spinules or perforated synapses is induced by environmental manipulation and, hence, indicative of synaptic plasticity (Applegate and Landfield, 1988; Schuster et al., 1990; Buchs and Muller, 1996). Similar to control afferent terminals, unlabeled inclusions, often characterized as spinules, dendrites, or vesicle-filled profiles, were also observed inside of GSP, CT, and IX terminals in sodium-restricted rats (e.g., Figs. 4 & 5). However, compared to controls, there was a significant increase in the incidence of these inclusions in CT terminals in sodium-restricted rats. On average, 10.0 ± 1.8% (v. control: 2.1 ± 0.5%; $P = 0.001$) of CT terminals observed within a given area had unlabeled inclusions, which were often identified as spinules

(Fig. 11A). The incidence of unlabeled inclusions in both GSP and IX terminals in sodium-restricted rats was not significantly different from their respective controls. That is, 6.8 ± 1.4% (v. control: 3.3 ± 1.0%; $P = 0.06$) of GSP terminals contained unlabeled inclusions, while 6.3 ± 1.5% (v. control: 7.9 ± 1.5%; $P = 0.5$) of IX terminals contained unlabeled inclusions (Fig. 11A). However, there were no significant differences in the occurrence of these unlabeled inclusions among the different nerve terminals in sodium-restricted rats (CT v. GSP $P = 0.2$, CT v. IX $P = 0.1$, GSP v. IX $P = 0.8$; Fig. 11A). Therefore, a higher incidence of spinules occurred overall in the NTS as a result of sodium restriction.

Perforations in synapses were also observed infrequently among all three gustatory terminals in sodium-restricted rats. On average 1.1 ± 0.7% (v. control: 1.8 ± 0.7%; $P = 0.4$) of the synapses of GSP terminals, 2.0 ± 0.6% (v. control: 2.3 ± 0.7%; $P = 0.8$) of the synapses of CT terminals, and 1.0 ± 0.2% (v. control: 1.3 ± 0.4%; $P = 0.6$) of the synapses of IX terminals were perforated (Fig. 11B). There were also no significant differences in the occurrence of these perforations among the three nerve terminals in sodium-restricted rats (CT v. GSP $P = 0.3$, CT v. IX $P = 0.1$, GSP v. IX $P = 0.9$; Fig. 11B).

Areal axon density: Total axon length was estimated and expressed relative to the area of the region of tissue that was examined in order to provide an estimate of the density of axons represented by each gustatory nerve. Compared to controls, there was a significant increase in the average total density of axon observed for CT and GSP axons in sodium-restricted rats (Fig. 12A). GSP axons occupied a mean length (± SEM) of 25.8

± 4.2 μm/ mm^2 (v. control: 13.2 ± 1.6 μm/ mm^2; $P = 0.01$). CT axons occupied a mean length (± SEM) of 48.6 ± 5.8 μm/ mm^2 (v. control: 12.5 ± 1.9 μm/ mm^2; $P = 0.0001$). Although not significant, the mean total density of axon observed in the dorsal NTS for IX axons in sodium-restricted rats appeared to increase compared to controls (Fig. 12A). IX axons occupied a mean length (± SEM) of 69.3 ± 11.3 μm/ mm^2 (v. control: 40.3 ± 7.6 μm/ mm^2). In sodium-restricted rats, IX and CT axons were significantly denser than GSP axons ($P = 0.002$ and $P = 0.006$, respectively; Fig. 12A). Interestingly, there was not a significant difference in the density of CT and IX axons in sodium-restricted rats ($P = 0.1$; Fig. 12A), whereas IX axons in controls were significantly denser than CT axons (May et al., submitted).

Synapsing frequency of axons: In order to determine if the relative differences in the synapsing patterns of GSP, CT, and IX axons were altered by dietary sodium restriction, the number of synapses on individual afferents was calculated and compared to controls. The calculation measured the probability of a synapse appearing on an axon segment. A result of 100% was interpreted to mean that every labeled axon segment observed had one synapse. Higher scores indicated that each observed axon segment had more than one synapse (e.g., 200% indicates two synapses per axon segment). Conversely, lower scores indicated that not every axon segment observed engaged in synaptic junctions (e.g., 50% indicates a synapse forms on every other axon segment encountered). Compared to their respective controls, synapses occurred significantly less frequently on GSP axons and IX axons in sodium-restricted rats (Fig. 12B). The frequency of synapses on GSP axons occurred at 51.7 ± 27.1% (v. control: 204.7 ±

39.2%; $P = 0.002$). Synapses occurred on IX axons at 117.5 ± 18.7% (v. control: 197.3 ± 20.7%; $P = 0.01$). However, compared to controls, there was not a significant difference in how often synapses occurred on CT axons in sodium-restricted rats. Synapse frequency occurred at 104.6 ± 13.1% (v. control: 106.9 ± 11.4%; $P = 0.9$) for CT axons. Furthermore, in sodium-restricted rats, synapses occurred significantly more often on CT and IX axons than on GSP axons ($P = 0.006$ and $P = 0.007$, respectively; Fig. 12B). There was not a significant difference in synapse frequency between CT and IX axons in sodium-restricted rats ($P = 0.6$; Fig. 12B).

Volumetric density of synapses: The relative density of synapses of labeled axons contained within the measured volume of tissue was also compared between GSP, CT, and IX afferents in sodium-restricted and control rats. Compared to controls, there was a significant 4X increase in the volumetric density of synapses of CT axons in sodium-restricted rats (Fig. 12C). A mean (± SEM) of 16.2 ± 1.7 synapses/ mm^3 (v. control: 4.9 ± 0.9 synapses/ mm^3; $P = 0.0001$) were found on CT axons (Fig. 12C). However, compared to their respective controls, there were no significant differences in the volumetric density of synapses from GSP axons and IX axons in sodium-restricted rats (Fig. 12C). A mean (± SEM) of 4.6 ± 0.7 synapses/ mm^3 were found on GSP axons (v. control: 4.4 ± 0.8 synapses/ mm^3; $P = 0.9$). A mean (± SEM) of 29.6 ± 5.9 synapses/ mm^3 were found on IX axons (v. control: 22.0 ± 4.1 synapses/ mm^3; $P = 0.3$). In control rats (May et al., submitted), IX axons accounted for the bulk of synapses made by gustatory afferents in the dorsal NTS. However, in sodium-restricted rats, the volumetric density of synapses made by IX axons was not significantly different from the volumetric density of

synapses made by CT axons (Fig. 12C). Synapses associated with both CT axons and IX axons in sodium-restricted rats were significantly denser in the dorsal NTS than synapses associated with GSP axons ($P = 0.0001$ and $P = 0.001$, respectively; Fig. 12C).

DISCUSSION

The morphological underpinnings of the central gustatory changes resulting from developmental dietary sodium restriction have been characterized in this study. Compared to controls (May et al., submitted), sodium restriction does not affect the general appearance typical of excitatory nerve terminals (i.e., vesicle shape and asymmetry of synaptic contacts) and does not affect certain distinguishing aspects of GSP, CT, and IX terminals (i.e., terminal area and postsynaptic target). However, distinct differences in the morphology and synaptic arrangements of the terminals of these three gustatory afferents are apparent, indicating a significant restructuring of neuropil.

In consideration of the effects of sodium restriction on the terminal field organization of gustatory nerves (May and Hill, submitted), we hypothesized that synaptic plasticity would be evident at the ultrastructural level that reflected the alterations of this organization. Since this dietary manipulation affected the terminal field morphology of the IXth nerve the greatest followed by the CT nerve, it was predicted that the IXth nerve would also display the most synaptic plasticity. Disruption of the GSP terminal field morphology was not apparent at the light level; therefore, alterations in the synaptic arrangements of GSP terminals were not expected. To the contrary, the results of this study revealed that dietary sodium restriction affects the

synaptic connections of all three gustatory nerves. Moreover, the most striking evidence for synaptic plasticity induced by dietary sodium restriction was reflected in CT axon terminal morphology, making the morphological alterations of IX and GSP terminals appear secondary to the synaptic plasticity associated with the CT nerve. Specifically, the CT nerve had the largest increase in afferent synaptic connections compared to controls, while connections of the IXth and GSP nerves were marginally affected. The most notable changes in both IX and GSP synapse morphology were an increase in synapse length and a decrease in synapse frequency.

Morphological Aberrations Indicative of Plasticity

Further evidence of synaptic plasticity in gustatory terminals was noted by irregularities in axon terminal morphology. Dendritic spinules, which occasionally appeared in the morphological landscape of normal gustatory nerve terminals (May et al., submitted), were also often noted in sodium-restricted rats. A striking 5X increase in these incidences occurred in CT terminals in sodium-restricted rats compared to control rats, but there was not a significant increase for GSP and IX terminals. Spinules, similar to those observed in this study and in May et al. (submitted), have been described in detail in other brain regions including area CA 1 of the hippocampus (Spacek and Harris, 2004), the dentate gyrus of the hippocampus (Tarrant and Routtenberg, 1977), the cerebellum (Eccles et al., 1967), frontal cortex (Cadete-Leite et al., 1986), sensorimotor cortex (Bozhilova-Pastirova and Ovtscharoff, 1999), and visual cortex (Erisir and Dreusicke, 2005). Protrusions of the postsynaptic membrane into presynaptic terminal endings such as these are often regarded as signs of synaptic plasticity. For example, the

frequency of spinules protruding into afferent terminals increases upon induction of long-term potentiation (LTP) in the hippocampus and the dentate gyrus (Applegate and Landfield, 1988; Schuster et al., 1990). In contrast, it appears that decreased activity carried by the CT nerve in sodium-restricted rats (Hill, 1987; Hill and Przekop, 1988; Vogt and Hill, 1993) results in an increased frequency of spinules.

The structural remodeling of dendritic processes provides a measurable representation of spine motility. This is significant with respect to synaptogenesis, since increases in spinules increase the potential for dendritic processes to receive synapses from presynaptic axons. This may be accomplished by either passively increasing the effective target area upon which synapses can form and/or actively recruiting axons with which to form synapses. Thus, the significant increase in spinules associated with CT terminals in sodium-restricted rats may facilitate synaptic plasticity by increasing the potential for these terminals to make synaptic contact with NTS cells.

Perforations of postsynaptic densities have also been implicated as an expression of synaptic plasticity by means of remodeling the synaptic membrane in response to increased activity. For example, in the hippocampus, an increase in perforated synapses also occurs with LTP induction (Buchs and Muller, 1996). In this system, an increase in the incidence of perforations was associated with the formation of new synapses (Toni et al., 2001). Numerous studies have hypothesized that perforated synapses result in the formation of additional synapses through the splitting of the postsynaptic density by the extension of a dendritic spinule (Calverley and Jones, 1990). However, alternative mechanisms for the creation of perforated synapses have also been proposed (Sorra et al.,

1998). Under normal developmental conditions, there was a low occurrence of perforated synapses in gustatory NTS neuropil (May et al., submitted). Dietary sodium restriction did not alter the frequency of these perforations. Furthermore, perforations in postsynaptic densities did not correlate with the increase in the protrusion of dendritic spinules into gustatory axon terminals. Thus, in the gustatory NTS, synaptic membrane remodeling in the form of perforated synapses did not appear related to extensions of dendritic spinules and, instead, appeared to be an intermittent feature of NTS morphology.

Plasticity in Distribution of Synapses

As indicated by areal axon density, developmental sodium restriction resulted in a substantial increase in the density of gustatory axon terminals in the dorsal NTS, but the most dramatic increase in terminal density was the 4-fold increase in CT terminations. Under normal diet conditions, IX axons occupied 4X more volume in the dorsal zone of the NTS compared to CT and GSP axons (May et al., submitted). However, with dietary sodium restriction, the density of CT axonal input was comparable with axonal input from the IXth nerve. Although CT terminal density was the most affected by dietary sodium-restriction, it is interesting that a trend of increased afferent terminal density occurred for the GSP and IX nerves as well. This trend, however, was not completely consistent with the specific increases in terminal field volume induced by sodium restriction reported in May and Hill (submitted). At the light microscopic level, developmental sodium restriction resulted in significant increases in both CT and IX terminal field volume in the dorsal zone of the NTS, but with no changes in the GSP

terminal field volume. Thus, ultrastructural analysis of these individual gustatory terminals reveals further evidence that the axonal input of the GSP nerve is affected as well by dietary sodium manipulation.

Synaptic Arrangement of Gustatory Afferents

With significant increases in axon density due to sodium restriction, a concomitant remodeling of the synaptic arrangements occurred uniquely for the three nerves. The model in figure 13 illustrates the synaptic arrangements of each gustatory nerve in the dorsal NTS resulting from density and frequency measurements of synapses.

GSP: For GSP axons, sodium restriction resulted in a 4-fold decrease in the frequency of synapses occurring on axon terminals. An average of two synaptic contacts were made for every identified axon terminal in control rats, but synaptic contacts were made less often in sodium-restricted rats. However, despite the decreased frequency of synapses occurring on an individual axon terminal, the overall density of synapses from GSP terminals in restricted rats did not change. Therefore, in order to maintain the same number of synapses and a decreased synaptic frequency, synapses must be distributed more diffusely upon single GSP terminals and additional GSP terminals must present in the neuropil of sodium-restricted rats (Fig. 13).

IX: Sodium restriction also resulted in a decreased frequency of synapses appearing on IX terminals. Normally, an average of two synapses appeared on every axon terminal; however, sodium restriction reduced the occurrence of synaptic contacts to an average of one per axon terminal. As with GSP terminals in sodium-restricted rats, the density of synapses associated with IX terminals in sodium-restricted rats in the

dorsal NTS did not change. Thus, as with GSP terminals in sodium-restricted rats, synapses were distributed more diffusely along the IX axon terminals in sodium-restricted rats (Fig. 13). A potential contributing factor to the redistribution of synapses associated with IX terminals may be related to the capacity of the postsynaptic target to receive synapses. Normally, the majority of large IX terminals form synapses with spines, allowing for a substantial increase in the packing density of the synaptic contacts with NTS cells. However, in sodium-restricted rats, half of the synapses made by IX terminals were with dendrites. Thus, by contacting dendritic shafts directly, large, individual IX terminals would be potentially relegated further from their target NTS soma, since the packing density of synaptic contacts upon dendrites can not be as compact as the density with spines.

CT: In contrast to the GSP and IXth nerves, the frequency of synapses occurring on CT axon terminals in sodium-restricted rats did not differ from controls. However, sodium restriction uniquely affected the density of synapses associated with CT terminals in the dorsal NTS. Specifically, the number of synapses associated with CT terminals in sodium-restricted rats quadrupled compared to control rats. Hence, as a result of sodium restriction, many more synapses associated with CT terminals were added without changing how frequently synapses occurred on individual axon terminals. Considering the parallel 4-fold increase in the total estimated CT axon length in sodium-restricted rats, the 4-fold increase in synapse density of CT terminals in sodium-restricted rats without a change in synapse frequency indicates that more synapses are present in the dorsal NTS. Furthermore, these additional synapses occur at the same interval on individual CT

terminals as in controls. Therefore, additional axon terminals are present in sodium-restricted rats, and each terminal bears the same number of synaptic contacts as their counterparts in control rats (Fig. 13). It is notable that dietary sodium manipulation results in a similar density of synaptic input to the dorsal NTS from both the CT and IXth nerves. This further highlights the dramatic increase in synapses associated with CT terminals as a result of developmental sodium restriction.

The synaptic contact of these additional terminals with NTS cells is potentially mediated by the increased presence of dendritic spinules, which may serve to recruit these additional terminals to their targets. With the addition of synaptic CT terminals to the neuropil of sodium-restricted rats, the distribution of these additional terminals onto NTS cells must be considered, as well. A population of CT terminals in sodium-restricted rats formed synapses with significantly larger caliber dendrites than GSP or IX terminals. Thus, these additional CT terminals form synaptic contacts closer to the soma of NTS cells than GSP and IX terminals, perhaps due to the competition for available synaptic sites.

Taken as a whole, developmental dietary sodium restriction affects the arrangement of synaptic terminations from each gustatory nerve uniquely. Considering that these terminations converge in the dorsal NTS vying for the same postsynaptic targets, it is possible that alterations in the synaptic arrangements of one gustatory nerve influences the synaptic arrangements of the other two gustatory nerves. That is, the addition of extra synapse-bearing axon terminals (i.e., CT terminals) will affect the dynamics of axonal terminations from all three gustatory nerves. A likely scenario for

the convergence of gustatory nerves onto NTS cells in sodium-restricted rats involves a restructuring or redistribution of synapses from GSP and IX axon terminals to accommodate the additional synaptic terminals of CT axons.

Wiring of the Gustatory Circuitry

May and Hill (submitted) described specific alterations in terminal field organization for the CT and IX nerves of sodium-restricted rats that involved a gross disruption of the normal boundaries of each terminal field. Upon electron microscopic inspection, it is now evident that not only are afferent terminals errant from their normal organization, but synaptic connections made by those terminals are uniquely altered as well. Traditional hypotheses for the link between dietary manipulation and anatomical alterations to the gustatory system have focused on activity-dependent effects (King and Hill, 1991; Krimm and Hill, 1997). This hypothesis is attractive because the terminations of the CT nerve, whose responsiveness to taste stimuli with sodium salt is selectively reduced as a result of sodium restriction (Hill, 1987; Hill and Przekop, 1988), undergoes the most plasticity (King and Hill, 1991; Lasiter and Diaz, 1992; Lasiter, 1995; Krimm and Hill, 1997; Pittman and Contreras, 2002). However, activity dependence on sodium alone cannot completely account for the unique reorganization of gustatory circuits of each nerve because not all gustatory nerves are highly responsive to NaCl (Formaker and Hill, 1991; Kitada et al., 1998). Furthermore, the dietary manipulation is implemented and terminal fields develop before taste receptors are able to functionally process chemical stimuli (Mistretta, 1972; Lasiter et al., 1989; Lasiter, 1992). Therefore, the basis for the plasticity induced by sodium restriction must lie fundamentally within the

processes that set up these individual afferent connections with their postsynaptic targets. Once connections are established, activity dependence may play a secondary role in the refinement of gustatory input. Perhaps this is why synapses associated with CT terminals are so abundant in sodium-restricted rats compared both to the synapses associated with CT terminals in controls and to the synapses associated with GSP and IX terminals in sodium-restricted rats. These additional synapses may have not been pruned due to the lack of adequate stimulation necessary to establish the appropriate, precise connections. This hypothesis is consistent with data from the normal development of gustatory nerve terminal fields; a 30% reduction in the total volume of the CT terminal field occurs between postnatal day 27 and adulthood (Hill et al., 2003).

Plasticity of Postsynaptic Elements

As an accompaniment to the alterations of the presynaptic inputs of sodium-restricted rats, the morphology of NTS neurons and their associated synaptic structures are also affected by dietary manipulation. Dietary sodium restriction results in gross increases in dendritic length and number (King and Hill, 1993). As shown here, spine motility, as evidenced by an increased incidence of spinules, increases as a whole. Hence, dietary sodium restriction also disrupts the normal arrangement of postsynaptic elements. These alterations may also influence the dynamics of synapse formation; however, it is not clear if alterations in the postsynaptic targets actively direct synaptic changes or if they are affected as a result of synaptic changes.

Implications for Function and Behavior

As a result of the modification of the axonal input from each gustatory afferent by developmental sodium restriction, corresponding functional alterations are also likely to occur. Indeed, changes in synaptic morphology can alter synaptic function and affect receptor targeting (Calverley and Jones, 1990). Furthermore, spine motility and dendritic restructuring can modulate the availability of postsynaptic targets (Dunaevsky et al., 2001; Deng and Dunaevsky, 2005) and lead to functional changes. Therefore, the normal degree of convergence of individual gustatory afferents onto NTS cells may be grossly altered as a result of dietary sodium restriction. Presumably, such changes in the connectivity of gustatory afferents would be reflected in the functional output of NTS cells. In fact, in sodium-restricted rats, a selective decrease in taste responses to sodium salt stimuli occurs in NTS neurons driven by stimulation of taste receptors of the CT nerve (Vogt and Hill, 1993). Upon repletion of dietary sodium, a substantial increase in neural taste responses exclusively to sodium salts occurs beyond that recorded in controls (Vogt and Hill, 1993). Thus, a hyper-responsiveness to sodium stimuli upon recovery from sodium restriction may physiologically represent the increased density of synaptic contacts associated with the CT nerve. (This assumes a lack of synaptic plasticity following dietary recovery.) Furthermore, alterations in the functional output of NTS cells would likely affect taste-mediated perception and behavior. Thus, the plasticity of both the pre- and postsynaptic elements of the gustatory relay of the NTS as a result of developmental dietary manipulation has important implications on the central processing of taste stimuli and related behaviors.

LITERATURE CITED

Applegate MD, Landfield PW. 1988. Synaptic vesicle redistribution during hippocampal frequency potentiation and depression in young and aged rats. J Neurosci 8:1096-1111.

Beaudet A, Sotelo C. 1981. Synaptic remodeling of serotonin axon terminals in rat agranular cerebellum. Brain Res 206:305-329.

Bozhilova-Pastirova A, Ovtscharoff W. 1999. Intramembranous structure of synaptic membranes with special reference to spinules in the rat sensorimotor cortex. Eur J Neurosci 11:1843-1846.

Buchs PA, Muller D. 1996. Induction of long-term potentiation is associated with major ultrastructural changes of activated synapses. Proc Natl Acad Sci U S A 93:8040-8045.

Buonomano DV, Merzenich MM. 1998. Cortical plasticity: from synapses to maps. Annu Rev Neurosci 21:149-186.

Cadete-Leite A, Tavares MA, Paula-Barbosa MM, Gray EG. 1986. 'Perforated' synapses in frontal cortex of chronic alcohol-fed rats. J Submicrosc Cytol 18:495-499.

Calverley RK, Jones DG. 1990. Contributions of dendritic spines and perforated synapses to synaptic plasticity. Brain Res Brain Res Rev 15:215-249.

Colonnier M. 1968. Synaptic patterns on different cell types in the different laminae of the cat visual cortex. An electron microscope study. Brain Res 9:268-287.

Colonnier M, Beaulieu C. 1985. An empirical assessment of stereological formulae applied to the counting of synaptic disks in the cerebral cortex. J Comp Neurol 231:175-179.

DeFelipe J, Marco P, Busturia I, Merchan-Perez A. 1999. Estimation of the number of synapses in the cerebral cortex: methodological considerations. Cereb Cortex 9:722-732.

Deng J, Dunaevsky A. 2005. Dynamics of dendritic spines and their afferent terminals: spines are more motile than presynaptic boutons. Dev Biol 277:366-377.

Dunaevsky A, Blazeski R, Yuste R, Mason C. 2001. Spine motility with synaptic contact. Nat Neurosci 4:685-686.

Eccles JC, Ito MSJ, Szentagothai J. 1967. The cerebellum as a neuronal machine. New York: Springer. p 127-130.

Erickson R. 1966. Nontraumatic headholders for mammals. Physiol Behav 1:97-98.

Erisir A, Dreusicke M. 2005. Quantitative morphology and postsynaptic targets of thalamocortical axons in critical period and adult ferret visual cortex. J Comp Neurol 485:11-31.

Formaker BK, Hill DL. 1991. Lack of amiloride sensitivity in SHR and WKY glossopharyngeal taste responses to NaCl. Physiol Behav 50:765-769.

Frazier LL, Brunjes PC. 1988. Unilateral odor deprivation: early postnatal changes in olfactory bulb cell density and number. J Comp Neurol 269:355-370.

Harris RM, Woolsey TA. 1981. Dendritic plasticity in mouse barrel cortex following postnatal vibrissa follicle damage. J Comp Neurol 196:357-376.

Hayat MA. 2000. Principles and techniques of electron microscopy. Biological applications. New York: Cambridge University Press.

Hill DL. 1987. Susceptibility of the developing rat gustatory system to the physiological effects of dietary sodium deprivation. J Physiol 393:413-424.

Hill DL, Przekop PR, Jr. 1988. Influences of dietary sodium on functional taste receptor development: a sensitive period. Science 241:1826-1828.

Hill DL, Sollars SI, May OL. 2003. Plasticity of the developing central gustatory brainstem. Chem Senses 28:J3.

Hubel DH, Wiesel TN. 1970. The period of susceptibility to the physiological effects of unilateral eye closure in kittens. J Physiol 206:419-436.

Katz LC, Crowley JC. 2002. Development of cortical circuits: lessons from ocular dominance columns. Nat Rev Neurosci 3:34-42.

King CT, Hill DL. 1991. Dietary sodium chloride deprivation throughout development selectively influences the terminal field organization of gustatory afferent fibers projecting to the rat nucleus of the solitary tract. J Comp Neurol 303:159-169.

King CT, Hill DL. 1993. Neuroanatomical alterations in the rat nucleus of the solitary tract following early maternal NaCl deprivation and subsequent NaCl repletion. J Comp Neurol 333:531-542.

Kitada Y, Mitoh Y, Hill DL. 1998. Salt taste responses of the IXth nerve in Sprague-Dawley rats: lack of sensitivity to amiloride. Physiol Behav 63:945-949.

Lasiter PS. 1992. Postnatal development of gustatory recipient zones within the nucleus of the solitary tract. Brain Res Bull 28:667-677.

Lasiter PS. 1995. Effects of orochemical stimulation on postnatal development of gustatory recipient zones within the nucleus of the solitary tract. Brain Res Bull 38:1-9.

Lasiter PS, Diaz J. 1992. Artificial rearing alters development of the nucleus of the solitary tract. Brain Res Bull 29:407-410.

Lasiter PS, Kachele DL. 1990. Effects of early postnatal receptor damage on development of gustatory recipient zones within the nucleus of the solitary tract. Brain Res Dev Brain Res 55:57-71.

Lasiter PS, Wong DM, Kachele DL. 1989. Postnatal development of the rostral solitary nucleus in rat: dendritic morphology and mitochondrial enzyme activity. Brain Res Bull 22:313-321.

May OL, Erisir A, Hill DL. 2005. Characterization of the ultrastructural morphology of the greater superficial petrosal, chorda tympani, and glossopharyngeal axons in the nucleus of the solitary tract in rat. (submitted).

May OL, Hill DL. 2005. Gustatory terminal field organization and developmental plasticity in the nucleus of the solitary tract revealed through triple fluorescent labeling. (submitted).

Mistretta CM. 1972. Topographical and histological study of the developing rat tongue, palate and taste buds. In: Bosma JF, Editor. Oral Sensation and Perception III. The Mouth of the Infant. Springfield: Charles C Thomas. p 163-187.

Peters A, Kaiserman-Abramof IR. 1969. The small pyramidal neuron of the rat cerebral cortex. The synapses upon dendritic spines. Z Zellforsch Mikrosk Anat 100:487-506.

Peters A, Palay SL, Webster HdF. 1970. The fine structures of the nervous system. New York: Harper and Row.

Pierce JP, Lewin GR. 1994. An ultrastructural size principle. Neuroscience 58:441-446.

Renehan WE, Massey J, Jin Z, Zhang X, Liu YZ, Schweitzer L. 1997. Developmental changes in the dendritic architecture of salt-sensitive neurons in the nucleus of the solitary tract. Brain Res Dev Brain Res 102:231-246.

Schuster T, Krug M, Wenzel J. 1990. Spinules in axospinous synapses of the rat dentate gyrus: changes in density following long-term potentiation. Brain Res 523:171-174.

Shepherd GM, Pologruto TA, Svoboda K. 2003. Circuit analysis of experience-dependent plasticity in the developing rat barrel cortex. Neuron 38:277-289.

Siekevitz P. 1985. The postsynaptic density: a possible role in long-lasting effects in the central nervous system. Proc Natl Acad Sci U S A 82:3494-3498.

Smith ZD, Gray L, Rubel EW. 1983. Afferent influences on brainstem auditory nuclei of the chicken: n. laminaris dendritic length following monaural conductive hearing loss. J Comp Neurol 220:199-205.

Sollars SI, Hill DL. 2000. Lack of functional and morphological susceptibility of the greater superficial petrosal nerve to developmental dietary sodium restriction. Chem Senses 25:719-727.

Sorra KE, Fiala JC, Harris KM. 1998. Critical assessment of the involvement of perforations, spinules, and spine branching in hippocampal synapse formation. J Comp Neurol 398:225-240.

Spacek J, Harris KM. 2004. Trans-endocytosis via spinules in adult rat hippocampus. J Neurosci 24:4233-4241.

Tarrant SB, Routtenberg A. 1977. The synaptic spinule in the dendritic spine: electron microscopic study of the hippocampal dentate gyrus. Tissue Cell 9:461-473.

Toni N, Buchs PA, Nikonenko I, Povilaitite P, Parisi L, Muller D. 2001. Remodeling of synaptic membranes after induction of long-term potentiation. J Neurosci 21:6245-6251.

Umbriaco D, Watkins KC, Descarries L, Cozzari C, Hartman BK. 1994. Ultrastructural and morphometric features of the acetylcholine innervation in adult rat parietal cortex: an electron microscopic study in serial sections. J Comp Neurol 348:351-373.

Vogt MB, Hill DL. 1993. Enduring alterations in neurophysiological taste responses after early dietary sodium deprivation. J Neurophysiol 69:832-841.

Wu K, Sachs L, Carlin RK, Siekevitz P. 1986. Characteristics of a Ca2+/calmodulin-dependent binding of the Ca2+ channel antagonist, nitrendipine, to a postsynaptic density fraction isolated from canine cerebral cortex. Brain Res 387:167-184.

FIGURE LEGENDS

Figure 1. Light micrographs of DAB-labeled chorda tympani (CT) nerve terminal field in the dorsal nucleus of the solitary tract (NTS) of a developmentally sodium-restricted, adult rat. **A.** A horizontal section through the brainstem displaying the densely labeled terminal field in the dorsal NTS. The border of the NTS is outlined (dotted line). The boxed area is magnified in B. R; rostral. L; lateral. **B.** Higher magnification of the periphery of the dense network of terminal field reveals the projection pattern of CT axon fibers, which displayed frequent swellings (arrowheads). Scale bar equals 10 μm.

Figure 2. Electron micrographs of DAB-labeled greater superficial petrosal (GSP) terminals in the dorsal zone of the NTS of a sodium-restricted rat. **A.** A labeled, vesicle-filled terminal (t*) forms synapses (arrows) on a dendrite (d) and vesicle-filled profile (t). **B.** A labeled terminal (t1*) engaged in a synaptic triad forms asymmetric synapses (arrows) on both a spine (s) and an unlabeled terminal (t). The unlabeled terminal (t) contains a dense-cored vesicle (arrowhead) and forms a synapse (arrow) on the same spine (s) as the labeled terminal (t1*). Glia (g) surrounds the entire arrangement including an additional labeled terminal (t2*) and a dendrite (d). Scale bar in B equals 0.5 μm.

Figure 3. Electron micrograph of DAB-labeled GSP terminal in the dorsal zone of the NTS of a sodium-restricted rat. The labeled terminal (t*) forms a synapse (arrow) on a dendritic shaft (d1), which is also engaged in a synaptic junction (arrow) with an unlabeled terminal (t). This unlabeled terminal contains dense-cored vesicles

(arrowheads). Additionally, the unlabeled terminal forms an excitatory synapse (arrow) on another segment of a dendrite (d2). Scale bar equals 0.5 μm.

Figure 4. Electron micrographs of DAB-labeled CT terminals in the dorsal zone of the NTS of a sodium-restricted rat. **A.** Two different labeled terminals (t1*, t2*) contain unlabeled inclusions. Some unlabeled inclusions observed in labeled profiles were assumed to be cross-sections of protruding spines and, hence, were labeled spinules (sp). Other unlabeled inclusions were identified as axon segments (t) when they contained synaptic vesicles. One of the labeled terminals (t1*) forms synapses (arrows) with two separate dendrites (d1, d2). An unlabeled terminal (t1) is also forming a synapse (arrow) with one of these dendrites (d1). Surrounding glia (g) suggests a glomerular structure. m; mitochondria. **B.** A labeled terminal (t*) that encloses both a spine and a vesicle-filled profile (t). This terminal (t*) forms synapses (arrows) with both a spine (s) that it surrounds and an unlabeled terminal (t1) that surrounds the labeled terminal. Scale bar in B equals 0.5 μm.

Figure 5. Electron micrograph of DAB-labeled CT terminals in the dorsal zone of the NTS of a sodium-restricted rat. Two labeled terminals (t1*, t2*) contain many spinules (sp) or other unlabeled inclusions (d3). Spines (s) protrude into both terminals. One of the labeled terminals (t1*) contains dense-cored vesicles (arrowheads) and forms synapses (arrows) with 2 separate dendrites (d1, d2) and a spinule. Scale bar equals 0.5 μm.

Figure 6. Electron micrograph of DAB-labeled IX terminals in the dorsal zone of the NTS of a sodium-restricted rat. Three closely apposed, labeled terminals (t1*, t2*,

t3*) are densely filled with synaptic vesicles. One terminal (t1*) forms a synapse (arrow) on a dendrite (d1). Another terminal (t2*) forms a synapse on spine. Scale bar equals 0.5 μm.

Figure 7. Electron micrograph of a large DAB-labeled glossopharygeal (IX) terminal in the dorsal zone of the NTS of a sodium-restricted rat. This terminal (t*) forms synapses (arrows) with three different spines (s1, s2, s3). Scale bar equals 0.5 μm.

Figure 8. A. Frequency distribution histogram comparing the terminal areas of DAB-labeled GSP, CT, and IX axons in control (outline) and sodium-restricted (solid bars) rats, measured on terminals that contained a synapse. Frequencies for each nerve are displayed as a percentage of the total to allow visual comparison between groups. The distribution of terminal area for GSP, CT and IX axons was not altered by diet manipulation. Similar to controls, in sodium-restricted rats a population of IX axon terminals were observed that were significantly larger than GSP and CT terminals. Median and population size (n) are indicated for each nerve in sodium-restricted rats. **B.** Mean terminal areas of GSP, CT, and IX axons in control (open bars) and sodium-restricted (closed bars) rats. Error bars indicate standard error. The square indicates a statistical significance of $P < 0.05$ within comparisons between gustatory nerves of sodium-restricted rats.

Figure 9. A. Frequency distribution histogram of the synapse lengths of GSP, CT, and IX axon terminals in control (outline) and sodium-restricted (solid bars) rats. Frequencies for each nerve are displayed as a percentage of the total to allow visual comparison between groups. Median and population size (n) are indicated for each nerve

in sodium-restricted rats. **B.** Mean synapse length of GSP, CT, and IX axon terminals in control (open bars) and sodium-restricted (closed bars) rats. In comparing sodium-restricted rats to controls, synapses associated with GSP and IX axon terminals are longer, while synapses associated with CT axon terminals are shorter (asterisks indicate an alpha value less than 0.05). In comparing the three gustatory afferents within sodium-restricted rats, synapses found on CT axon terminals were significantly shorter than synapses on GSP and IX terminals (square indicates alpha values less than 0.05). Error bars indicate standard error.

Figure 10. A. Preference for the postsynaptic targets of GSP, CT, and IX axons in control (open bars) and sodium-restricted (closed bars) rats. Preference is indicated by the percentage of total synapses terminating on dendrites (hatched bars), spines (open bars), and axons (closed bars). In sodium-restricted rats, the majority synapses of GSP and CT axon terminals occurred on dendrites while the majority of synapses of IX terminals occurred on spines (squares indicate a statistical significance of $P < 0.02$). Compared to controls, a significant shift from the targeting of spines to the targeting of dendrites occurred in IX terminals of sodium-restricted rats (asterisks indicate a statistical significance of $P < 0.02$). **B.** Frequency distribution histogram of the caliber of the dendrites postsynaptic to GSP, CT, and IX axon terminals in control (outline) and sodium-restricted (solid bars) rats. Frequencies for each nerve are displayed as a percentage of the total to allow visual comparison between groups. In sodium-restricted rats, a population of CT terminals contacted larger caliber dendrites than GSP and IX

terminals. Median and population size (n) are indicated for each nerve in sodium-restricted rats.

Figure 11. **A.** Mean percentage of GSP, CT, and IX axon terminals in control (open bars) and sodium-restricted (closed bars) rats that contained unlabeled inclusions. In sodium-restricted rats, CT terminals contained significantly more of these inclusions than controls (asterisk indicates a statistical significance of $P < 0.02$). **B.** Mean percentage of postsynaptic densities associated with GSP, CT, and IX axon terminals in control (open bars) and sodium-restricted (closed bars) rats that were perforated. Perforations of postsynaptic densities were rarely observed for each nerve terminal. The incidence of perforations was not altered by dietary manipulation. (See Results for definitions.) Error bars indicate standard error.

Figure 12. **A.** Areal axon density of GSP, CT, and IX axons in control (open bars) and sodium-restricted (closed bars) rats per mm^2 of the dorsal NTS. In comparing the total axon density of gustatory nerves of sodium-restricted rats to controls, GSP and CT axons were significantly denser upon dietary manipulation (asterisks indicate a statistical significance of $P < 0.02$). However, the CT and IX axons of sodium-restricted rats were denser than GSP axons located in the same region (squares indicate a statistical significance of $P < 0.02$). **B.** Extrapolated synapse frequency of GSP, CT, and IX axons in control (open bars) and sodium-restricted (closed bars) rats. Compared to controls, synapses occurred less frequently on GSP and IX axons in sodium-restricted rats (asterisks indicate a statistical significance of $P < 0.02$). However, in comparing the synapse frequency between gustatory axons in sodium-restricted rats, CT and IX axons

formed synapses at a significantly higher frequency than GSP axons (squares indicate a statistical significance of $P < 0.02$). **C.** Volumetric density of synapses associated with GSP, CT, and IX axons in control (open bars) and sodium-restricted (closed bars) rats. Dietary sodium manipulation resulted in a significant four-fold increase in the number of synapses present on CT axons compared to controls (asterisk indicates a statistical significance of $P < 0.02$). In the NTS of sodium-restricted rats, significantly more synapses were associated with CT and IX axons compared to GSP axons (squares indicate a statistical significance of $P < 0.02$). See Methods for calculations. Error bars indicate standard error.

Figure 13. Model of synapse plasticity of gustatory primary afferents in the dorsal NTS. GSP, IX, and CT axon terminals (ellipses) of control and sodium-restricted rats form synapses (filled circles) on dendritic shafts and spines. **GSP:** As a result of sodium restriction, the frequency of synapses associated with GSP axon terminals decreases, but the density of synaptic input by GSP afferents does not change. Thus, compared to controls, additional axon terminals bear fewer synaptic contacts. **IX:** IX axon terminals are larger than GSP and CT terminals. Similar to GSP afferents, synapses occur less frequently on individual terminals of the IXth nerve of sodium-restricted rats; however, the density of synaptic input from this nerve does not change. Therefore, compared to controls, fewer synaptic contacts occur on additional, individual axon terminals. Interestingly, a larger percentage of IX axon terminals in sodium-restricted rats formed synapses on dendrites compared to controls. **CT:** Compared to controls, synapses associated with CT axon terminals in sodium-restricted rats quadrupled in

density, but the number of synapses associated with each individual axon terminal was not different. Therefore, compared to controls, CT axon terminals in sodium-restricted rats engaged in more synaptic contacts by increased axonal input. These additional synapse bearing axon terminals targeted larger caliber dendrites compared to axon terminals of the GSP and IX nerves in sodium-restricted rats.

FIGURE 1.

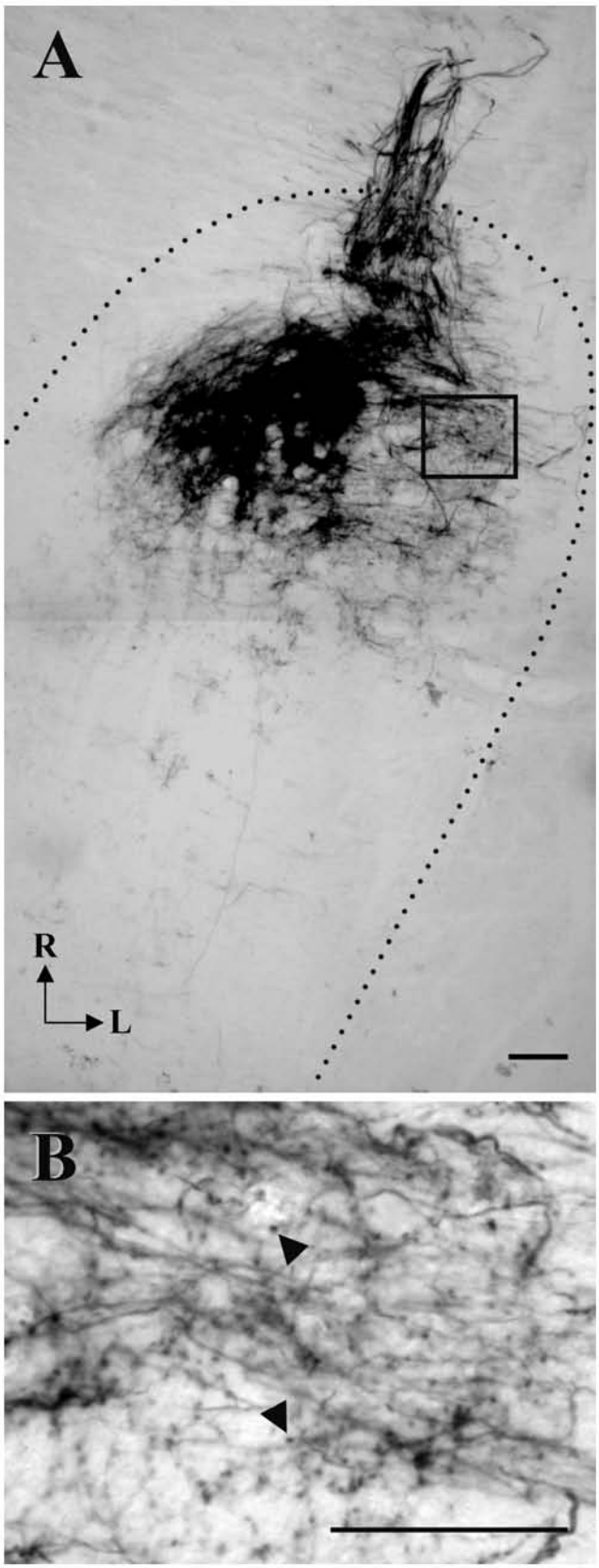

FIGURE 2.

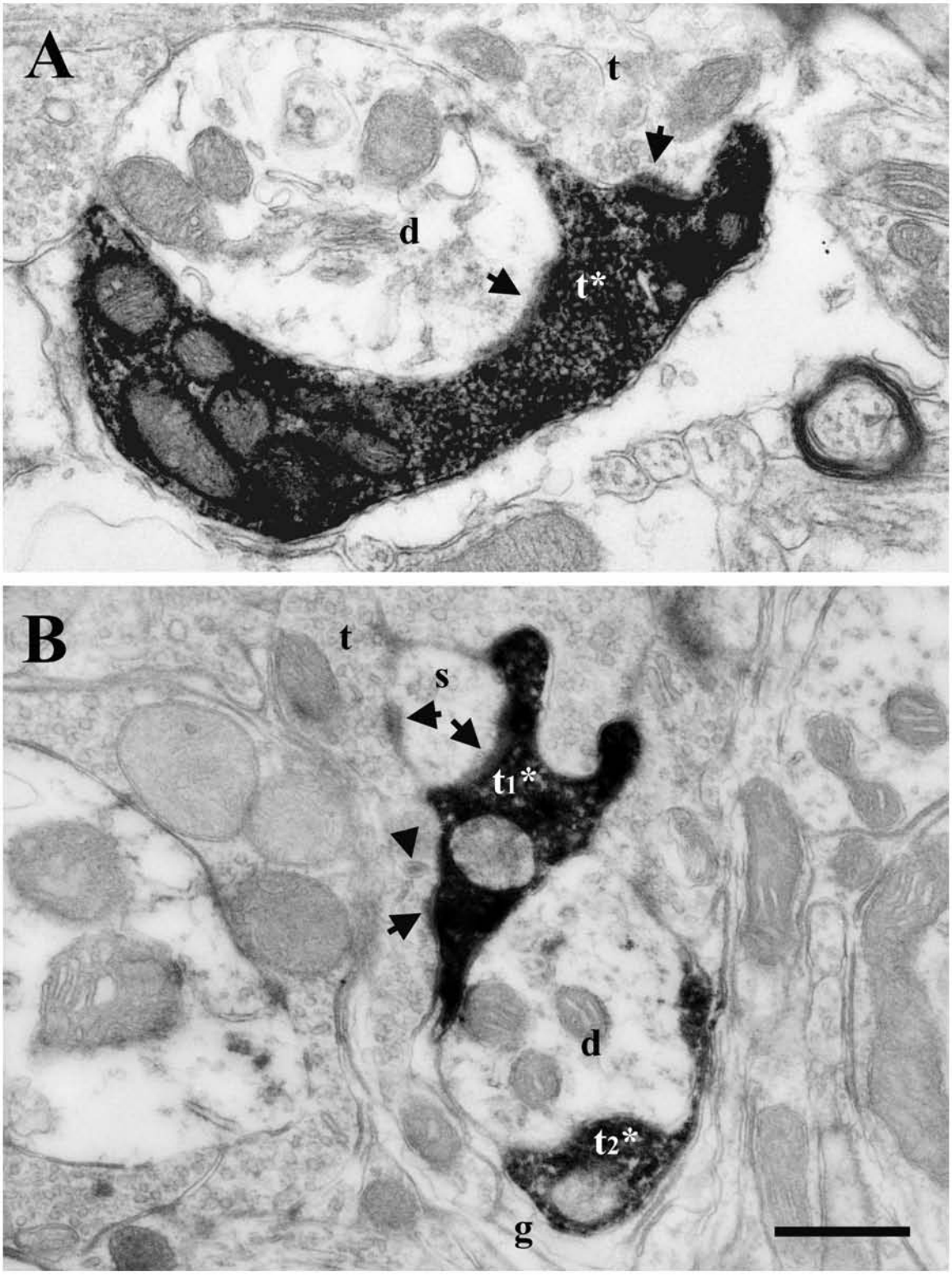

FIGURE 3.

FIGURE 4.

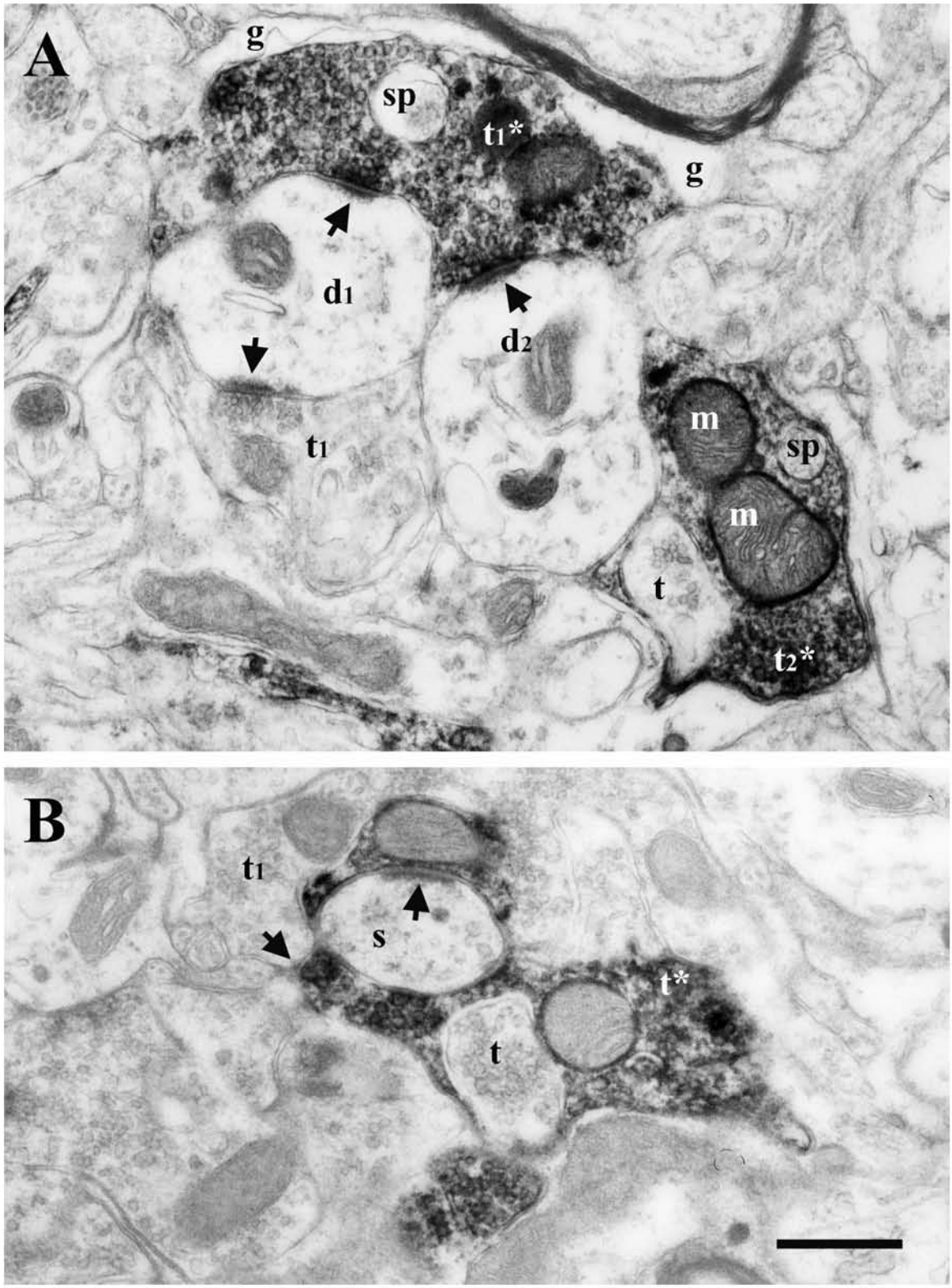

FIGURE 5.

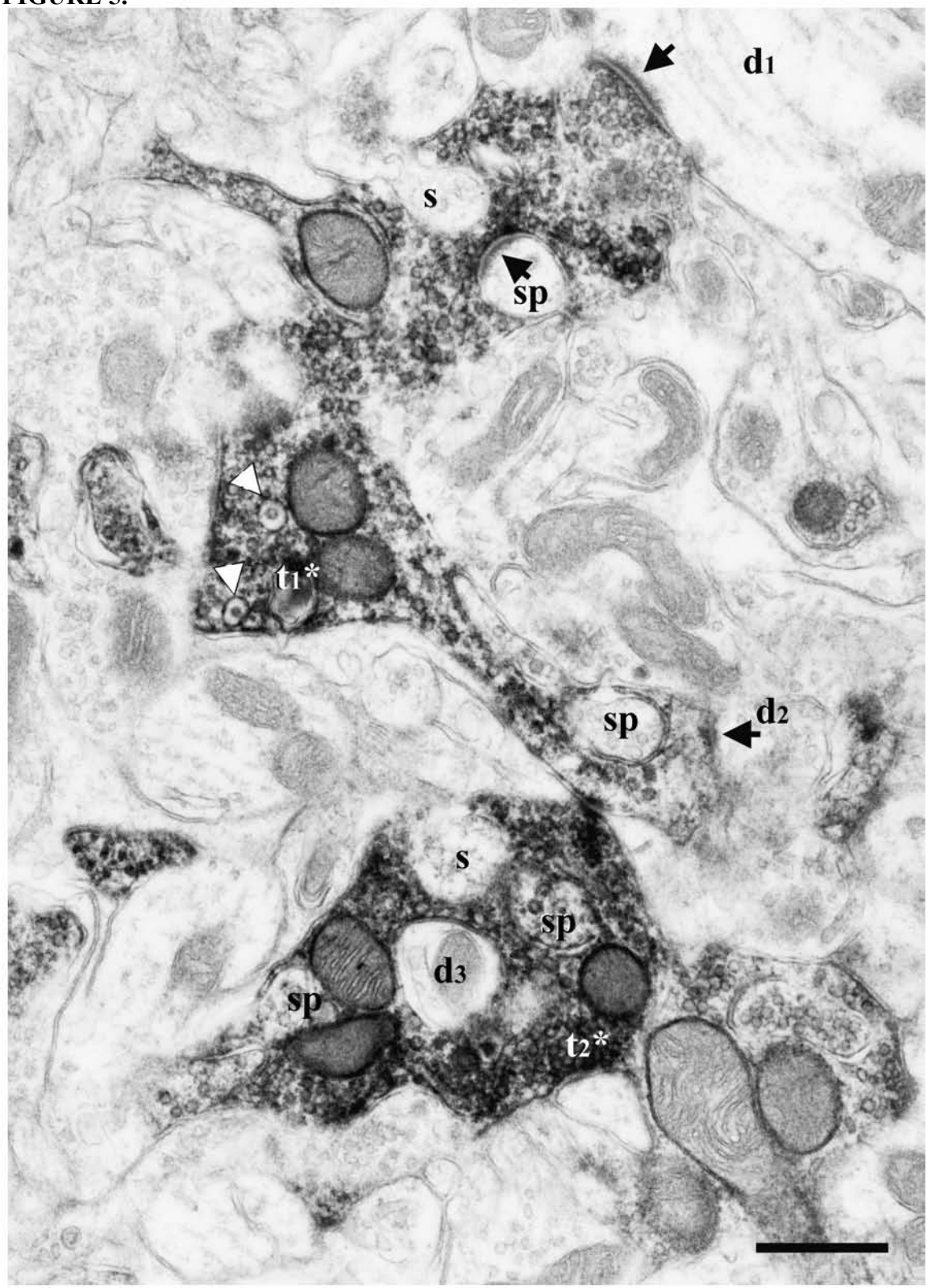

FIGURE 6.

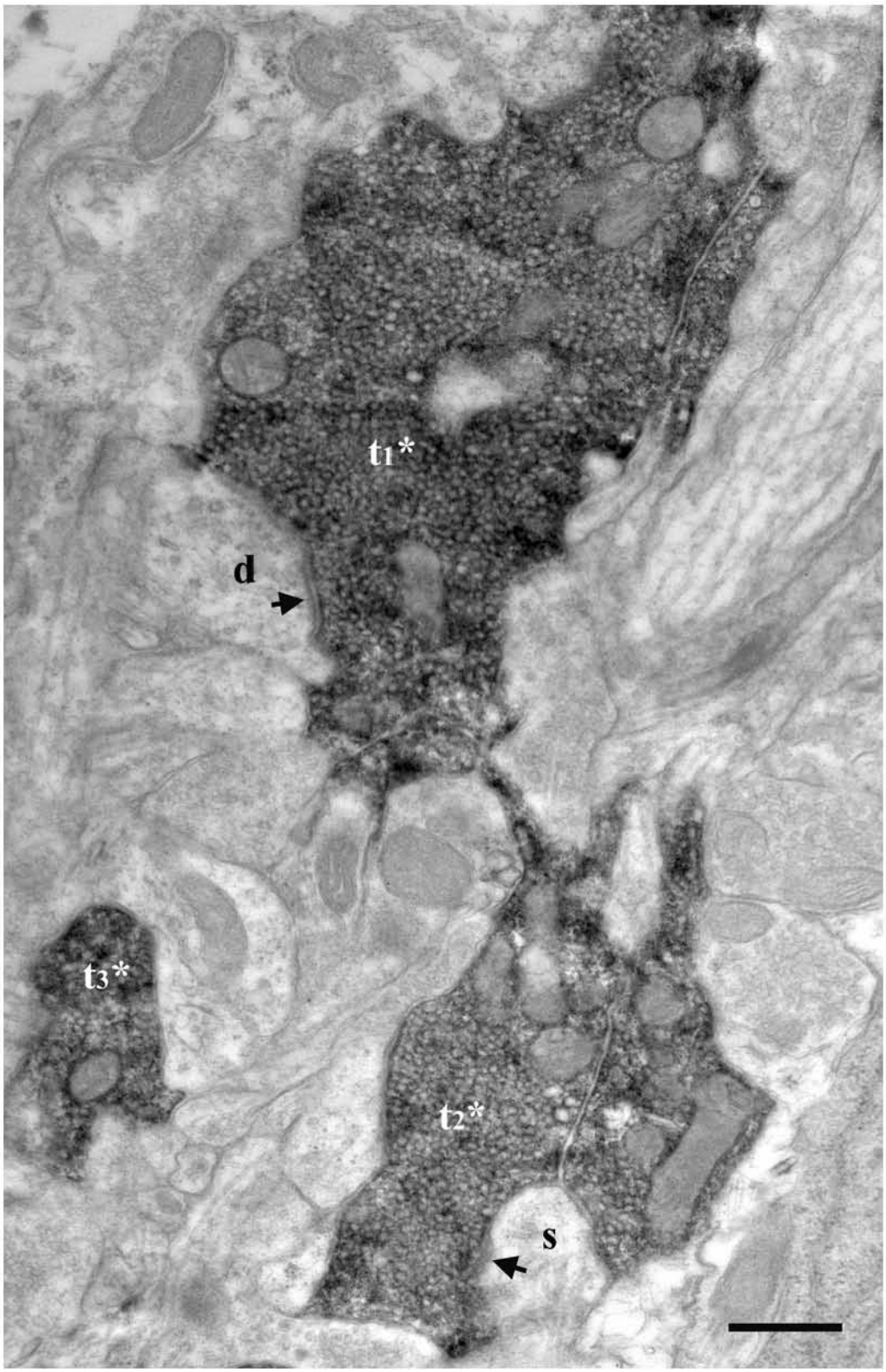

FIGURE 7.

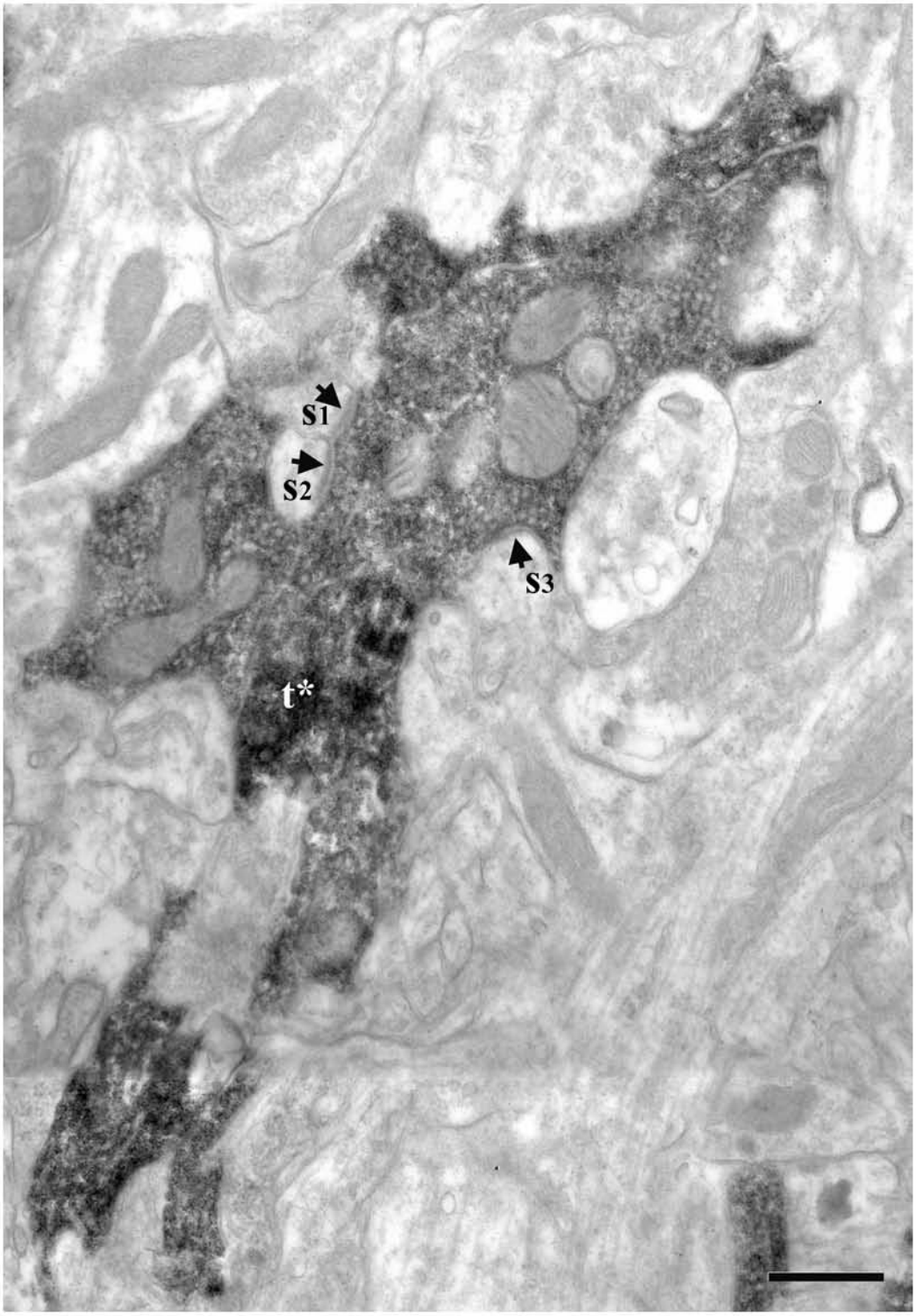

FIGURE 8.

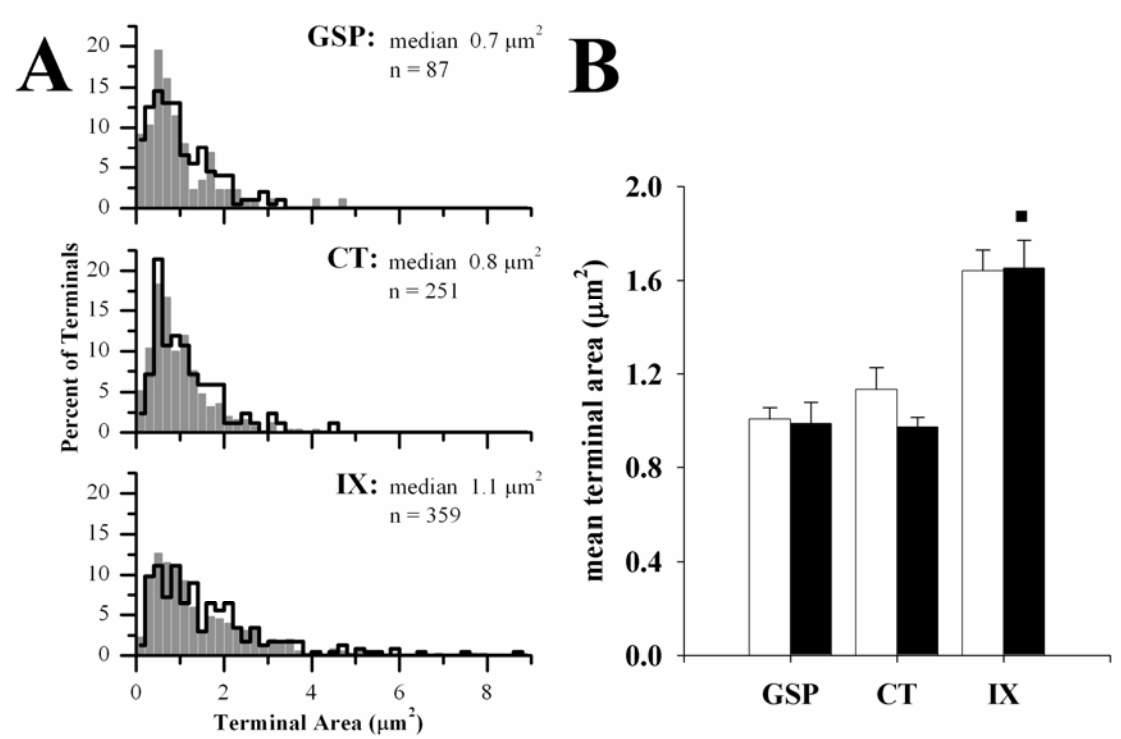

FIGURE 9.

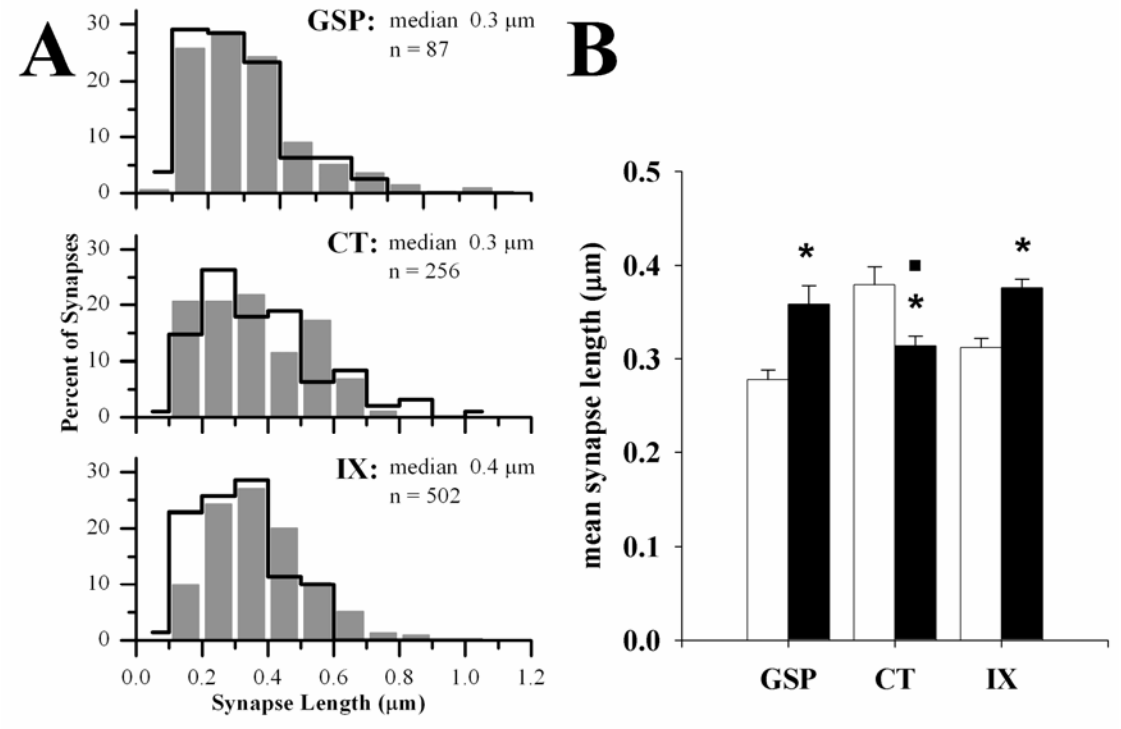

FIGURE 10.

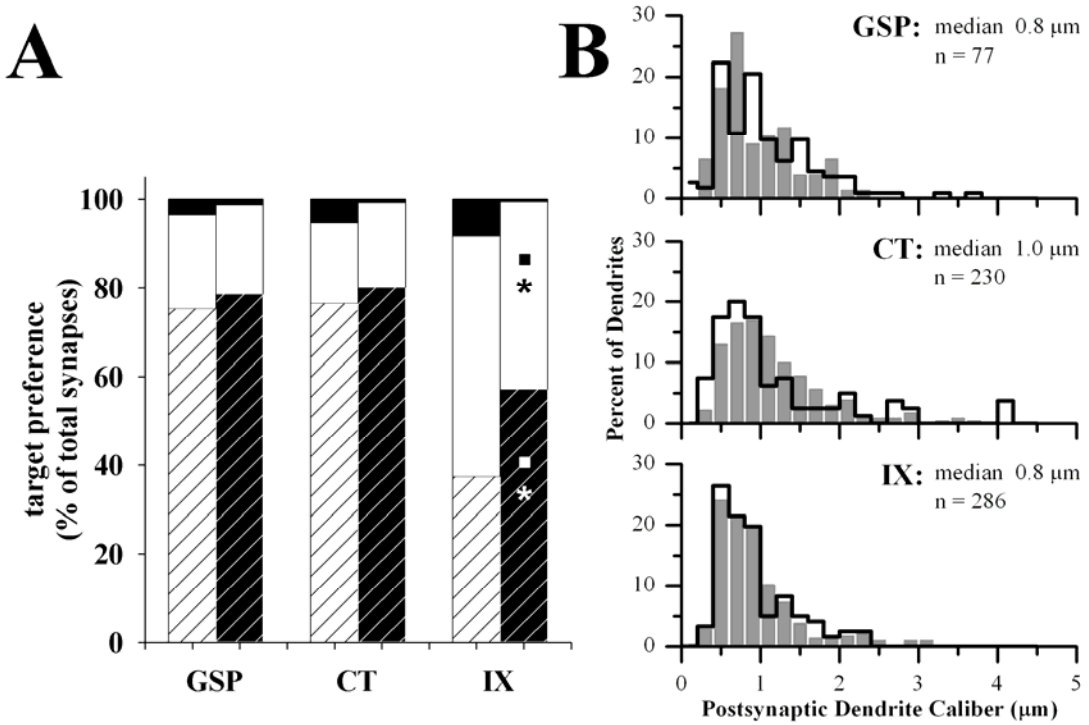

FIGURE 11.

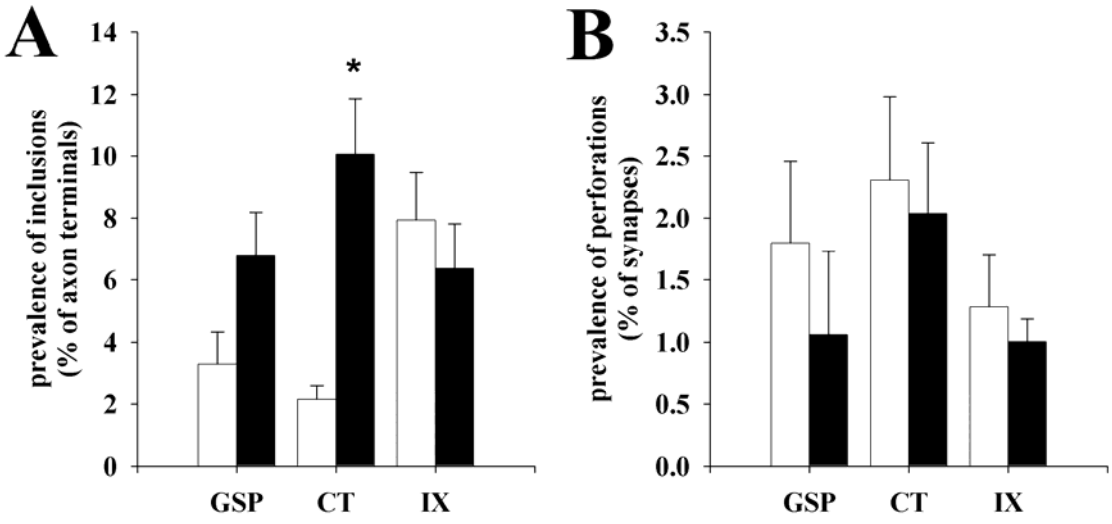

FIGURE 12.

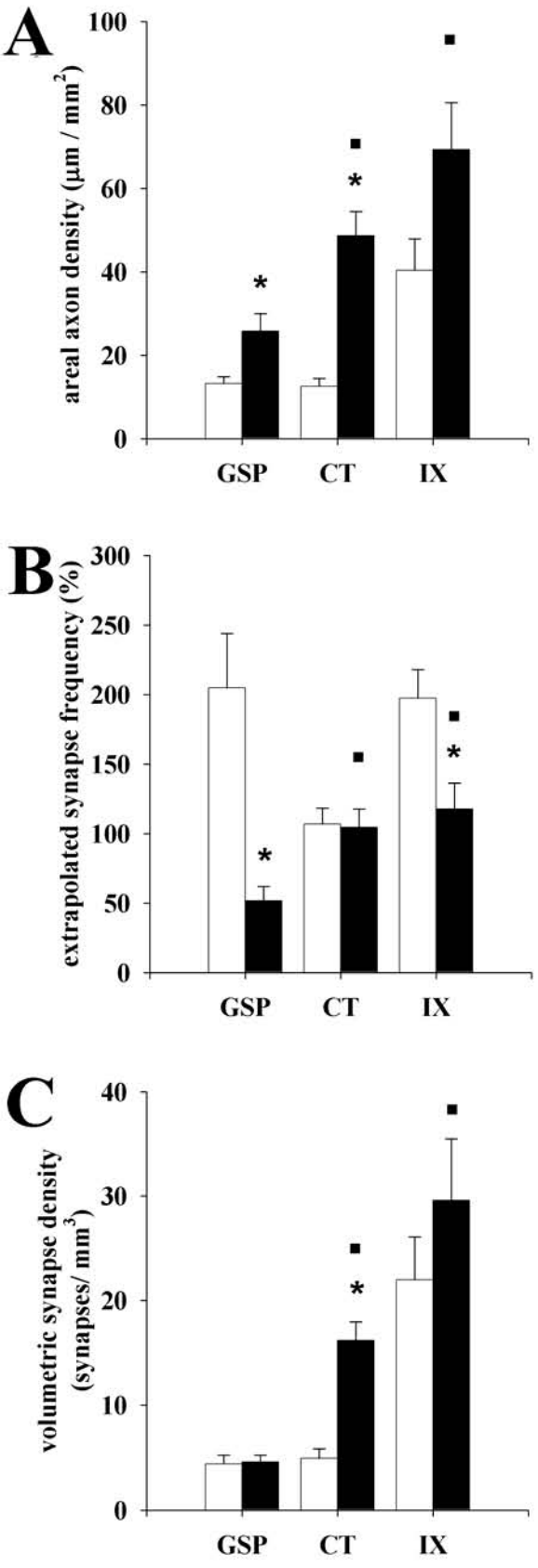
A
areal axon density (µm / mm²)
100
80
60
40
20
0
GSP
CT
IX
B
extrapolated synapse frequency (%)
300
250
200
150
100
50
0
GSP
CT
IX
C
volumetric synapse density (synapses/ mm³)
40
30
20
10
0
GSP
CT
IX

FIGURE 13.

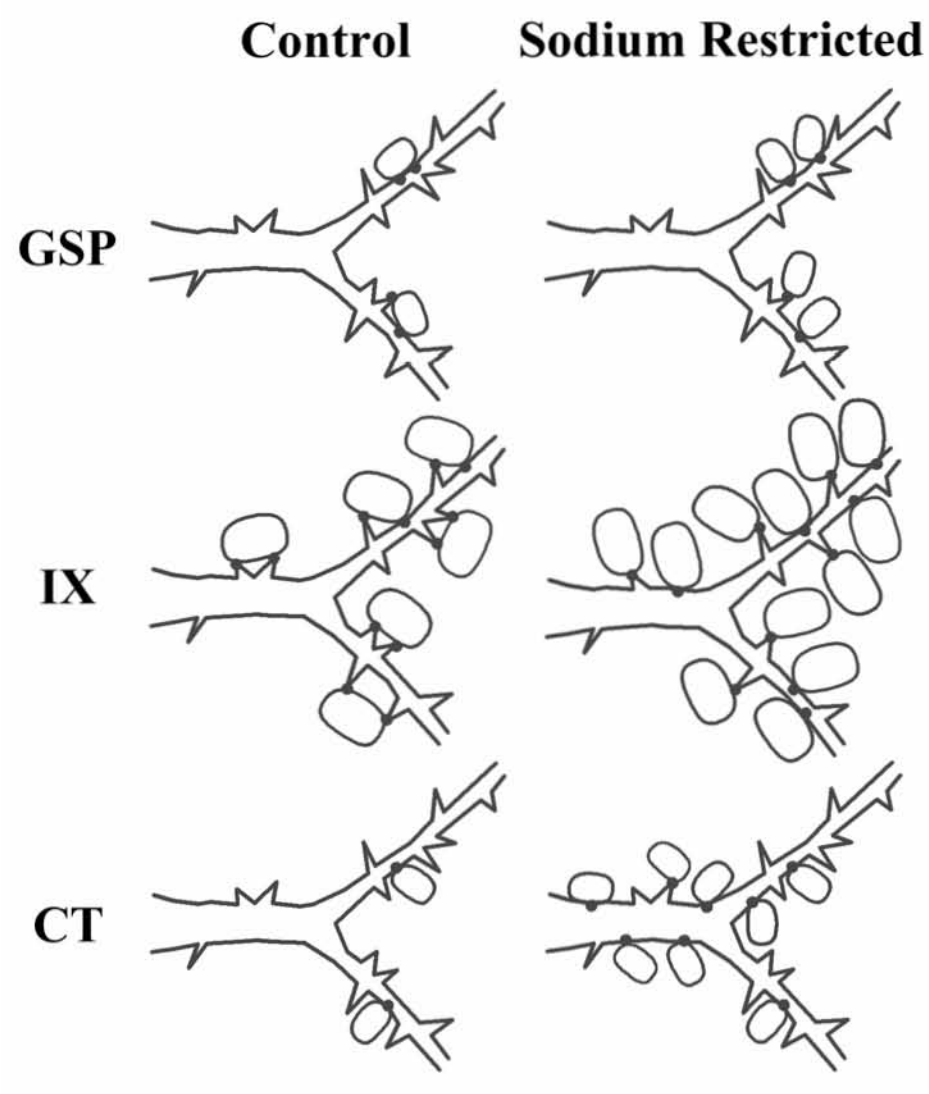

CHAPTER V

General Discussion

Organization of the Central Gustatory System

The experiments presented in Chapters II-IV provide a clearer understanding of the organization of the central gustatory system at the first afferent relay in the brainstem. Through improved methods of visualizing gustatory terminal fields concurrently, it is now evident that gustatory afferents terminate in a hierarchical pattern from dorsal to ventral in the sequence: the glossopharyngeal (IX) nerve, the greater superficial petrosal (GSP) nerve, and the chorda tympani (CT) nerve. Further, these terminations overlap considerably, most notably in the dorsal most portion of the nucleus of the solitary tract (NTS). Specifically, at this portion of the NTS there is a convergence of all three gustatory afferents. Furthermore, for the first time, the distinguishing morphological ultrastructure of gustatory afferent terminals has been described in rat. These results provide evidence that each of the three gustatory afferents maintains unique synaptic morphologies while most likely converging onto the same NTS cells.

Altogether, these results provide new insight on how the circuitry of the gustatory brainstem is wired during development, and as a result of those established synaptic connections, how taste stimulus information is processed at that first relay. For instance, as proposed in Chapter III, the morphological differences manifested in the terminal endings and the establishment of synaptic connectivity, be it driven by cues guiding the presynaptic terminal or attracted by the postsynaptic element, appear related to gustatory nerve identity. That is, the morphological dichotomy of gustatory nerves was proposed to reflect the developmental time course of maturation of afferent terminations, the nature of the stimulus information being transmitted by each gustatory nerve (be it aversive or

appetitive), and the impetus for that stimulus to be processed. As stipulated by the results of the experiments described in both Chapters II and III, a combination of morphologically distinct gustatory afferents potentially converge onto the same cells within the NTS. Compared to other extensively studied sensory systems, such as the visual system and the somatosensory system, convergence of separate afferents onto single NTS cells is a unique aspect of the taste system. Although speculative, this convergence of gustatory afferents may function to maximize the gain in processing neural responses and, in turn, to modulate input from separate receptors to guide taste-related behavior. Thus, the gustatory system provides an exceptional model of the synaptic integration of distinct sensory afferents.

Plasticity of Central Gustatory System

By perturbing this model system, the mechanisms involved in establishing synaptic connections during normal development are more clearly understood. With the implementation of a sodium-restricted diet during a critical period of development, the normal borders that define the IX and CT fields were severely disrupted (Chapter II); however, the GSP terminal field was not affected. By sheer magnitude of disruption of terminal field morphology, a time course for terminal field development of the different gustatory afferents in the NTS was predicted in Chapter II. I hypothesized that of the three gustatory nerves, the boundaries of the terminal field of the GSP nerve are determined earliest in development, before the effects of early dietary manipulation are expressed. Then, the initial development of the CT terminal field closely trails the development of the GSP terminal field (Lasiter, 1992) but is grossly misshapen by the

onset of the effects of sodium restriction. Finally, the IXth nerve begins to terminate in the NTS (Lasiter, 1992); however, the terminal field of this nerve is organized when the consequences of sodium restriction are fully realized and, thus, is malformed. Although, the ultimate time course of the development of the three gustatory afferents has not been demonstrated, this predicted time line of terminal field development is in accord with the results of previous research (Lasiter, 1992; Harada et al., 2000).

Previous investigations (King and Hill, 1991; Sollars and Hill, 2000) of the effects of developmental sodium restriction reported terminal field distortion for only the CT nerve. Since the CT nerve is uniquely associated with the transduction of sodium stimuli on the anterior tongue (Hill, 1987; Hill and Przekop, 1988), the effects of developmental sodium restriction were believed to result from the lack of neural activity dependent on stimulation from sodium ions. However, in the current experiments, the IXth nerve terminal fields were also affected by dietary manipulation. Activity dependence cannot explain the gross disruption of IX terminal field boundaries because the IXth nerve produces insubstantial taste responses to sodium salts (Formaker and Hill, 1991; Kitada et al., 1998). Further, the processes that determine abnormal terminal field development are enabled before taste receptor cells are functional. For instance, taste receptor cells on the anterior tongue are not functional until birth (Mistretta, 1972), but a discrete period from E3-E12 where a sodium-restricted diet is implemented is sufficient to cause alterations in terminal field formation (Krimm and Hill, 1997). Also, Stewart et al. (1993) demonstrated that the levels of sodium in the milk of sodium-restricted dams were equivalent to the levels of sodium in the milk of control mothers. Therefore, pups born to

sodium-restricted mothers are not truly restricted of sodium until weaning. Thus, an activity-dependent mechanism cannot fully explain the alterations in terminal field development as a result of sodium restriction.

Therefore, the reduced presence of sodium in the diet must indirectly affect the formation of terminal field boundaries in the NTS by disrupting a wide-ranging element of development as a whole. Indeed, the physiological consequences of prenatal dietary manipulations extend beyond the gustatory system and include alterations in the levels of hormones such as aldosterone (Kifor et al., 1991; Lehoux et al., 1994) and growth factors such as IGF1 (Fliesen et al., 1989; Dentremont et al., 1999). Additional factors and molecular cues involved in the guidance of gustatory afferents to the NTS and the formation of boundaries of the termination zones may also be disrupted. Indeed, a host of axon guidance and inhibitory molecules including (but not limited to) proteoglycans, extracellular matrix molecules, hox and oncogenes, semaphorins, and other growth-promoting or growth-inhibiting molecules are downregulated at the end of development (Letourneau, et al., 1994; Silver, 1994; Faissner and Steindler, 1995; Steindler et al., 1998)

Given the specific alterations of terminal field formation resulting from dietary sodium restriction that were evident with fluorescent confocal microscopy, we hypothesized that discernable, ultrastructural differences would be apparent most notably for IX afferents and also for CT afferents but not for GSP afferents. However, as described in Chapter IV, the electron microscopic examination of IX, CT, and GSP afferent terminals did not corroborate this prediction. A significant remodeling occurred

uniquely for all three gustatory afferents, but the largest effects of dietary sodium restriction occurred with CT axons. The synaptic input associated with the CT nerve quadrupled; whereas, the synaptic input associated with the IXth and GSP nerves remained the same. However, the frequency with which synapses occurred on IX and GSP axons decreased. Thus, in contrast to the effects of dietary sodium restriction revealed with fluorescent confocal microscopy, at the ultrastructural level, the most dramatically altered gustatory afferent was the CT nerve. The IXth and GSP nerves appeared to be affected secondarily as a result of increased synaptic connectivity of the CT nerve. Since the exuberant synaptic input of the CT nerve appears to be the driving force behind the synaptic alterations related to the IXth and GSP nerves, neural activity may play a role in the configuration of gustatory afferent synaptic connections during normal development. This is in sharp contrast to the proposition in Chapter II that extenuating factors other than activity dependence shape terminal field morphology. These differences reinforce the necessity of diverse experimental approaches to yield insight on the establishment of the circuitry of brainstem. Indeed, the combined light and electron microscopic observations, in conjunction with previous studies examining the structure and function of the gustatory brainstem, lead to several predictions that reconcile the role of activity dependence in the establishment of the connectivity of the three gustatory afferents during development.

Development of Gustatory Afferent Connectivity

It is apparent that the mature patterns of synaptic connections of gustatory afferents are established by two distinct phases of development. During an early phase of

development, the initial organization of neural circuits is dependent on a variety of molecular cues that guide axons to generally appropriate regions, where they establish connections with their postsynaptic targets, well in advance of functional interactions with the environment. Later in development, as these connections become functional, they are more specifically refined by appropriate stimulation. That is, in an activity-dependent manner, some connections are pared back while others are reinforced. Indeed, classic neuronal development has been repeatedly described as a pivotal process in which precise patterns of synaptic connections emerge from a prior period of more coarsely organized connections (Stryker and Harris, 1986; Katz and Shatz, 1996; Katz and Crowley, 2002). As postulated by Hebb, synaptic connections are strengthened and consolidated by correlated neural activity and weakened or eliminated by discordant activity (Hebb, 1949).

Thus, with plasticity of gustatory afferents induced by a paradigm of restricted dietary sodium, one can begin to predict the mechanisms involved in the integration of gustatory afferents onto NTS neurons during normal development. The effects of dietary sodium restriction are manifested during both of these periods of growth and refinement but perhaps have different degrees of influence dependent on both the developmental stage of the particular gustatory afferent and the requisite stimulation of the receptive fields of each gustatory nerve. Thus, perhaps the afferent terminations of the GSP nerve are least affected by dietary sodium restriction because they are established in the NTS first, in advance of the disruption of the boundary determining factors within the NTS. Next, the afferent terminations of the CT nerve are established; however, dietary sodium

restriction affects the molecular cues that establish the normal boundaries of the CT terminal field. Thus, the CT terminal field extends beyond its normal parameters. Moreover, as the taste receptors associated with the CT nerve become functional, CT afferents do not receive sufficient stimulation from sodium. Thus, these afferents do not receive the appropriate neural activity that would normally refine their synaptic connections. Without adequate pruning of synapses, more synapses are integrated within the NTS neuropil, which ultimately affects the distribution of synapses associated with the GSP and IX axons by relegating these synapses further apart. The afferent terminations of the IXth nerve are established well after the development of both the GSP and CT terminal fields is underway. Since this nerve terminates in an area of the NTS where the signals involved in establishing normal terminal field boundaries are grossly disrupted, the IXth nerve makes errant connections throughout the dorsal-ventral extent of the NTS. However, later in development the taste receptors associated with the IXth nerve are sufficiently stimulated. Thus, adequate neural activity pares down the synaptic connections of IX afferents. In summary, during early development, terminal fields are established by axon path-finding and boundary-forming signals; later in development, neural activity refines the synaptic connections of the terminal fields established earlier in development. Furthermore, restricting dietary sodium is effective in both derailing the background of necessary molecular signals involved in establishing appropriate terminal field boundaries and disrupting the refinement of synaptic connections specifically associated with the CT nerve.

Future Studies

While the comprehensive results of these experiments have clarified our understanding of the organization of the relay of the gustatory brainstem, many questions regarding the nature of the circuitry remain to be elucidated. Clearly, the most imperative aspect in understanding the mechanisms involved in the development of gustatory afferent circuitry is to definitively describe the developmental time course of the three gustatory terminal fields. Upon establishing this sequence of development, the effects of dietary sodium restriction on the mechanisms involved in framing gustatory connections can be more thoroughly examined. As an example, one potential method to determine the finer details of the establishment of the gustatory circuitry would involve the use of brain explant cocultures, which are widely employed to study axon-target interactions, differentiation of neuronal phenotypes, and functional connectivity (Grigaliunas et al., 2002; Liu et al., 2004; Ozdinler et al., 2004; Ulupinar et al., 2004). Since many aspects of neural activity can be recapitulated in vitro, biological phenomena that are difficult to tease apart in vivo become more readily accessible in a culture system. A technique such as this could potentially be applied to the NTS in order to determine the molecular framework of guidance and repellent molecules employed to establish the gustatory circuitry in early development.

Further, the results of the experiments presented in this dissertation reveal the necessity for a more tangible demonstration of convergence of gustatory afferents onto the same neurons in the NTS. This could be achieved at the ultrastructural level by dual labeling of gustatory afferents. Furthermore, great insight to convergence within the gustatory circuitry could be gained by identifying the postsynaptic elements and the

contribution inhibitory input has on modulating the neural transmission of the three gustatory afferents.

Finally, in conjunction with identifying the gustatory circuitry resulting from normal development, these same techniques could be applied to an examination of synaptic plasticity resulting from dietary sodium restriction. Additionally, potential factors (e.g., receptors) that mediate this plasticity could be identified and characterized. The *N*-methyl-D-aspartate (NMDA) receptor channel is a prime candidate for a substrate designed to detect coincident neural activity (Constantine-Paton et al., 1990) and, thus, may play a role in the gustatory system in the refinement of synaptic connections via experience-dependent plasticity. While as a whole, the findings reported in this dissertation establish a better foundation for the organization of the circuitry of the first relay of the central gustatory system. Perhaps more importantly, new experimental avenues that further delineate this organization are now possible to explore.

LITERATURE CITED

Constantine-Paton M, Cline HT, Debski E. 1990. Patterned activity, synaptic convergence, and the NMDA receptor in developing visual pathways. Annu Rev Neurosci 13:129-154.

Dentremont KD, Ye P, D'Ercole AJ, O'Kusky JR. 1999. Increased insulin-like growth factor-I (IGF-I) expression during early postnatal development differentially increases neuron number and growth in medullary nuclei of the mouse. Brain Res Dev Brain Res 114:135-141.

Faissner A, Steindler D. 1995. Boundaries and inhibitory molecules in developing neural tissues. Glia 13:233-254.

Fliesen T, Maiter D, Gerard G, Underwood LE, Maes M, Ketelslegers JM. 1989. Reduction of serum insulin-like growth factor-I by dietary protein restriction is age dependent. Pediatr Res 26:415-419.

Formaker BK, Hill DL. 1991. Lack of amiloride sensitivity in SHR and WKY glossopharyngeal taste responses to NaCl. Physiol Behav 50:765-769.

Grigaliunas A, Bradley RM, MacCallum DK, Mistretta CM. 2002. Distinctive neurophysiological properties of embryonic trigeminal and geniculate neurons in culture. J Neurophysiol 88:2058-2074.

Harada S, Yamaguchi K, Kanemaru N, Kasahara Y. 2000. Maturation of taste buds on the soft palate of the postnatal rat. Physiol Behav 68:333-339.

Hebb DO. 1949. The Organization of Behavior. New York: Wiley.

Hill DL. 1987. Susceptibility of the developing rat gustatory system to the physiological effects of dietary sodium deprivation. J Physiol 393:413-424.

Hill DL, Przekop PR, Jr. 1988. Influences of dietary sodium on functional taste receptor development: a sensitive period. Science 241:1826-1828.

Katz LC, Crowley JC. 2002. Development of cortical circuits: lessons from ocular dominance columns. Nat Rev Neurosci 3:34-42.

Katz LC, Shatz CJ. 1996. Synaptic activity and the construction of cortical circuits. Science 274:1133-1138.

Kifor I, Moore TJ, Fallo F, Sperling E, Menachery A, Chiou CY, Williams GH. 1991. The effect of sodium intake on angiotensin content of the rat adrenal gland. Endocrinology 128:1277-1284.

King CT, Hill DL. 1991. Dietary sodium chloride deprivation throughout development selectively influences the terminal field organization of gustatory afferent fibers projecting to the rat nucleus of the solitary tract. J Comp Neurol 303:159-169.

Kitada Y, Mitoh Y, Hill DL. 1998. Salt taste responses of the IXth nerve in Sprague-Dawley rats: lack of sensitivity to amiloride. Physiol Behav 63:945-949.

Krimm RF, Hill DL. 1997. Early prenatal critical period for chorda tympani nerve terminal field development. J Comp Neurol 378:254-264.

Lasiter PS. 1992. Postnatal development of gustatory recipient zones within the nucleus of the solitary tract. Brain Res Bull 28:667-677.

Lehoux JG, Bird IM, Rainey WE, Tremblay A, Ducharme L. 1994. Both low sodium and high potassium intake increase the level of adrenal angiotensin-II receptor type 1, but not that of adrenocorticotropin receptor. Endocrinology 134:776-782.

Letourneau PC, Condic ML, Snow DM. 1994. Interactions of developing neurons with the extracellular matrix. J Neurosci 14:915-928.

Liu HX, Maccallum DK, Edwards C, Gaffield W, Mistretta CM. 2004. Sonic hedgehog exerts distinct, stage-specific effects on tongue and taste papilla development. Dev Biol 276:280-300.

Mistretta CM. 1972. Topographical and histological study of the developing rat tongue, palate and taste buds. In: Oral Sensation and Perception III. The Mouth of the Infant. Bosma JF, Editor. Springfield: Charles C Thomas. p 163-187.

Ozdinler PH, Ulupinar E, Erzurumlu RS. 2004. Local neurotrophin effects on central trigeminal axon growth patterns. Brain Res Dev Brain Res 151:55-66.

Silver J. 1994. Inhibitory molecules in development and regeneration. J Neurol 242:S22-24.

Sollars SI, Hill DL. 2000. Lack of functional and morphological susceptibility of the greater superficial petrosal nerve to developmental dietary sodium restriction. Chem Senses 25:719-727.

Steindler DA, Kukekov VG, Thomas LB, Fillmore H, Suslov O, Scheffler B, O'Brien TF, Kusakabe M, Laywell ED. 1998. Boundary molecules during brain development, injury, and persistent neurogenesis--in vivo and in vitro studies. Prog Brain Res 117:179-196.

Stewart RE, Tong H, McCarty R, Hill DL. 1993. Altered gustatory development in Na(+)-restricted rats is not explained by low Na+ levels in mothers' milk. Physiol Behav 53:823-826.

Stryker MP, Harris WA. 1986. Binocular impulse blockade prevents the formation of ocular dominance columns in cat visual cortex. J Neurosci 6:2117-2133.

Ulupinar E, Unal N, Erzurumlu RS. 2004. Morphometric analysis of embryonic rat trigeminal neurons treated with different neurotrophins. Anat Rec A Discov Mol Cell Evol Biol 277:396-407.